LHAASO results from first years of observation

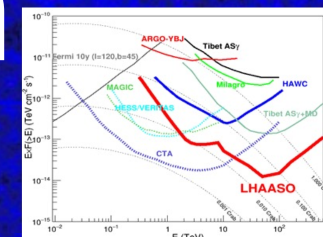

Dmitri Semikoz

APC, Paris

Summary of LHAASO results presented at

First LHAASO symposium+ several recent papers.

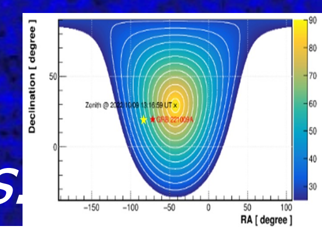

Many thanks to the following LHAASO speakers for sharing their slides:
Zhen Cao, Songzhan Chen, Ruoyu Liu, Siming Liu, Xiangyu Wang,
Ruizhi Yang, Qiang Yuan

Plan

- Introduction: LHAASO
- 1 LHAASO catalog of sources
  - PWN
  - SN remnants
  - Star Clusters
- Diffuse galactic emission
- GRB 221009A (including km2a 2310.08845)
- Cygnus region (2310.10100)
- Conclusions

Introduction: LHAASO detector

based on talk of
Zhen Cao

The ultimate goal is to identify origins of CRs

Large High Altitude Air Shower Observatory

LHAASO

Scientific Goals

γ-ray astronomy

Survey for sources (above 500 GeV)

PeVatrons (above 100 TeV)

All kind of sources: SNR, PWN, MYC, binary, pulsar

AGN, GRB etc.

Cosmic Ray Physics

The knees

Compositions : individual species H, He and Fe

Anisotropy: (1 TeV to 10 PeV)

New Physics Front: DM, LIV, etc.

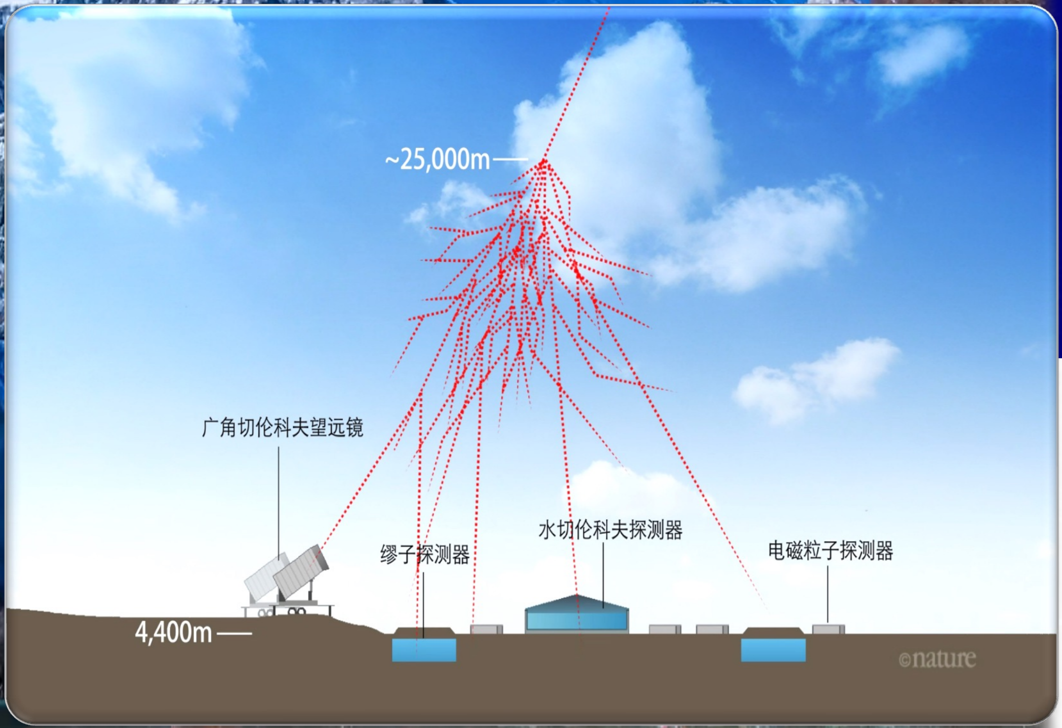

LHAASO
高海拔宇宙线观测站

LHAASO Layout

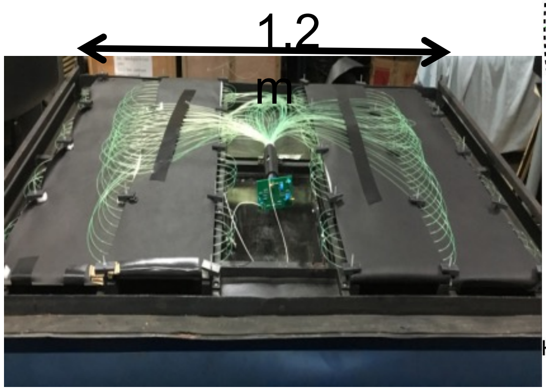

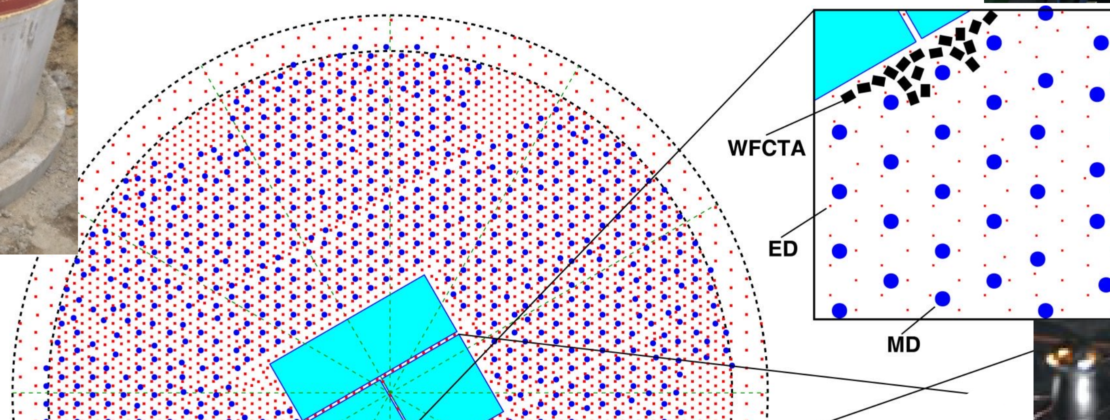

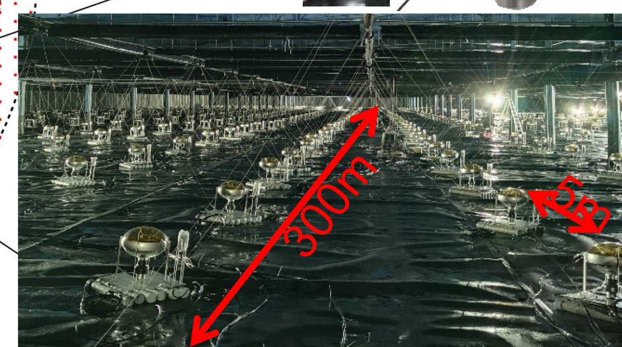

LHAASO-WCDA

Water Cherenkov Detector Array

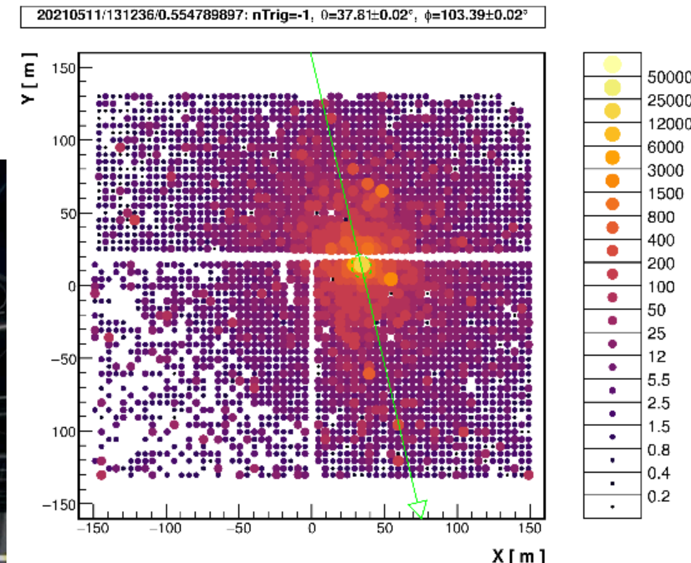

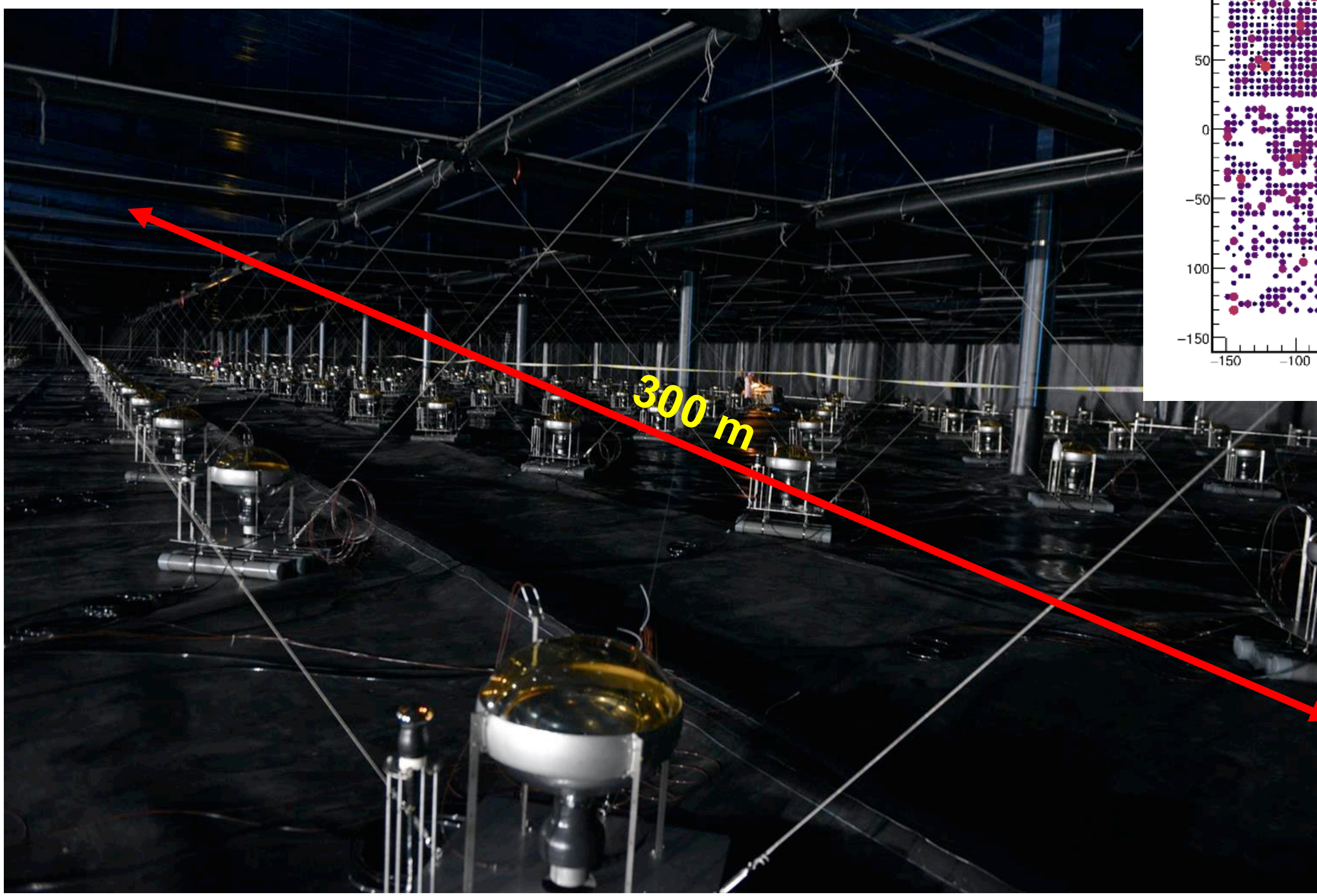

- **Area :**
  78,000 m²
- **Detector units :**
  3120
- **Energy Range :**
  0.1-10 TeV

LHAASO
高海拔宇宙线观测站

LHAASO-KM2A

Selection of γ–rays out of CR background

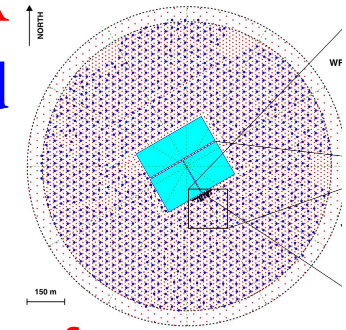

Active Area for Muons vs. Array Area: 4%

~1 PeV CR event: many muons

~1 PeV γ–ray event : very few muons

~1 PeV from the Crab

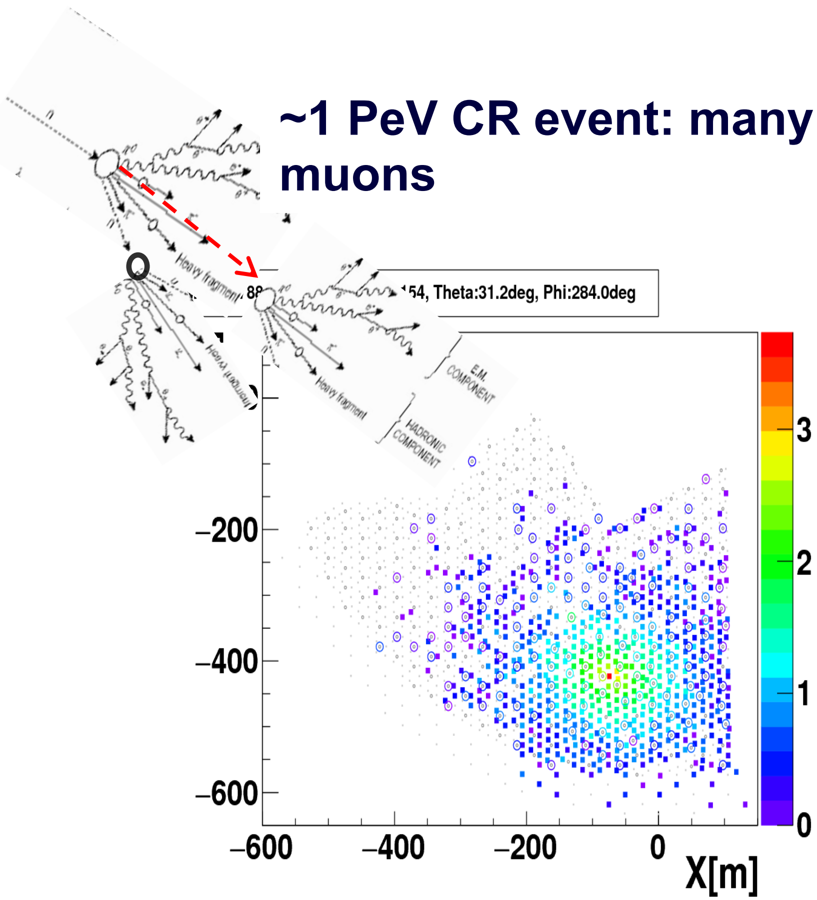

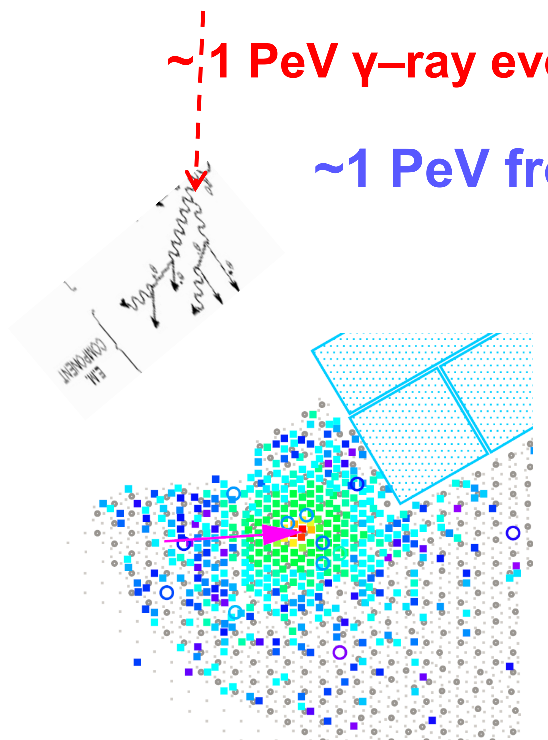

- **Area : 1.3 km²**
- **Detectors : 5216 ED, 1188 MD**
- **Energy Range : 0.01-10 PeV**

LHAASO 高海拔宇宙线观测站

LHAASO-WFCTA

Separate of individual CR species & measure the knees

~0.1 PeV CR event

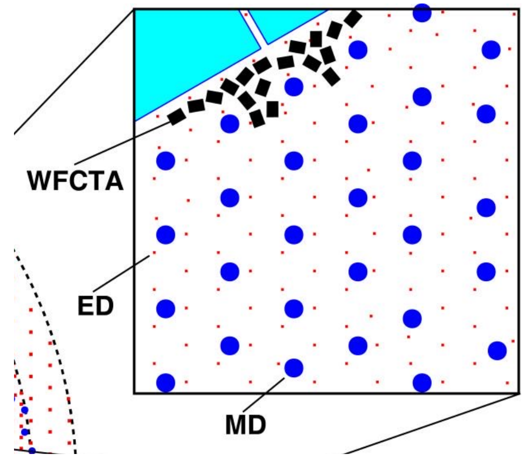

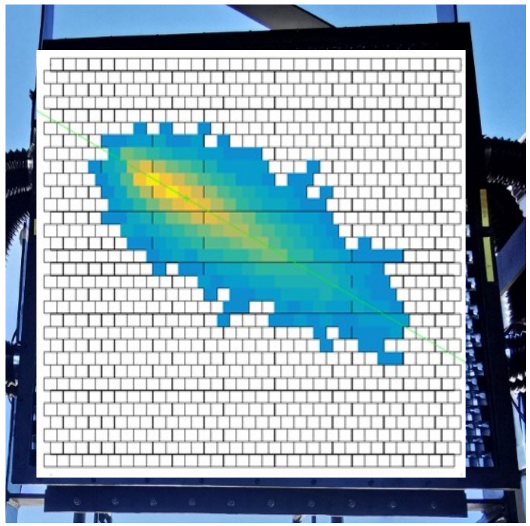

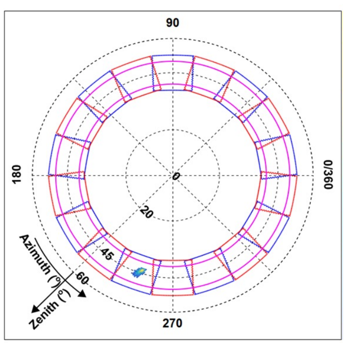

WFCTA: 18 IACTs

- Mirror: 5 m^2
- SiPM camera
- FOV: 16×16°
- Pixel size: 0.5°
- Energy: 0.1-100 PeV

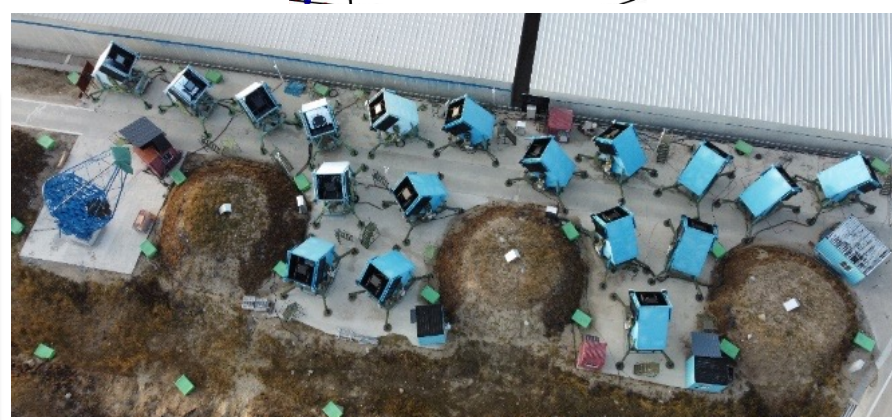

CR Background rejection in WCDA

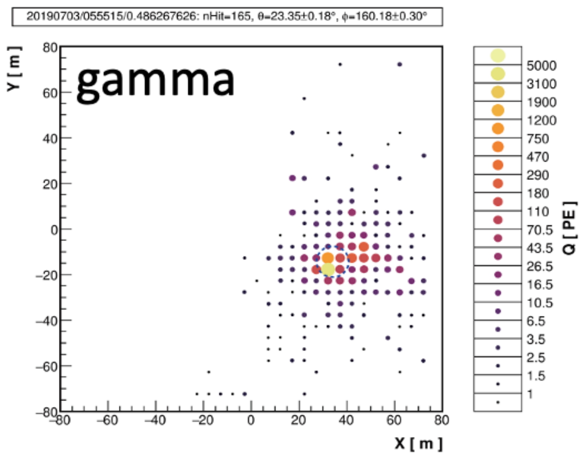

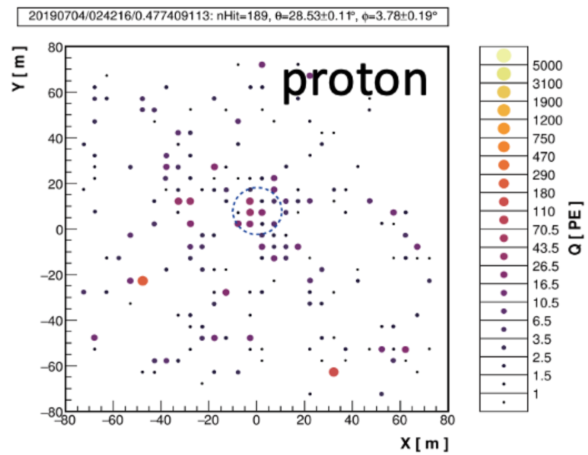

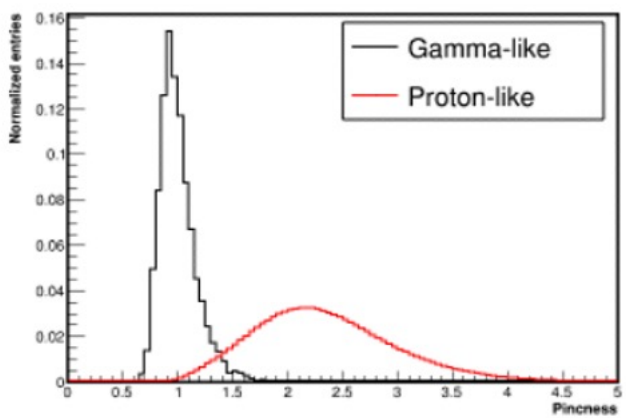

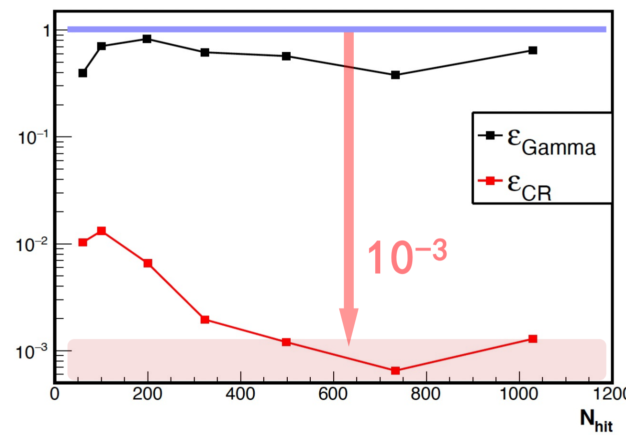

CR background Rejection in KM2A

- Counting number of measured muons in a shower
- Cutting on ratio N_{μ}/N_e<**1/230**
- BG-free (N_{γ}>10N_{CR}) Photon Counting

for showers with E>100 TeV from the Crab

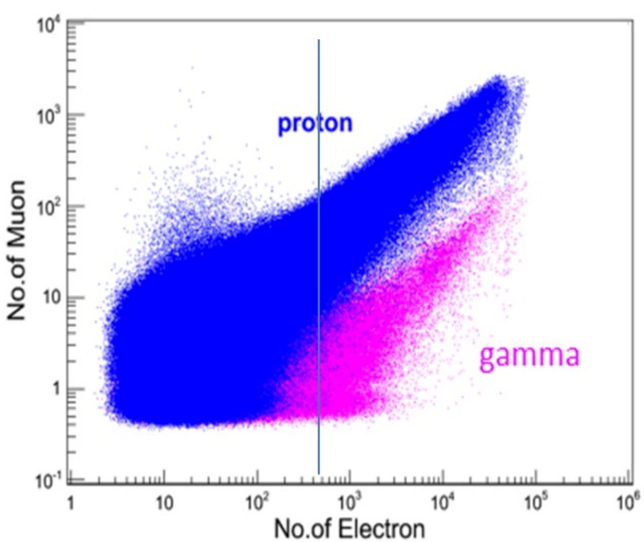

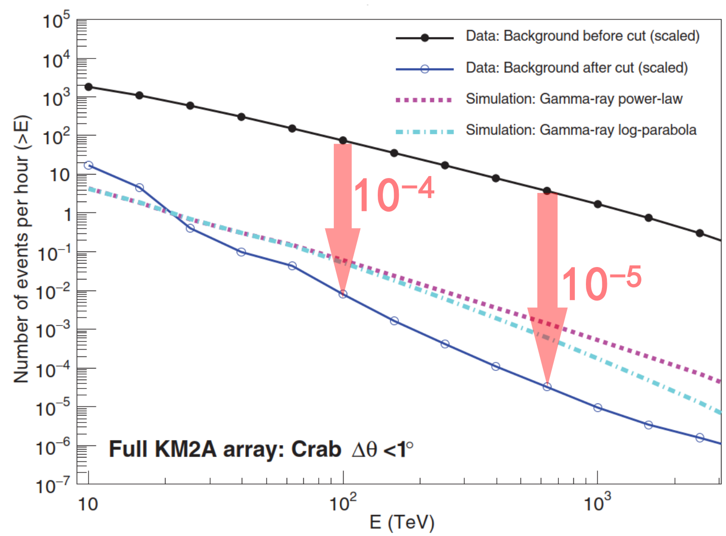

LHAASO Coll., ***Science***, 373, 425 (2021)

Multi-Messenger Collaboration Network

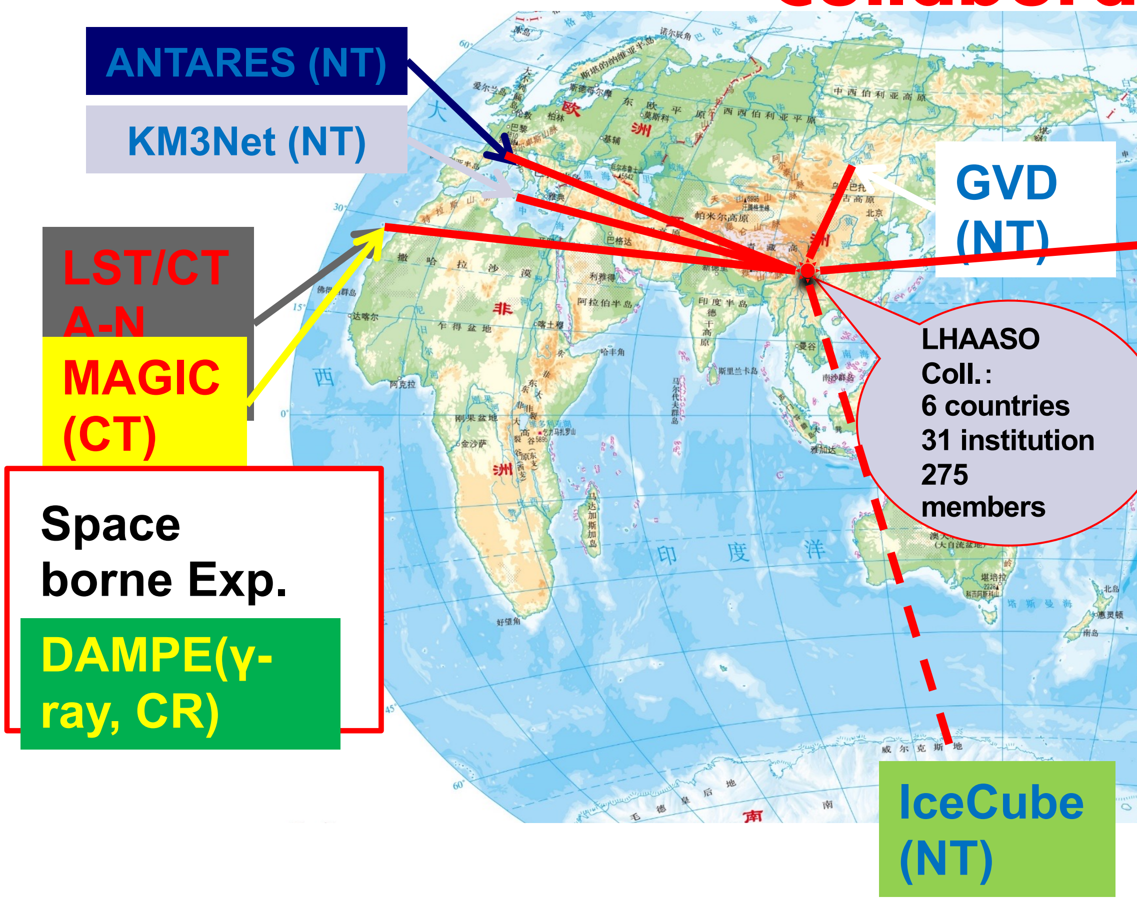

Zhen Cao,[1,2,3] F. Aharonian,[4,5] Q. An,[6,7] Axikegu,[8] L.X. Bai,[9] Y.X. Bai,[1,3] Y.W. Bao,[10] D. Bastieri,[11] X.J. Bi*,[1,2,3] Y.J. Bi,[1,3] H. Cai,[12] J.T. Cai,[11] Zhe Cao,[6,7] J. Chang,[13] J.F. Chang,[1,3,6] B.M. Chen,[14] E.S. Chen*,[1,2,3] J. Chen,[9] Liang Chen,[1,2,3] Liang Chen,[15] Long Chen,[8] M.J. Chen,[1,3] M.L. Chen,[1,3,6] Q.H. Chen,[8] S.H. Chen,[1,2,3] S.Z. Chen,[1,3] T.L. Chen,[16] X.L. Chen,[1,2,3] Y. Chen,[10] N. Cheng,[1,3] Y.D. Cheng,[1,3] S.W. Cui,[14] X.H. Cui,[17] Y.D. Cui,[18] B. D'Ettorre Piazzoli,[19] B.Z. Dai,[20] H.L. Dai,[1,3,6] Z.G. Dai,[7] Danzengluobu,[16] D. della Volpe,[21] X.J. Dong,[1,3] K.K. Duan,[13] J.H. Fan,[11] Y.Z. Fan,[13] Z.X. Fan,[1,3] J. Fang,[20] K. Fang,[1,3] C.F. Feng,[22] L. Feng,[13] S.H. Feng,[1,3] Y.L. Feng,[13] B. Gao,[1,3] C.D. Gao,[22] L.Q. Gao*,[1,2,3] Q. Gao,[16] W. Gao,[22] M.M. Ge,[20] L.S. Geng,[1,3] G.H. Gong,[23] Q.B. Gou,[1,3] M.H. Gu,[1,3,6] F.L. Guo,[15] J.G. Guo,[1,2,3] X.L. Guo,[8] Y.Q. Guo,[1,3] Y.Y. Guo,[1,2,3,13] Y.A. Han,[24] H.H. He,[1,2,3] H.N. He,[13] J.C. He,[1,2,3] S.L. He,[11] X.B. He,[18] Y. He,[8] M. Heller,[21] Y.K. Hor,[18] C. Hou,[1,3] X. Hou,[25] H.B. Hu,[1,2,3] S. Hu,[9] S.C. Hu,[1,2,3] X.J. Hu,[23] D.H. Huang,[8] Q.L. Huang,[1,3] W.H. Huang,[22] X.T. Huang,[22] X.Y. Huang,[13] Z.C. Huang,[8] F. Ji,[1,3] X.L. Ji,[1,3,6] H.Y. Jia,[8] K. Jiang,[6,7] Z.J. Jiang,[20] C. Jin,[1,2,3] T. Ke,[1,3] D. Kuleshov,[26] K. Levochkin,[26] B.B. Li,[14] Cheng Li,[6,7] Cong Li,[1,3] F. Li,[1,3,6] H.B. Li,[1,3] H.C. Li,[1,3] H.Y. Li,[7,13] Jian Li,[7] Jie Li,[1,3,6] K. Li,[1,3] W.L. Li,[22] X.R. Li,[1,3] Xin Li,[6,7] Xin Li,[8] Y. Li,[9] Y.Z. Li,[1,2,3] Zhe Li,[1,3] Zhuo Li,[27] E.W. Liang,[28] Y.F. Liang,[28] S.J. Lin,[18] B. Liu,[7] C. Liu,[1,3] D. Liu,[22] H. Liu,[8] H.D. Liu,[24] J. Liu,[1,3] J.L. Liu,[29] J.S. Liu,[18] J.Y. Liu,[1,3] M.Y. Liu,[16] R.Y. Liu,[10] S.M. Liu,[8] W. Liu,[1,3] Y. Liu,[11] Y.N. Liu,[23] Z.X. Liu,[9] W.J. Long,[8] R. Lu,[20] H.K. Lv,[1,3] B.Q. Ma,[27] L.L. Ma,[1,3] X.H. Ma,[1,3] J.R. Mao,[25] A. Masood,[8] Z. Min,[1,3] W. Mitthumsiri,[30] T. Montaruli,[21] Y.C. Nan,[22] B.Y. Pang,[8] P. Pattarakijwanich,[30] Z.Y. Pei,[11] M.Y. Qi,[1,3] Y.Q. Qi,[14] B.Q. Qiao,[1,3] J.J. Qin,[7] D. Ruffolo,[30] V. Rulev,[26] A. Sáiz,[30] L. Shao,[14] O. Shchegolev,[26,31] X.D. Sheng,[1,3] J.R. Shi,[1,3] H.C. Song,[27] Yu.V. Stenkin,[26,31] V. Stepanov,[26] Y. Su,[13] Q.N. Sun,[8] X.N. Sun,[28] Z.B. Sun,[32] P.H.T. Tam,[18] Z.B. Tang,[6,7] W.W. Tian,[2,17] B.D. Wang,[1,3] C. Wang,[32] H. Wang,[8] H.G. Wang,[11] J.C. Wang,[25] J.S. Wang,[29] L.P. Wang,[22] L.Y. Wang,[1,3] R.N. Wang,[8] W. Wang,[18] W. Wang,[12] X.G. Wang,[28] X.J. Wang,[1,3] X.Y. Wang,[10] Y. Wang,[8] Y.D. Wang,[1,3] Y.J. Wang,[1,3] Y.P. Wang,[1,2,3] Z.H. Wang,[9] Z.X. Wang,[20] Zhen Wang,[29] Zheng Wang,[1,3,6] D.M. Wei,[13] J.J. Wei,[13] Y.J. Wei,[1,2,3] T. Wen,[20] C.Y. Wu,[1,3] H.R. Wu,[1,3] S. Wu,[1,3] W.X. Wu,[8] X.F. Wu,[13] S.Q. Xi,[1,3] J. Xia,[7,13] J.J. Xia,[8] G.M. Xiang,[2,15] D.X. Xiao,[16] G. Xiao,[1,3] H.B. Xiao,[11] G.G. Xin,[12] Y.L. Xin,[8] Y. Xing,[15] D.L. Xu,[29] R.X. Xu,[27] L. Xue,[22] D.H. Yan,[25] J.Z. Yan,[13] C.W. Yang,[9] F.F. Yang,[1,3,6] J.Y. Yang,[18] L.L. Yang,[18] M.J. Yang,[1,3] R.Z. Yang,[7] S.B. Yang,[20] Y.H. Yao,[9] Z.G. Yao,[1,3] Y.M. Ye,[23] L.Q. Yin,[1,3] N. Yin,[22] X.H. You,[1,3] Z.Y. You,[1,2,3] Y.H. Yu,[22] Q. Yuan*,[13] H.D. Zeng,[13] T.X. Zeng,[1,3,6] W. Zeng,[20] Z.K. Zeng,[1,2,3] M. Zha,[1,3] X.X. Zhai,[1,3] B.B. Zhang,[10] H.M. Zhang,[10] H.Y. Zhang,[22] J.L. Zhang,[17] J.W. Zhang,[9] L.X. Zhang,[11] Li Zhang,[20] Lu Zhang,[14] P.F. Zhang,[20] P.P. Zhang,[14] R. Zhang,[7,13] S.R. Zhang,[14] S.S. Zhang,[1,3] X. Zhang,[10] X.P. Zhang,[1,3] Y.F. Zhang,[8] Y.L. Zhang,[1,3] Yi Zhang*,[1,13] Yong Zhang,[1,3] B. Zhao,[8] J. Zhao,[1,3] L. Zhao,[6,7] L.Z. Zhao,[14] S.P. Zhao*,[13,22] F. Zheng,[32] Y. Zheng,[8] B. Zhou,[1,3] H. Zhou,[29] J.N. Zhou,[15] P. Zhou,[10] R. Zhou,[9] X.X. Zhou,[8] C.G. Zhu,[22] F.R. Zhu,[8] H. Zhu,[17] K.J. Zhu,[1,2,3,6] and X. Zuo[1,3]

LHAASO sensitivity

With large FOV and high sensitivity, LHAASO is an ideal detector for sky survey to search VHE and UHE sources!

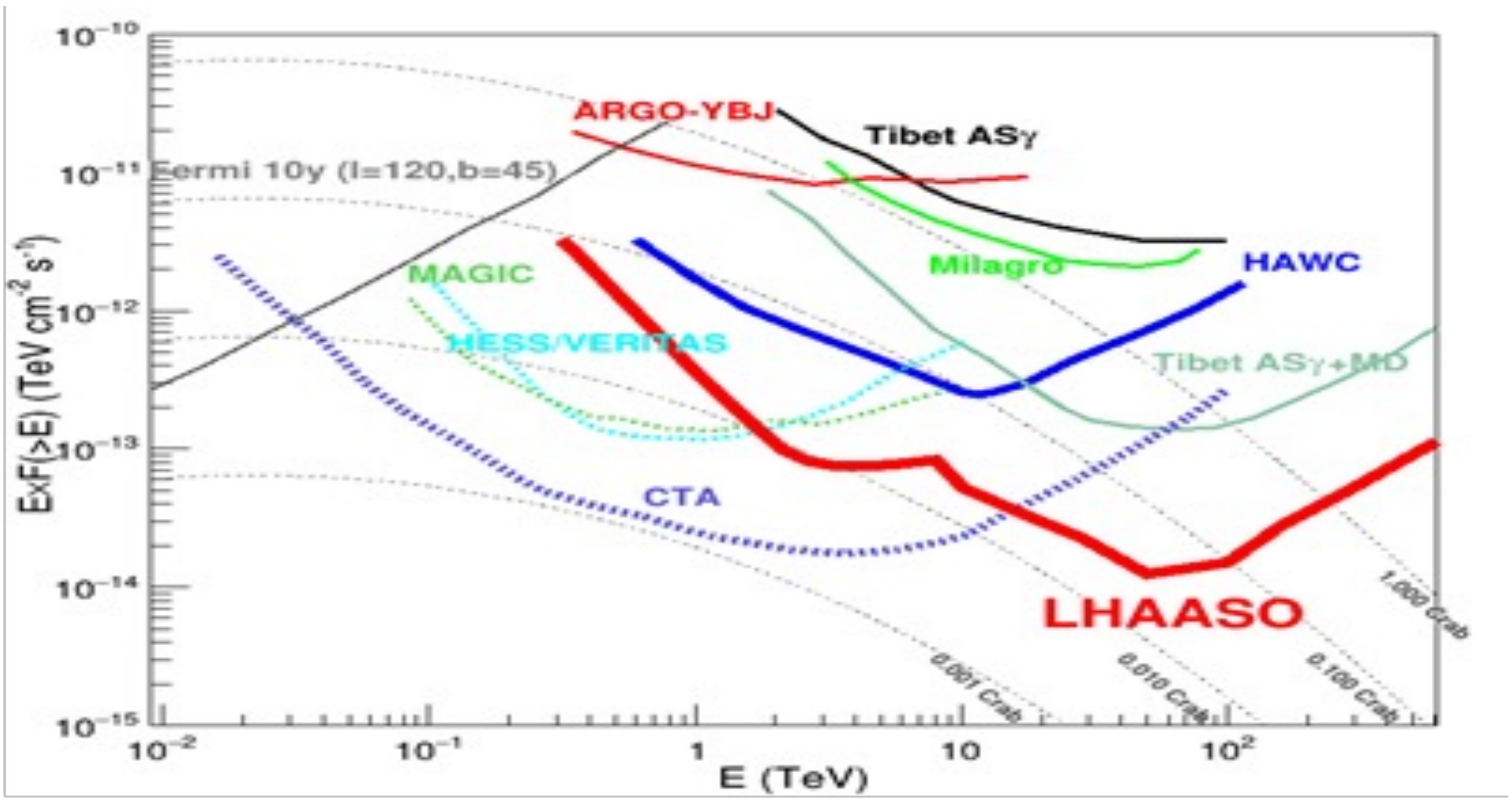

Field of view for GRB/TOO

1/7 of the sky at any time

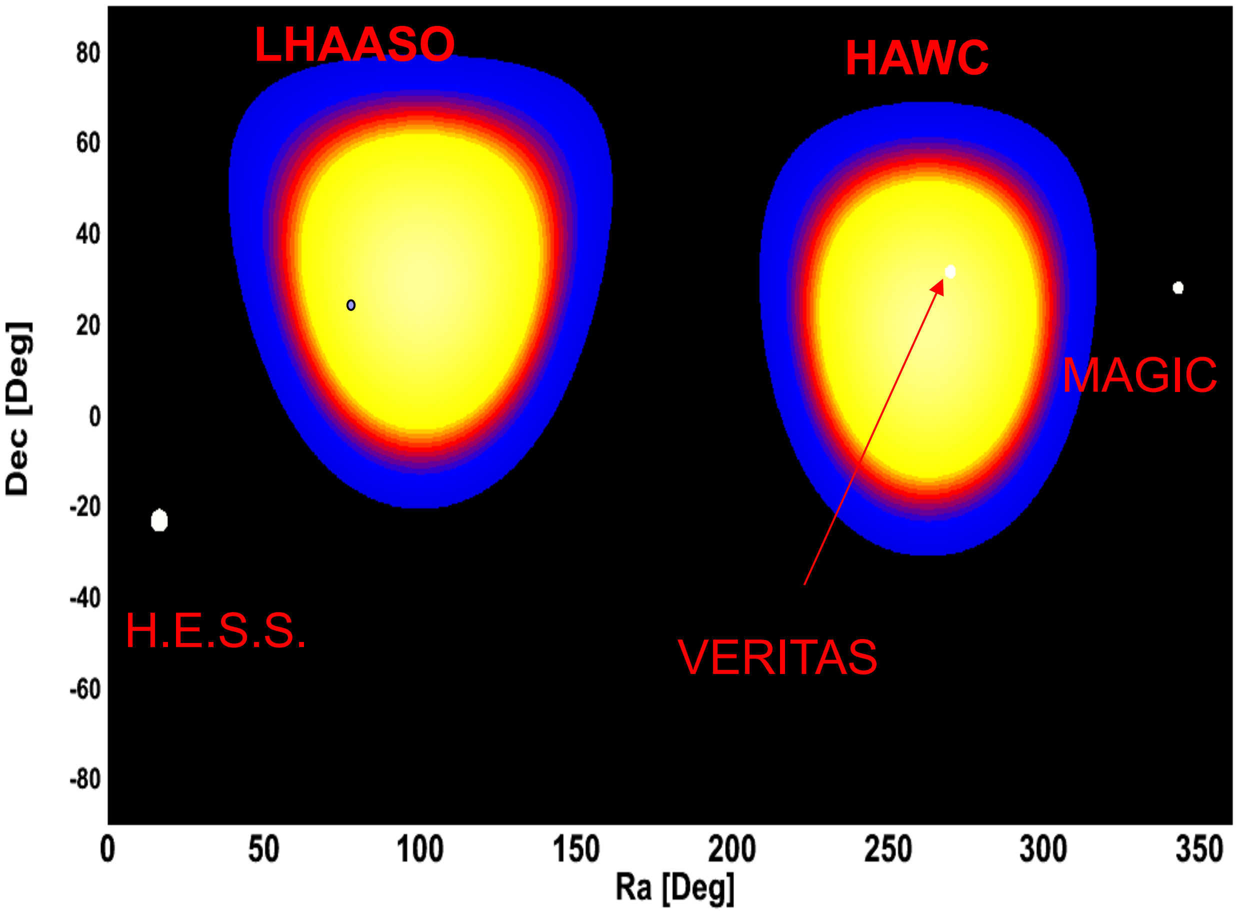

1 LHAASO catalog

based on talk of

Chen Songzhan

LHAASO data used for catalog analysis

KM2A

- 2019-12 to 2022-09
- 933 days (~730 days full array)
- 1.3×10^7 gamma-like events

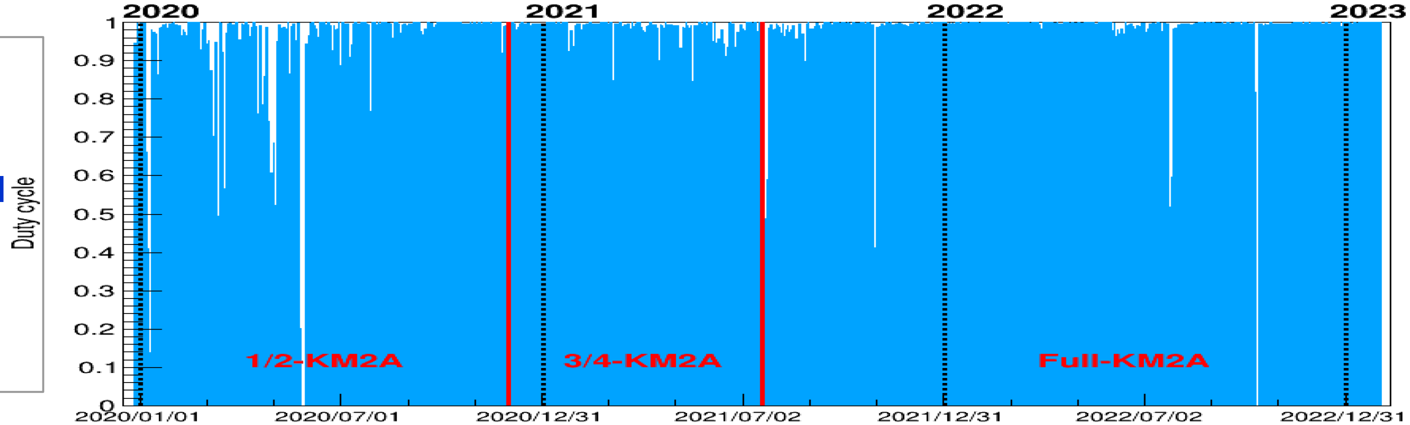

WCDA

- 2021-03 to 2022-09
- 508 days
- 1.3×10^9 gamma-like events

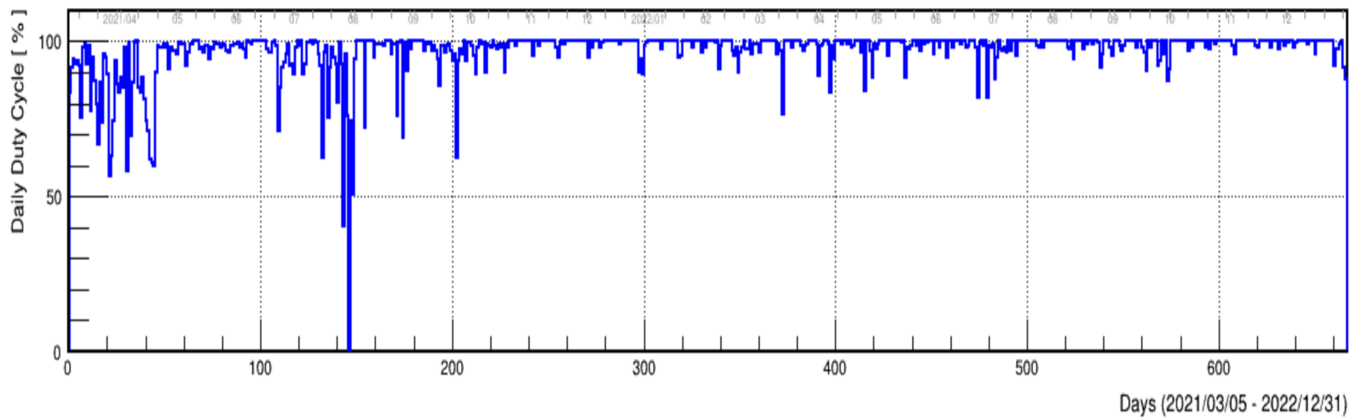

Background estimation method

- **Direct integration method:** 10 hours, Galactic plane (|b|<10º) and known sources (δθ<5º) are excluded.
- **Galactic diffuse emission** (DGE) template is added as background gamma-ray source.

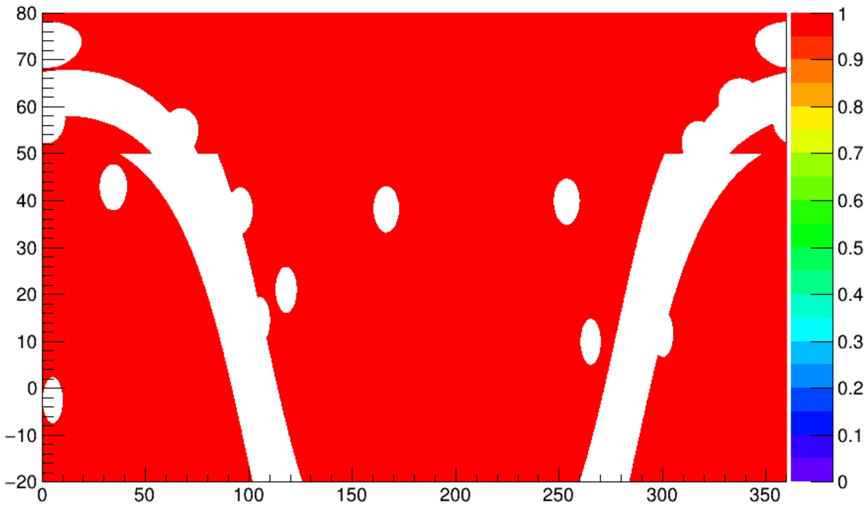

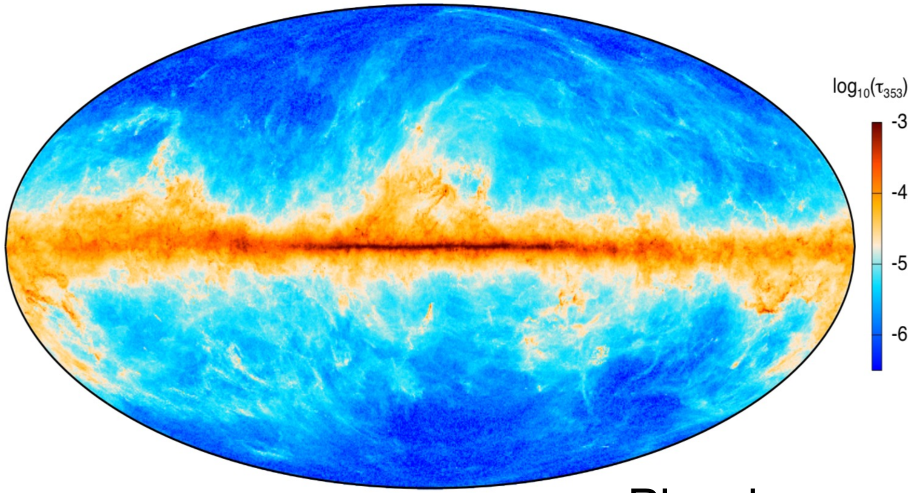

Planck dust

Binned Likelihood method for source fitting

- **Space bin:** 0.1°x0.1° for Ra:0°-360°, Dec:-20°-80°
- **WCDA energy bin:** N_{hit}100-200, 200-300, 300-500, 500-800, ≥800
- **KM2A energy bin:** E_{rec} 25-40, 40-63, 63-100, 100-160, 160-250, 250-400, 400-630, 630-1000, 1000-1600, >1600 TeV

$$P(N^{\mathrm{on}}_{i,j}|\lambda_{i,j}) = \frac{\lambda_{i,j}^{N^{\mathrm{on}}_{i,j}} e^{-\lambda_{i,j}}}{N^{\mathrm{on}}_{i,j}!}$$

$$\ln L(\Theta|N_{\mathrm{on}}) = \sum_{i}^{N_{\mathrm{bins}}} \sum_{j}^{\mathrm{ROI}} \left(N^{\mathrm{on}}_{i,j} \ln\lambda_{i,j} - \lambda_{i,j} - \ln N^{\mathrm{on}}_{i,j}!\right)$$

$$\lambda_{i,j} = N^{\mathrm{bk}}_{i,j} + \sum_{k}^{N_{\mathrm{src}}} N^{\mathrm{s}}_{k,i,j}$$

$$TS = -2\left(\ln L_0 - \ln L_1\right)$$

Point gamma-ray source searching

- The candidates with significance **>5σ** are used to determine ROI and also as **seeds** for next fitting.

WCDA SED: power-law with a index of

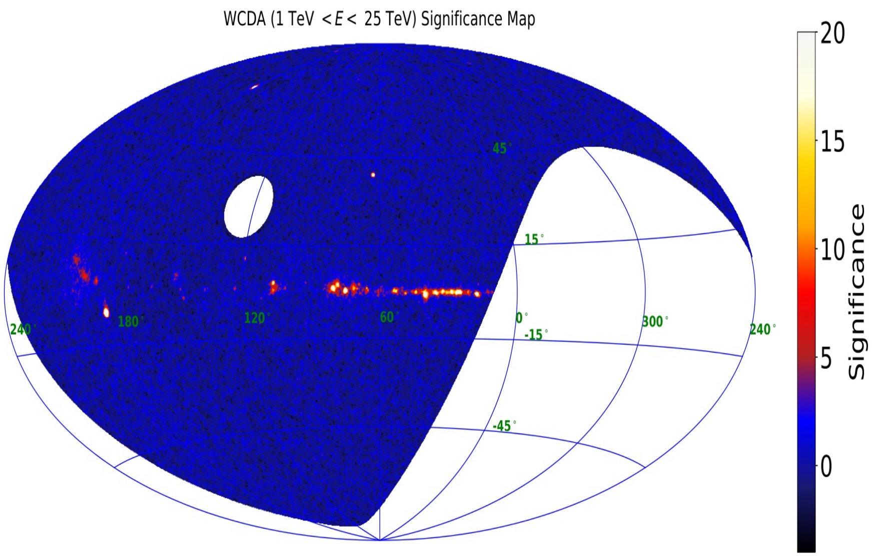

KM2A SED: power-law with a index of -3.0

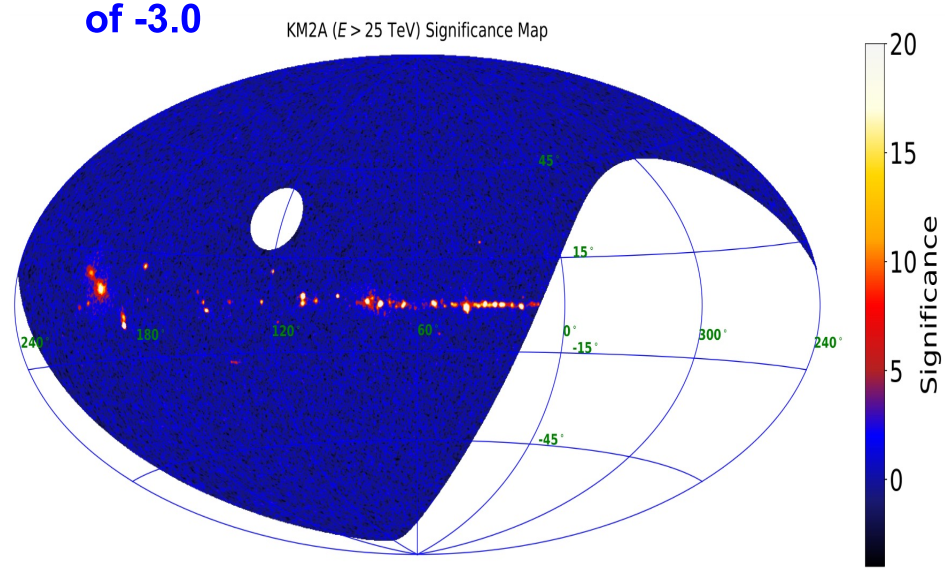

Features of WCDA and KM2A sources

- **WCDA detected 69 sources at >5σ (TS>37) and extension <2º**
- **KM2A detected 75 sources at >5σ (TS>37) and extension <2º**

Location uncertainty vs TS

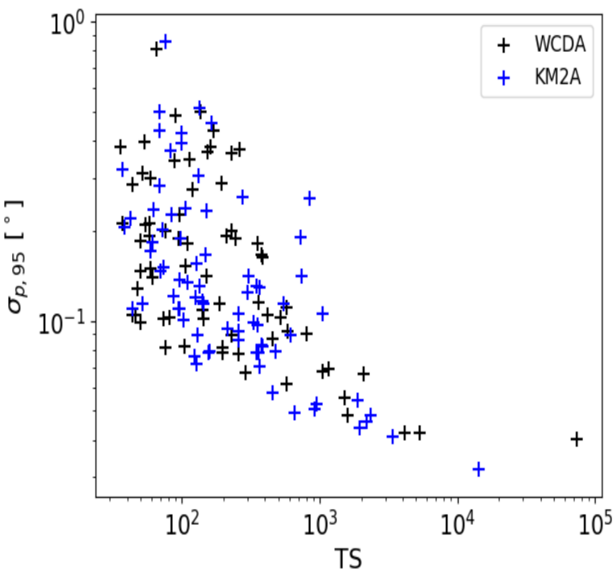

Source extension

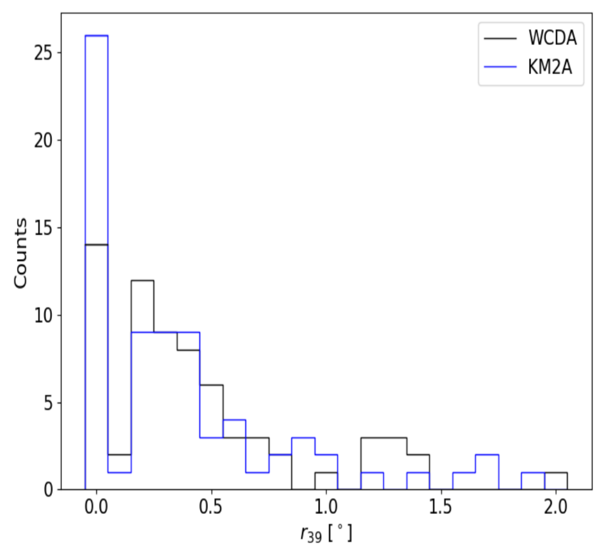

Spectral index

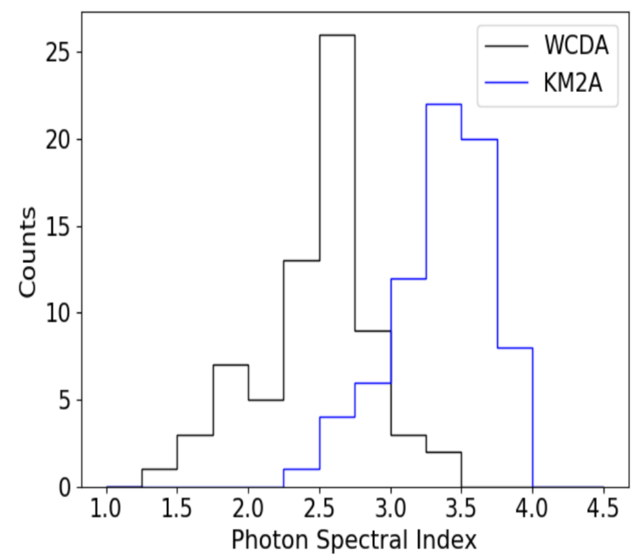

Construction of the 1st LHAASO sources

WCDA&KM2A

- Space Angle
- Position error
- Source extension

90 1st LHAASO sources

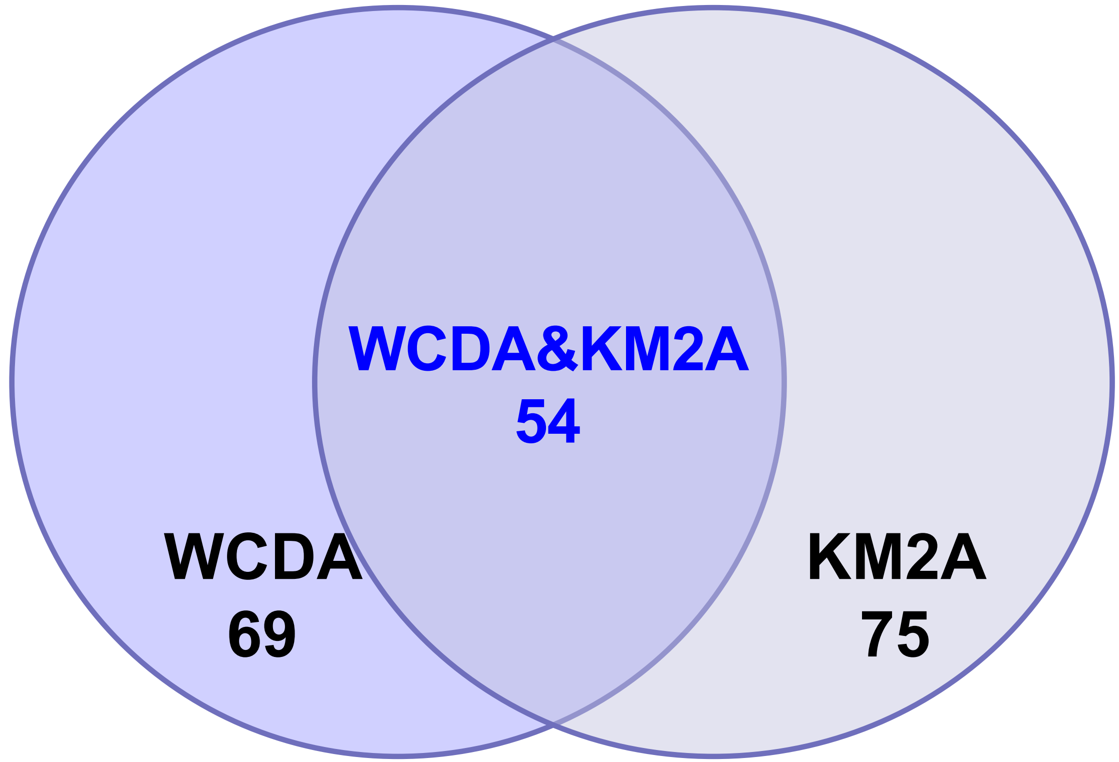

UHE gamma-ray sources

- The position and extension achieved by KM2A at >25 TeV are used.
- Sources with significance >4σ at >100 TeV are labeled as UHE sources

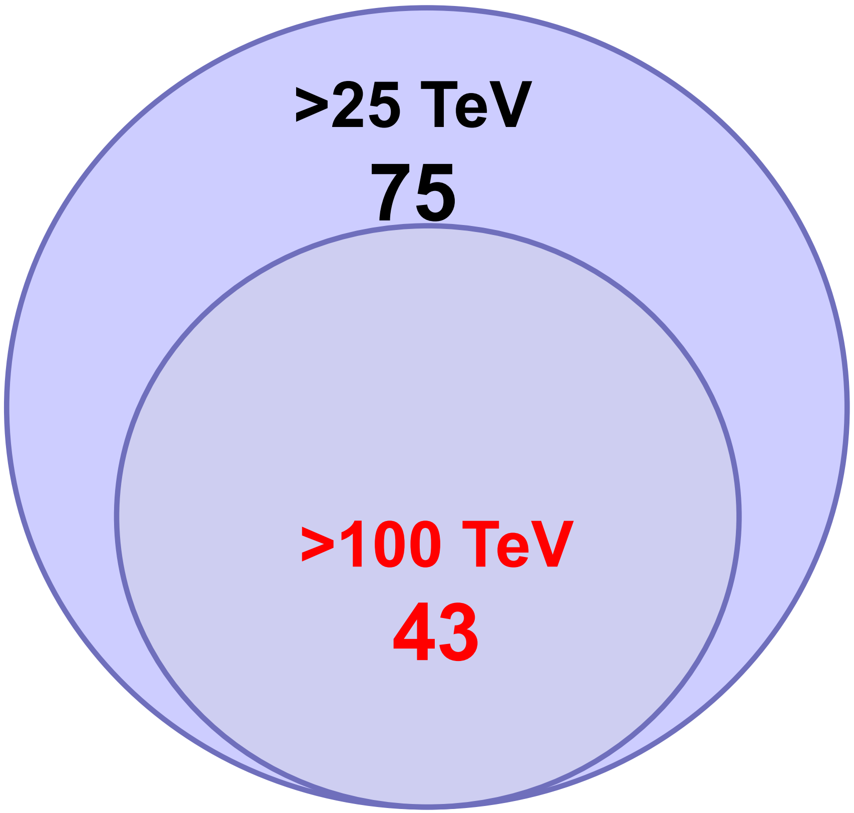

1^{st} LHAASO source catalog

Source name	Components	α_{2000}	δ_{2000}	$\sigma_{p,95,stat}$	r_{39}	TS	N_0	Γ	TS_{100}	Asso.(Sep.[°])
1LHAASO J0007+5659u	KM2A	1.86	57.00	0.12	<0.18	86.5	0.33±0.05	3.10±0.20	43.6	
	WCDA						<0.27			
1LHAASO J0007+7303u	KM2A	1.91	73.07	0.07	0.17±0.03	361.0	3.41±0.27	3.40±0.12	171.6	CTA 1 (0.12)
	WCDA	1.48	73.15	0.10	<0.22	141.6	5.01±1.11	2.74±0.11		
1LHAASO J0056+6346u	KM2A	14.10	63.77	0.08	0.24±0.03	380.2	1.47±0.10	3.33±0.10	94.1	
	WCDA	13.78	63.96	0.15	0.33±0.07	106.1	1.45±0.41	2.35±0.13		
1LHAASO J0206+4302u	KM2A	31.70	43.05	0.13	<0.27	96.0	0.24±0.03	2.62±0.16	82.8	
	WCDA						<0.09			
1LHAASO J0212+4254u	KM2A	33.01	42.91	0.20	<0.31	38.4	0.12±0.03	2.45±0.23	30.2	
	WCDA						<0.07			
1LHAASO J0216+4237u	KM2A	34.10	42.63	0.10	<0.13	102.0	0.18±0.03	2.58±0.17	65.6	
	WCDA						<0.20			
1LHAASO J0249+6022	KM2A	42.39	60.37	0.16	0.38±0.08	148.8	0.93±0.09	3.82±0.18		
	WCDA	41.52	60.49	0.40	0.71±0.10	53.3	1.96±0.51	2.52±0.16		
1LHAASO J0339+5307	KM2A	54.79	53.13	0.11	<0.22	144.0	0.58±0.06	3.64±0.16		LHAASO J0341+5258 (0.37)
	WCDA						<0.21			
1LHAASO J0343+5254u*	KM2A	55.79	52.91	0.08	0.20±0.02	388.1	1.07±0.07	3.53±0.10	20.2	LHAASO J0341+5258 (0.28)
	WCDA	55.34	53.05	0.18	0.33±0.05	94.1	0.29±0.13	1.70±0.19		

82 sources with the Galactic latitude |b|<12º

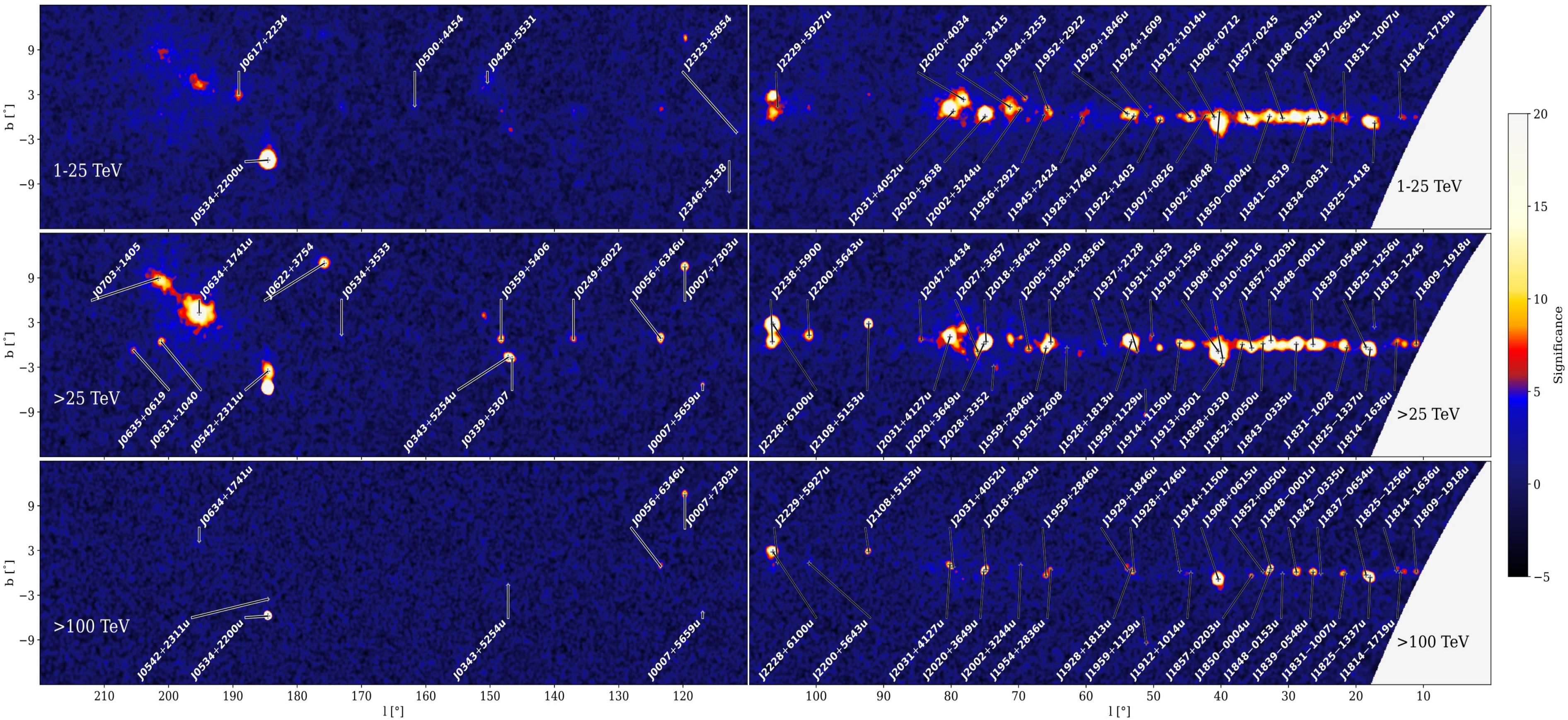

8 sources with the Galactic latitude |b|>12º

Mrk 421 z=0.031 | **1ES 1727+502** z=0.055 | **4 AGNs** | **Mrk 501** z=0.034 | **NGC 4278** z=0.002

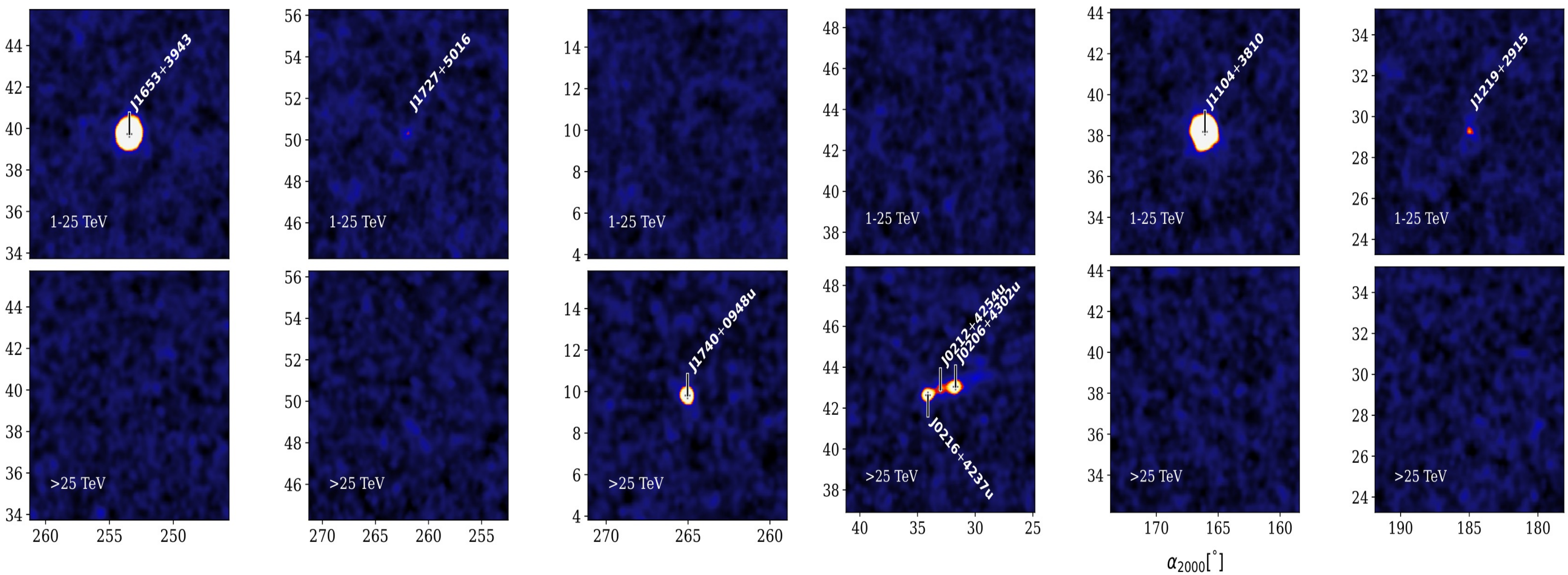

Association with known TeV Sources

- **58 sources with TeVCat+3HAWC association**
- **32 new sources (25+7)**

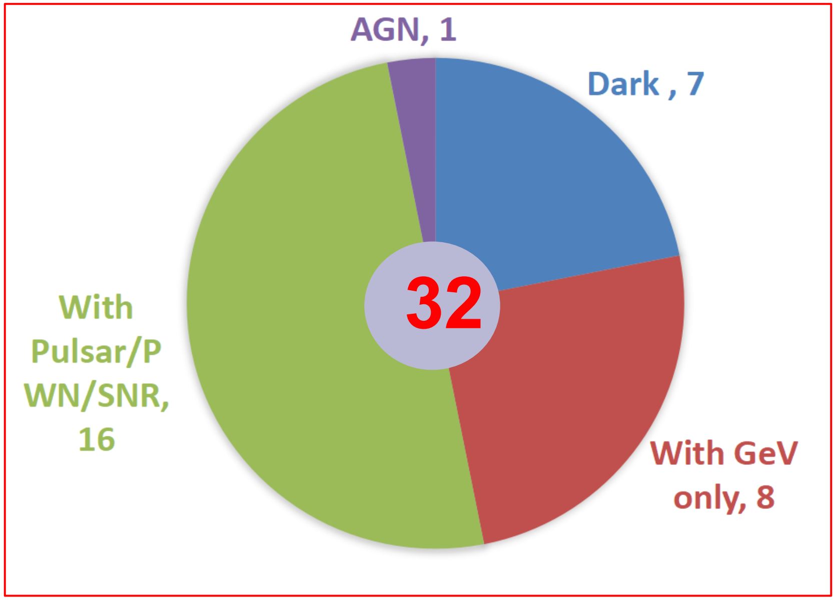

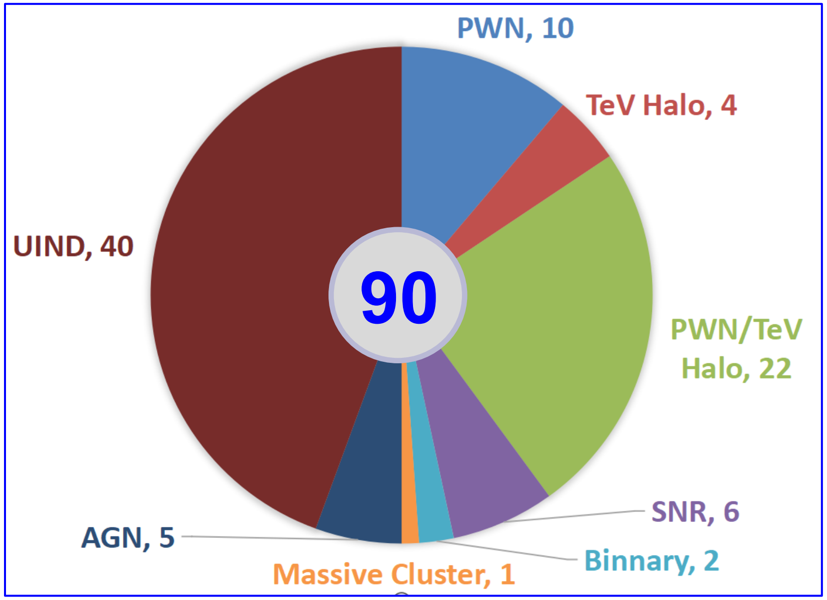

Association with ATNF pulsars

- 65 1LHAASO sources with pulsar nearby <0.5°.
- 35 associations with chance coincide probability <1%. (13 labeled as PWN or Halo in TeVCat)
- 22 new possible PWN/TeV Halo

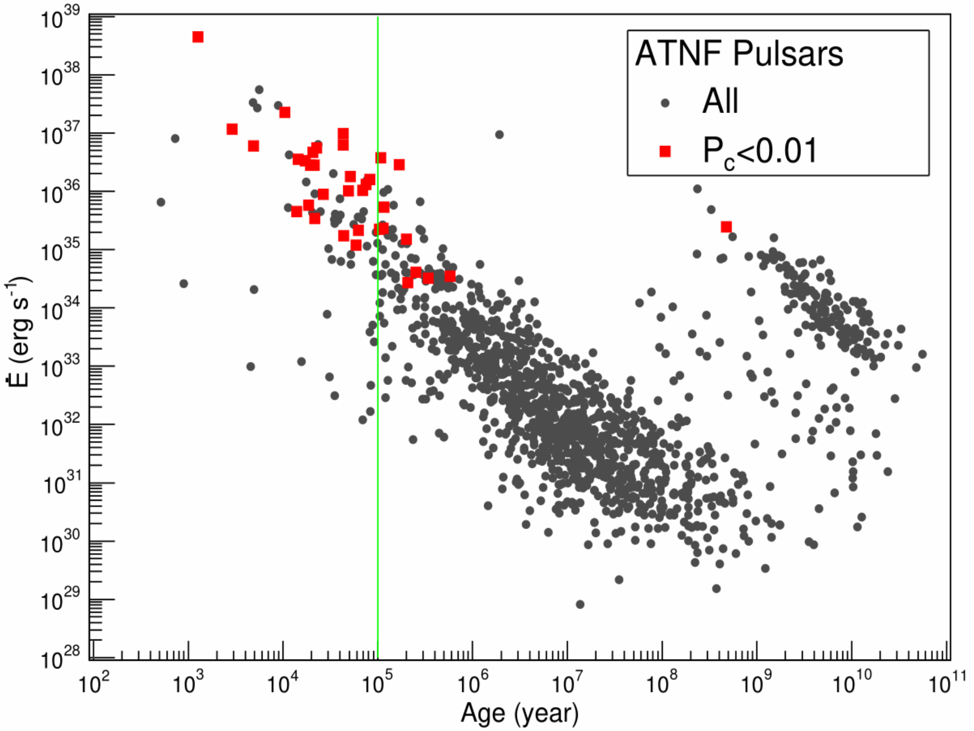

PeVatrons

- 51% (35/69) 1-25TeV sources are UHE sources.
- 57% (43/75) >25TeV sources are UHE sources.
- 19% (8/43) UHE sources are not detected at 1-25TeV (new class?).

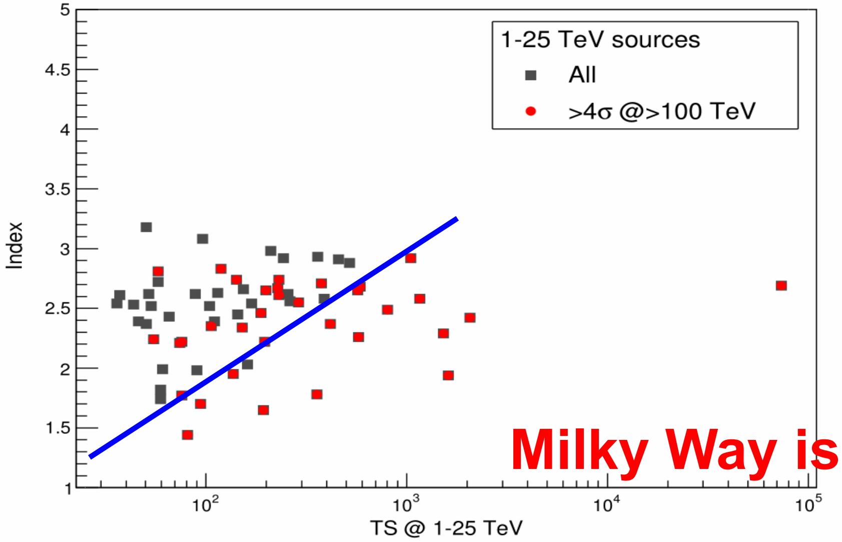

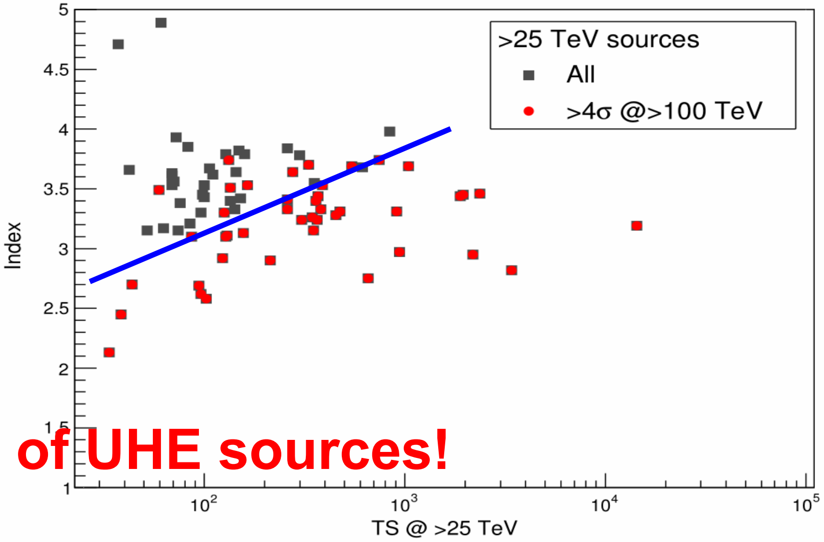

Milky Way is full of UHE sources!

1 LHAASO catalog

- **90 in 1st LHAASO sources.**
- **32 new discoveries**
- **43 UHE**

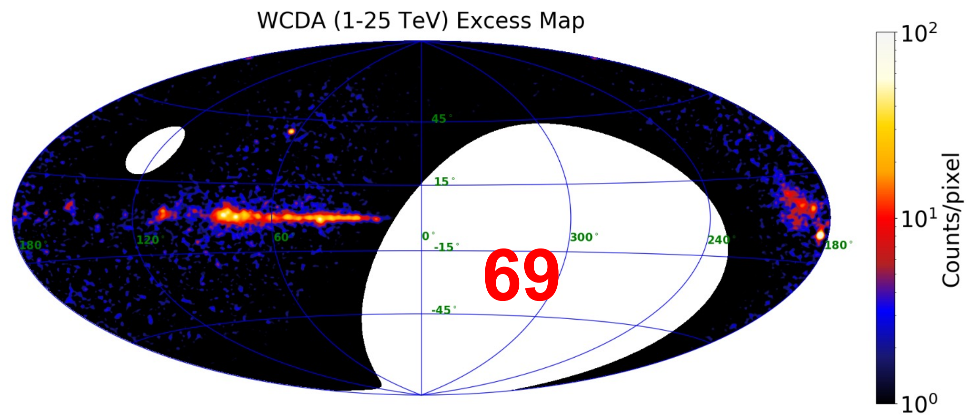

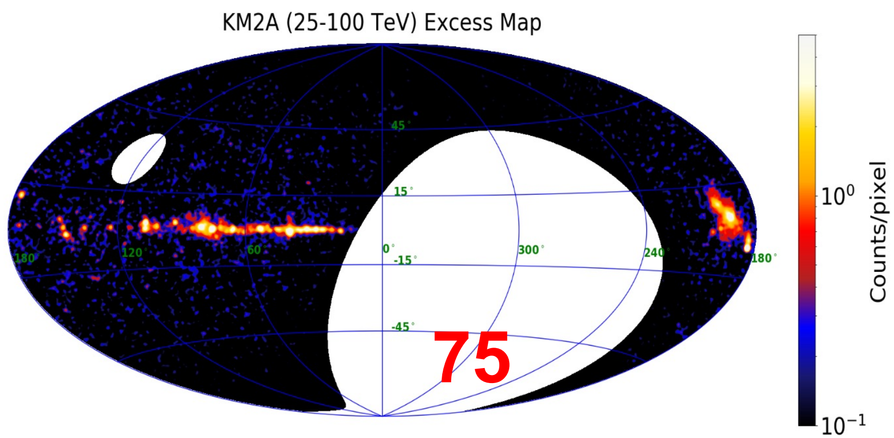

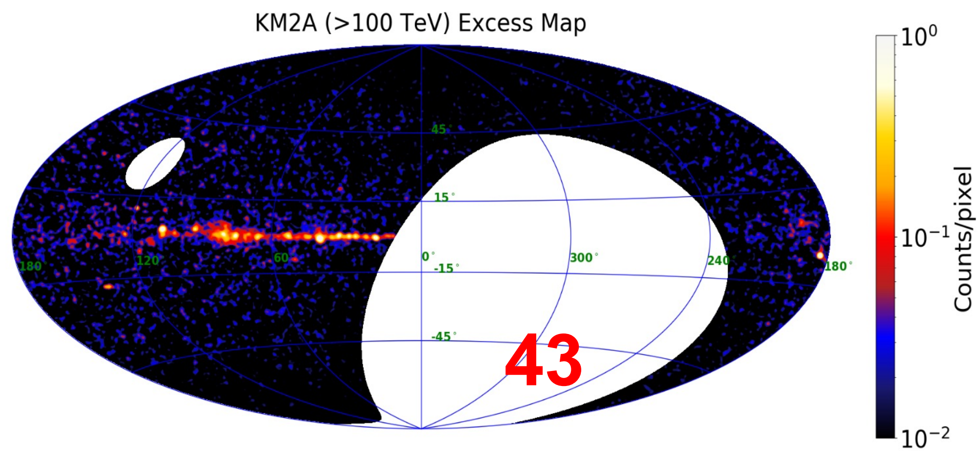

Pulsar Wind Nebulas

based on talk of Ruoyu Liu

Pulsars as Counterparts of VHE gamma-ray sources

Pulsars – the most commonly potential counterparts of detected VHE gamma-ray emitter

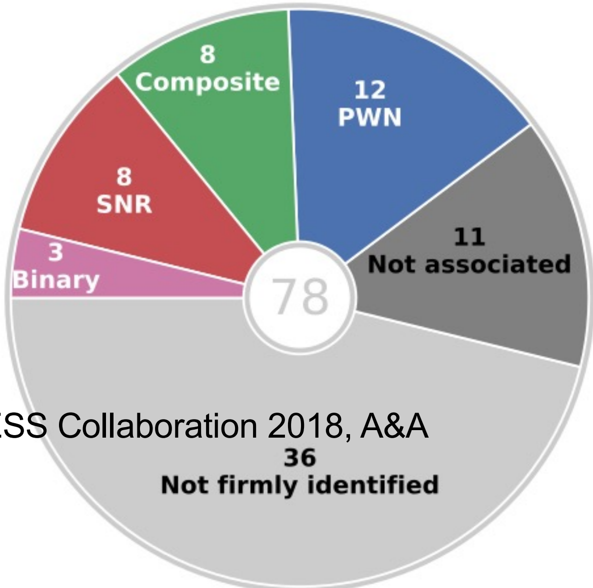

HESS Collaboration 2018, A&A

14 firmly identified PWN by HESS

HGPS name	ATNF name	Canonical name	lg $\dot{E}$	τ_c (kyr)	d (kpc)	PSR offset (pc)	Γ	R_{PWN} (pc)	$L_{1-10\,TeV}$ (10^{33} erg s^{-1})
J1813−178[1]	J1813−1749		37.75	5.60	4.70	<2	2.07 ± 0.05	4.0 ± 0.3	19.0 ± 1.5
J1833−105	J1833−1034	G21.5−0.9[2]	37.53	4.85	4.10	<2	2.42 ± 0.19	<4	2.6 ± 0.5
J1514−591	B1509−58	MSH 15−52[3]	37.23	1.56	4.40	<4	2.26 ± 0.03	11.1 ± 2.0	52.1 ± 1.8
J1930+188	J1930+1852	G54.1+0.3[4]	37.08	2.89	7.00	<10	2.6 ± 0.3	<9	5.5 ± 1.8
J1420−607	J1420−6048	Kookaburra (K2)[5]	37.00	13.0	5.61	5.1 ± 1.2	2.20 ± 0.05	7.9 ± 0.6	44 ± 3
J1849−000	J1849−0001	IGR J18490−0000[6]	36.99	42.9	7.00	<10	1.97 ± 0.09	11.0 ± 1.9	12 ± 2
J1846−029	J1846−0258	Kes 75[2]	36.91	0.728	5.80	<2	2.41 ± 0.09	<3	6.0 ± 0.7
J0835−455	B0833−45	Vela X[7]	36.84	11.3	0.280	2.37 ± 0.18	1.89 ± 0.03	2.9 ± 0.3	0.83 ± 0.11*
J1837−069[8]	J1838−0655		36.74	22.7	6.60	17 ± 3	2.54 ± 0.04	41 ± 4	204 ± 8
J1418−609	J1418−6058	Kookaburra (Rabbit)[5]	36.69	10.3	5.00	7.3 ± 1.5	2.26 ± 0.05	9.4 ± 0.9	31 ± 3
J1356−645[9]	J1357−6429		36.49	7.31	2.50	5.5 ± 1.4	2.20 ± 0.08	10.1 ± 0.9	14.7 ± 1.4
J1825−137[10]	B1823−13		36.45	21.4	3.93	33 ± 6	2.38 ± 0.03	32 ± 2	116 ± 4
J1119−614	J1119−6127	G292.2−0.5[11]	36.36	1.61	8.40	<11	2.64 ± 0.12	14 ± 2	23 ± 4
J1303−631[12]	J1301−6305		36.23	11.0	6.65	20.5 ± 1.8	2.33 ± 0.02	20.6 ± 1.7	96 ± 5

Among the 47 sources not yet identified, most of them (36) have possible associations with cataloged objects, notably PWNe and energetic pulsars that could power VHE PWN. —— HGPS

We have presented the third catalog of steady gamma-ray emitters detected by HAWC using 1523 days of data. The catalog consists of 65 sources, including two blazars. The most abundant source class among the potential counterpart of HAWC sources in the Galactic plane is pulsars (56). —— 3HWC (HAWC Collaboration 2020, ApJ)

From PWN to Pulsar Halos

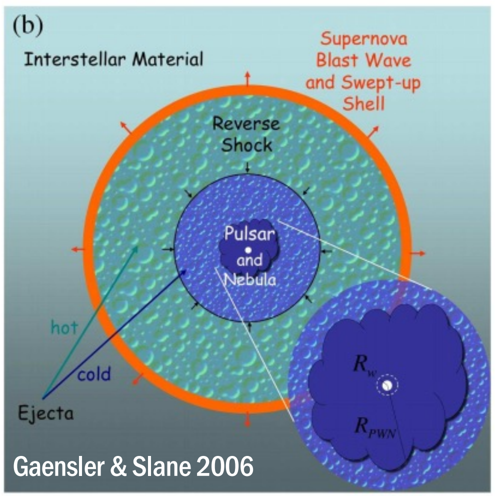

Gaensler & Slane 2006

Conservation of Momentum: Natal kick velocity: 400-500 km/s

$$t_{cross} = 44\left(\frac{E_{SN}}{10^{51}\mathrm{ergs}}\right)^{1/3}\left(\frac{n_0}{1\ \mathrm{cm}^{-3}}\right)^{-1/3}\left(\frac{V_{\mathrm{PSR}}}{500\ \mathrm{km\ s}^{-1}}\right)^{-5/3}\ \mathrm{kyr}.$$

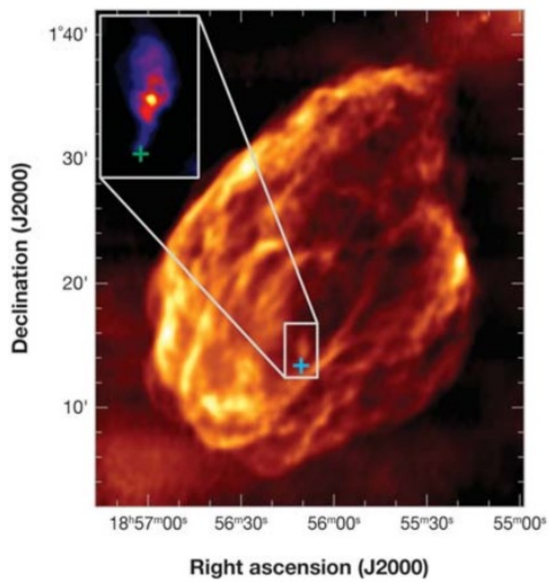

Giacani et al. 1997 Frail et al. 1996

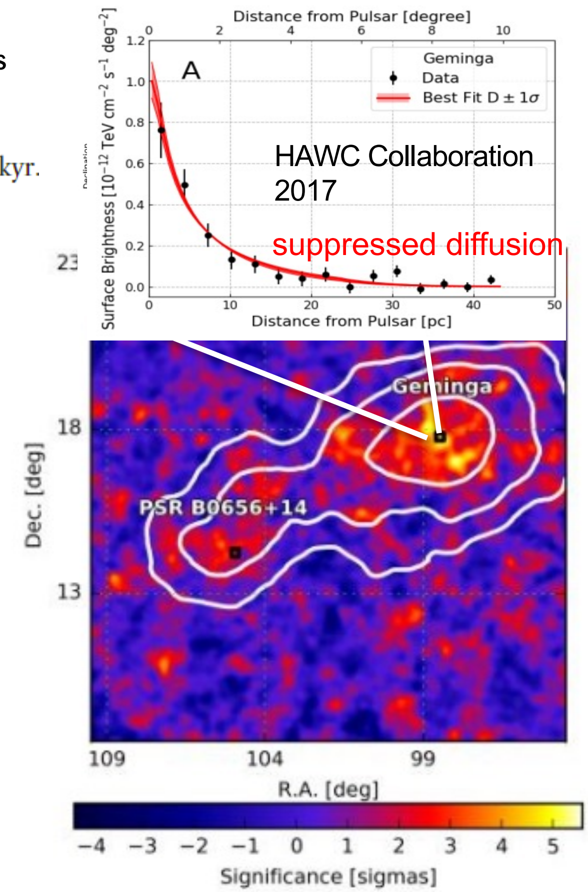

Three Evolution Stages

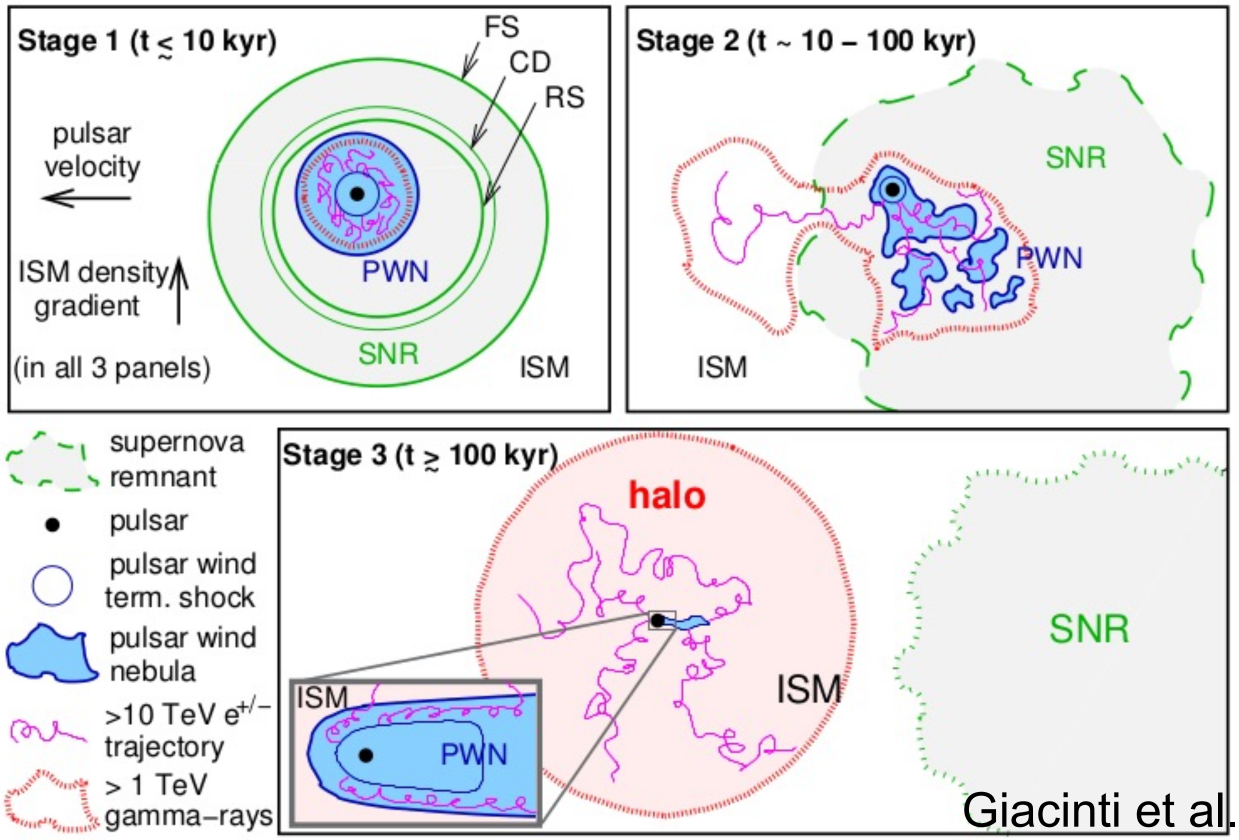

Giacinti et al. 2020

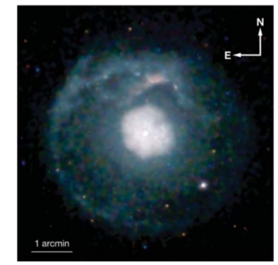

SNR G21.5-0.9
PSR J1833-1034

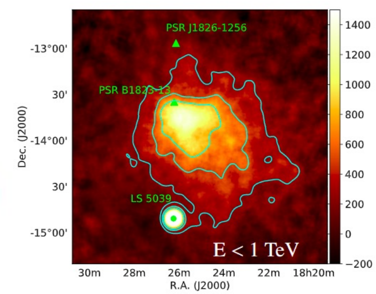

HESS J1825-137
PSR J1826-1334

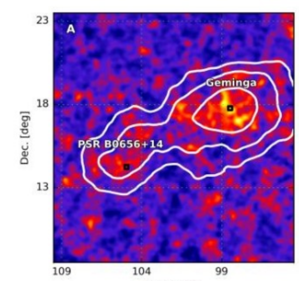

Geminga
Monogem

1LHAASO Catalogue

35 sources associated with pulsars with $\dot{E} > 10^{34} \mathrm{erg/s}$ at a chance probablity <1%
(65 have ≥1 pulsar within 0.5 deg)

Source name	PSR name	dist.(°)	Distance (kpc)	τ_c (kyr)	$\dot{E}$ (ergs/s)	P_c	Identified type in TeVCat
1LHAASO J0007+7303u	PSR J0007+7303	0.05	1.40	14	4.5e+35	7.3e-05	PWN
1LHAASO J0216+4237u	PSR J0218+4232	0.33	3.15	476000	2.4e+35	3.6e-03	
1LHAASO J0249+6022	PSR J0248+6021	0.16	2.00	62	2.1e+35	1.5e-03	
1LHAASO J0359+5406	PSR J0359+5414	0.15	-	75	1.3e+36	7.2e-04	
1LHAASO J0534+2200u	PSR J0534+2200	0.01	2.00	1	4.5e+38	3.2e-06	PWN
1LHAASO J0542+2311u	PSR J0543+2329	0.30	1.56	253	4.1e+34	8.3e-03	
1LHAASO J0622+3754	PSR J0622+3749	0.09	-	208	2.7e+34	2.5e-04	PWN/TeV Halo
1LHAASO J0631+1040	PSR J0631+1037	0.11	2.10	44	1.7e+35	3.5e-04	PWN
1LHAASO J0634+1741u	PSR J0633+1746	0.12	0.19	342	3.3e+34	1.3e-03	PWN/TeV Haloa
1LHAASO J0635+0619	PSR J0633+0632	0.39	1.35	59	1.2e+35	9.4e-03	
1LHAASO J1740+0948u	PSR J1740+1000	0.21	1.23	114	2.3e+35	1.4e-03	
1LHAASO J1809-1918u	PSR J1809-1917	0.05	3.27	51	1.8e+36	6.2e-04	
1LHAASO J1813-1245	PSR J1813-1245	0.01	2.63	43	6.2e+36	6.3e-06	
1LHAASO J1825-1256u	PSR J1826-1256	0.09	1.55	14	3.6e+36	1.6e-03	
1LHAASO J1825-1337u	PSR J1826-1334	0.11	3.61	21	2.8e+36	2.8e-03	PWN/TeV Halo
1LHAASO J1837-0654u	PSR J1838-0655	0.12	6.60	23	5.6e+36	2.2e-03	PWN
1LHAASO J1839-0548u	PSR J1838-0537	0.20	-	5	6.0e+36	6.1e-03	
1LHAASO J1848-0001u	PSR J1849-0001	0.06	-	43	9.8e+36	1.2e-04	PWN
1LHAASO J1857+0245	PSR J1856+0245	0.16	6.32	21	4.6e+36	3.1e-03	PWN
1LHAASO J1906+0712	PSR J1906+0722	0.19	-	49	1.0e+36	5.9e-03	
1LHAASO J1908+0615u	PSR J1907+0602	0.23	2.37	20	2.8e+36	6.8e-03	
1LHAASO J1912+1014u	PSR J1913+1011	0.13	4.61	169	2.9e+36	1.5e-03	
1LHAASO J1914+1150u	PSR J1915+1150	0.09	14.01	116	5.4e+35	1.8e-03	
1LHAASO J1928+1746u	PSR J1928+1746	0.04	4.34	83	1.6e+36	1.6e-04	
1LHAASO J1929+1846u	PSR J1930+1852	0.29	7.00	3	1.2e+37	2.6e-03	PWN
1LHAASO J1954+2836u	PSR J1954+2836	0.01	1.96	69	1.1e+36	1.6e-05	PWN
1LHAASO J1954+3253	PSR J1952+3252	0.33	3.00	107	3.7e+36	6.7e-03	
1LHAASO J1959+2846u	PSR J1958+2845	0.10	1.95	22	3.4e+35	2.8e-03	PWN
1LHAASO J2005+3415	PSR J2004+3429	0.25	10.78	18	5.8e+35	9.9e-03	
1LHAASO J2005+3050	PSR J2006+3102	0.20	6.04	104	2.2e+35	9.2e-03	
1LHAASO J2020+3649u	PSR J2021+3651	0.05	1.80	17	3.4e+36	1.5e-04	PWN
1LHAASO J2028+3352	PSR J2028+3332	0.36	-	576	3.5e+34	8.0e-03	
1LHAASO J2031+4127u	PSR J2032+4127	0.08	1.33	201	1.5e+35	1.0e-03	PWN
1LHAASO J2228+6100u	PSR J2229+6114	0.27	3.00	10	2.2e+37	2.2e-03	PWN
1LHAASO J2238+5900	PSR J2238+5903	0.07	2.83	27	8.9e+35	3.0e-04	

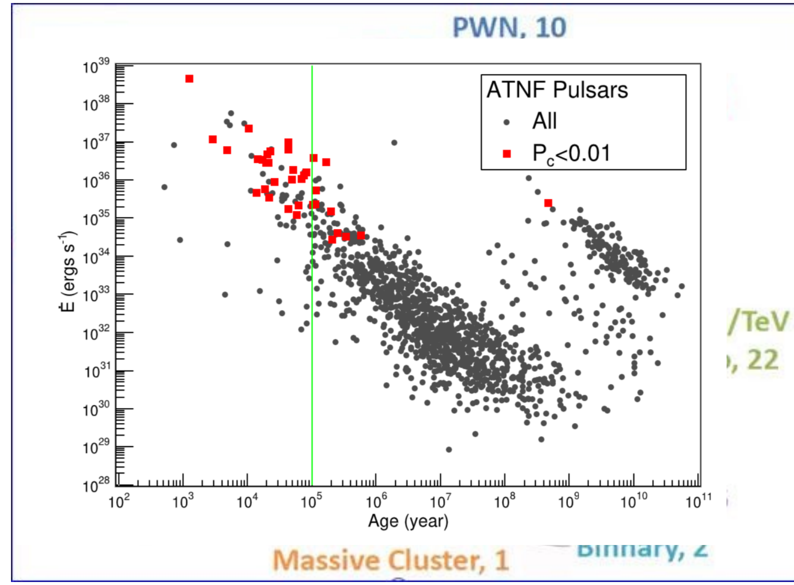

$$P_c = 1 - e^{r^2/r_0^2} \qquad r_0 = [\pi \rho(\dot{E})]^{-1/2}$$

$$|b - b_c| < 2.5^\circ \ \& \ |l - l_c| < 10^\circ$$

Crab: PWN as a Super-PeVatron of protons?

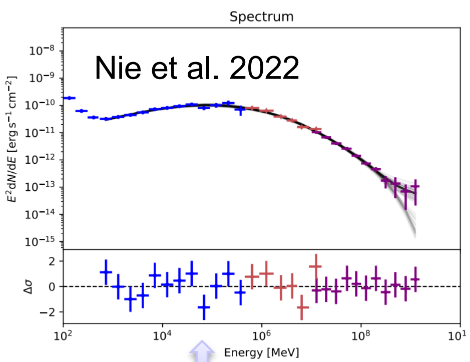

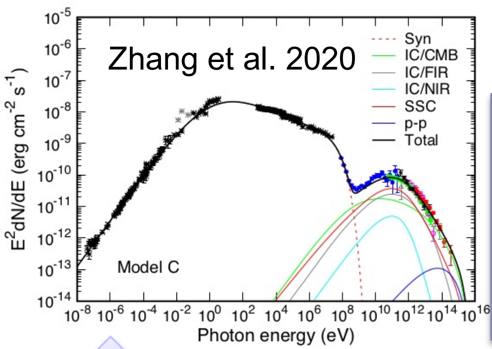

Estimation with a leaky box model

$$F(E_p) = \frac{c}{4\pi}\frac{\eta_p L_{s,\mathrm{tot}} t_{\mathrm{esc}}}{2\pi R_{\mathrm{Gal}}^2 H_{\mathrm{CR}} \ln(E_{p,\max}/E_{p,\min})}$$
$$\approx 2\times 10^3 \left(\frac{f_{\mathrm{pul}}\eta_p L_{s,\mathrm{tot}}}{10^{39}\,\mathrm{erg\ s^{-1}}}\right)\left(\frac{E_p}{10\,\mathrm{PeV}}\right)^{-1/3} \times \left(\frac{H_{\mathrm{CR}}}{4\,\mathrm{kpc}}\right)\left(\frac{R_{\mathrm{Gal}}}{15\,\mathrm{kpc}}\right)^{-2} \mathrm{eV\ cm^{-2}s^{-1}sr^{-1}}$$

Lepto-Hadronic fitting

$W_p \sim 1\%\ W_{rot}$ inside the nebula

Considering escape

$W_p \sim (10\text{-}50)\%$

may account for 10-100PeV protons if each pulsars can accelerate protons >10PeV when they were young

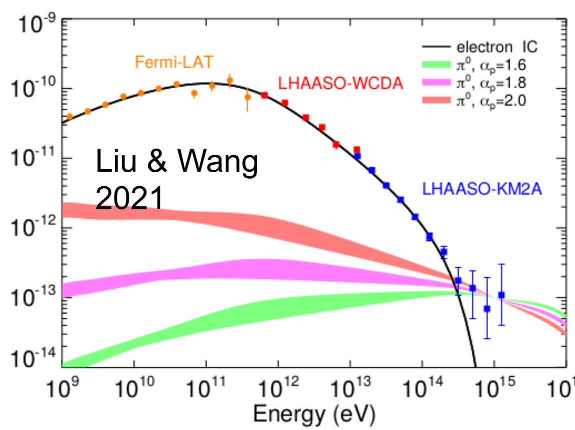

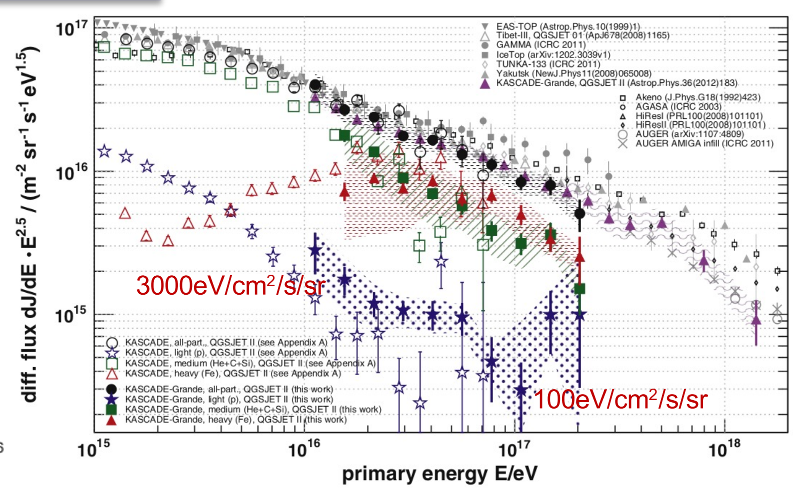

KASCADE-Grande Collaboration 2014

LHAASO J0621+3755

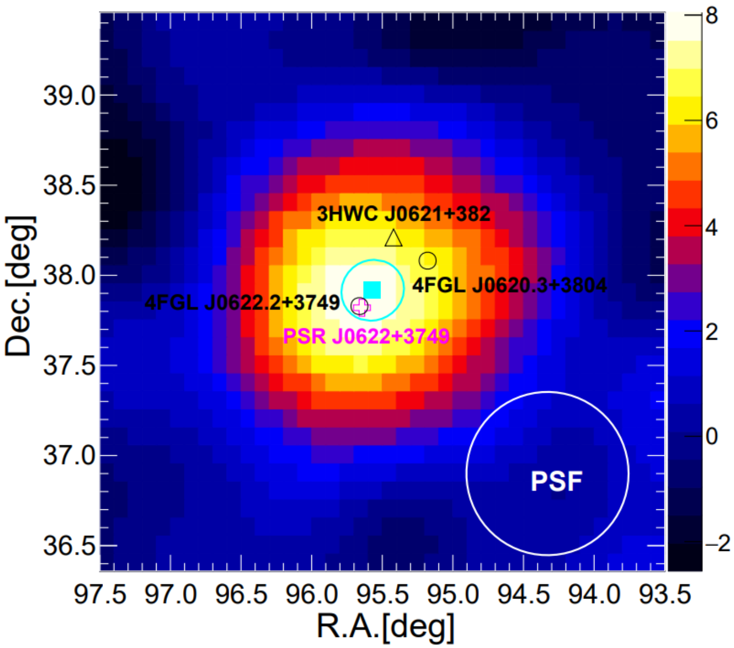

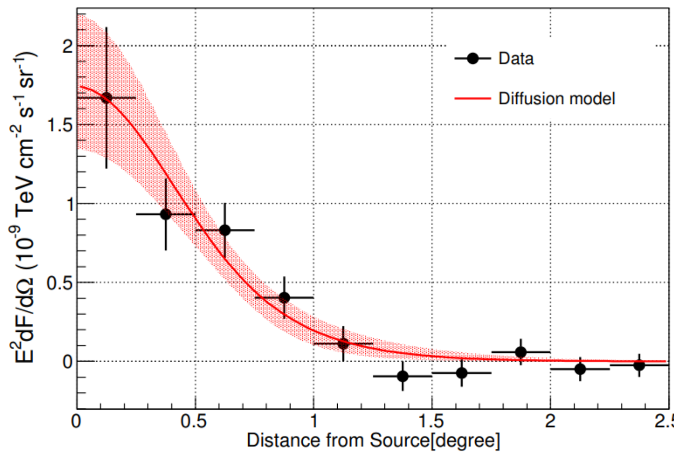

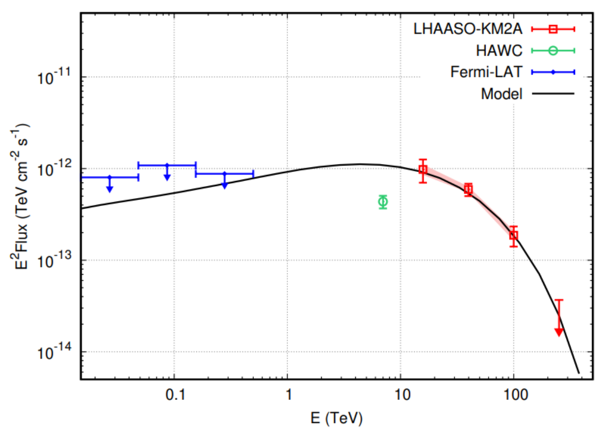

$D \approx (8.9\,^{+4.5}_{-3.9})\ \mathrm{x}10^{27}(d/1.6\ \mathrm{kpc})^2\ \mathrm{cm}^2\mathrm{s}^{-1}$ for $E_e \sim 160$ TeV

LHAASO Collaboration 2021, PRL

Highlight Talks in PWN/Pulsar Halos by LHAASO

Renfeng Xu's talk

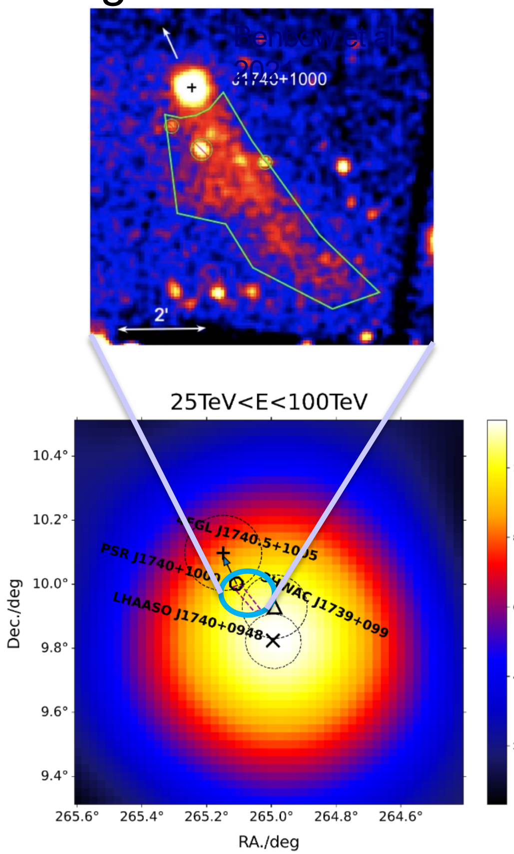

Dr. Zhe Li's talk

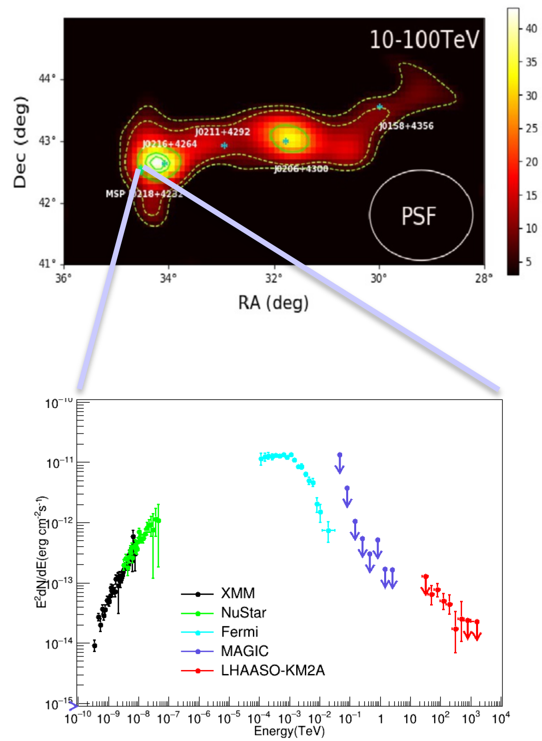

Dr. Yingying Guo's talk

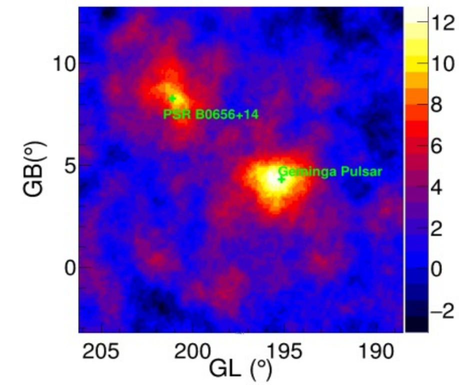

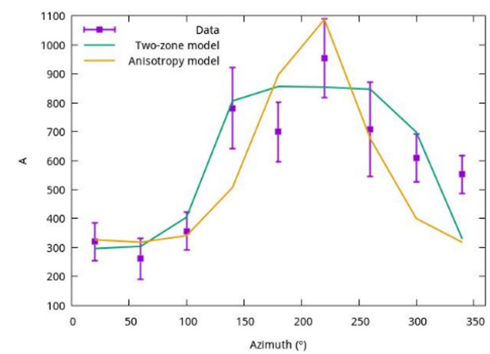

Super Nova Remnants

based on talk of
Siming Liu

Origin of Cosmic Rays

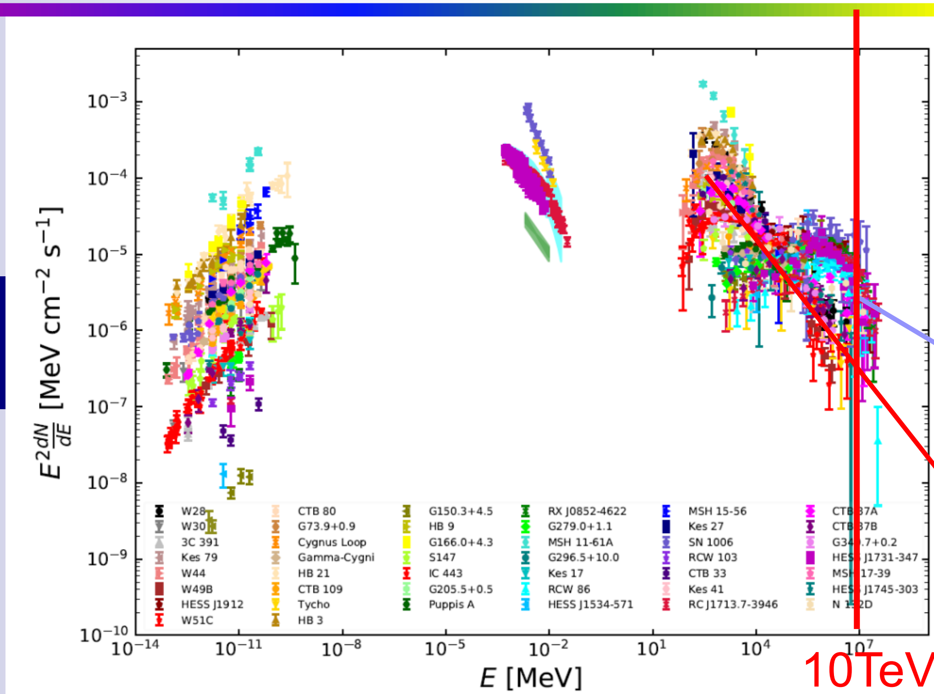

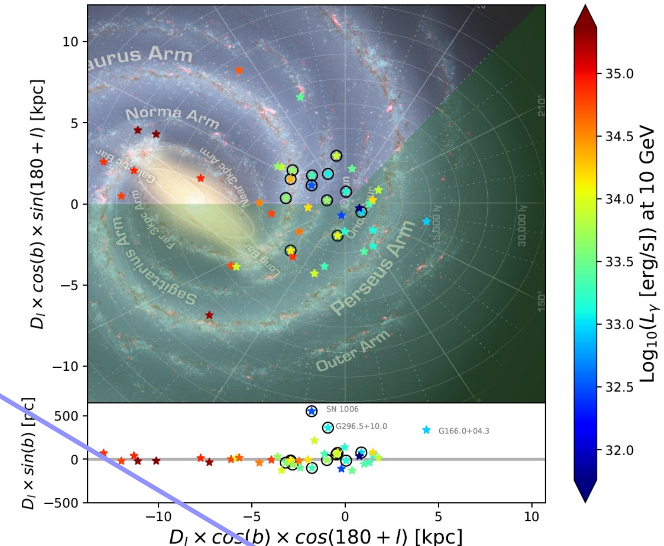

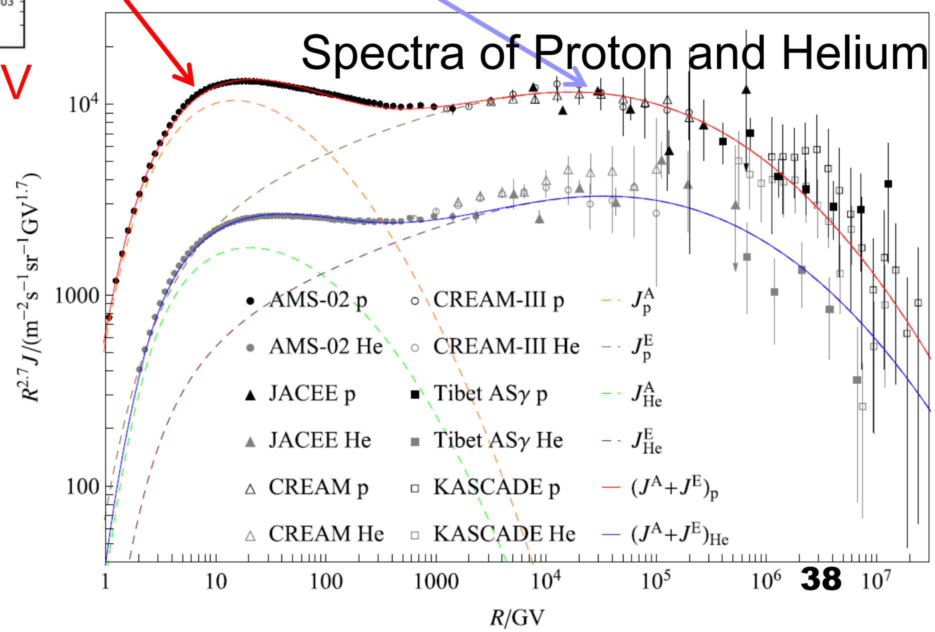

Multiwavelength spectra of 44 SNRs normalized at 100 GeV and their distribution in the

Reviews of Modern Plasma Physics (2022) 6:19
https://doi.org/10.1007/s41614-022-00080-6

REVIEW PAPER

The origin of galactic cosmic rays

Siming Liu[1] · Houdun Zeng[2,4] · Yuliang Xin[1] · Yiran Zhang[3]

LHAASO

7 SNRs Detected by LHAASO

Cas A; IC 443; W51C; Gamma-Cygni; G106.3+2.7; G69.7+1.0; G150.3+4.5

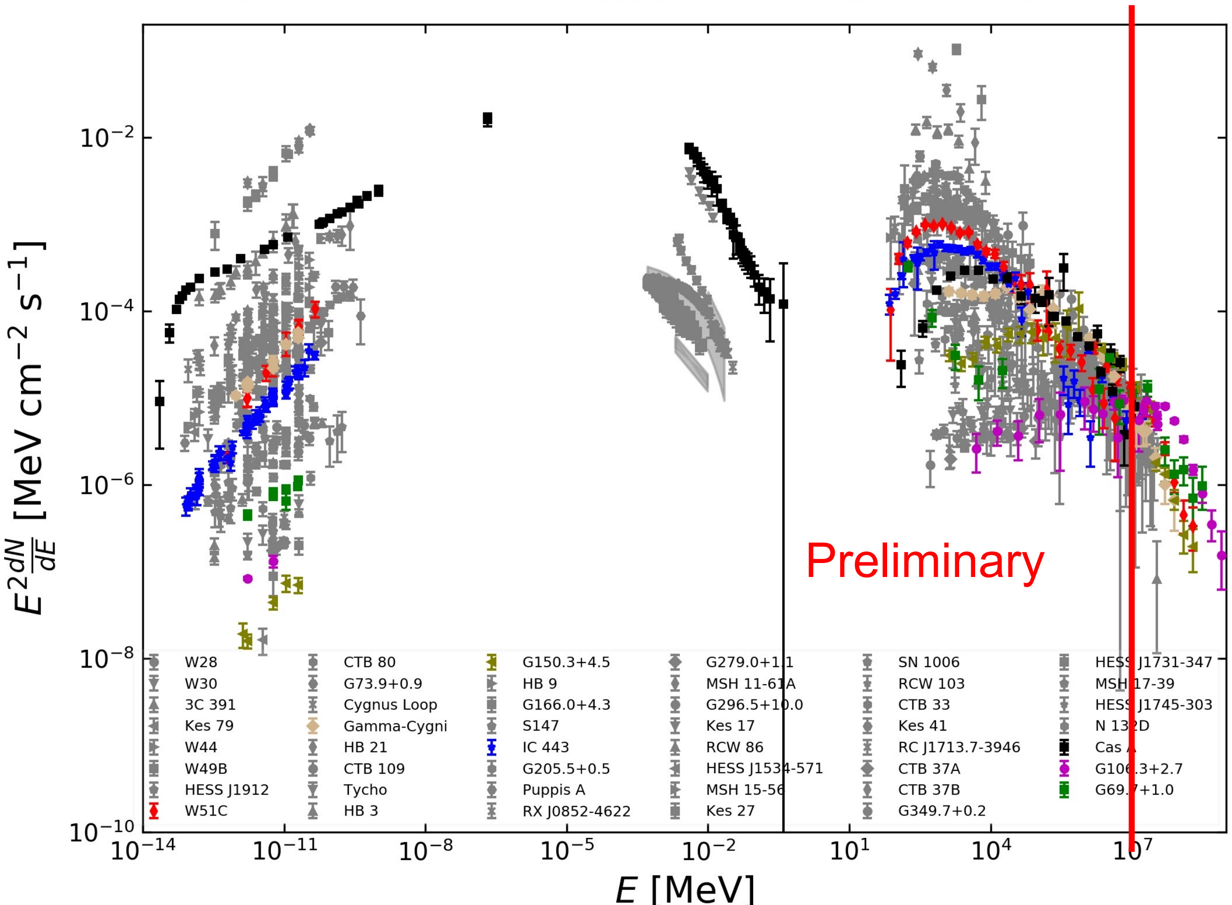

The higher energy spectra are softer (but harder than an exponential cutoff)

ϒ Cygni SNR

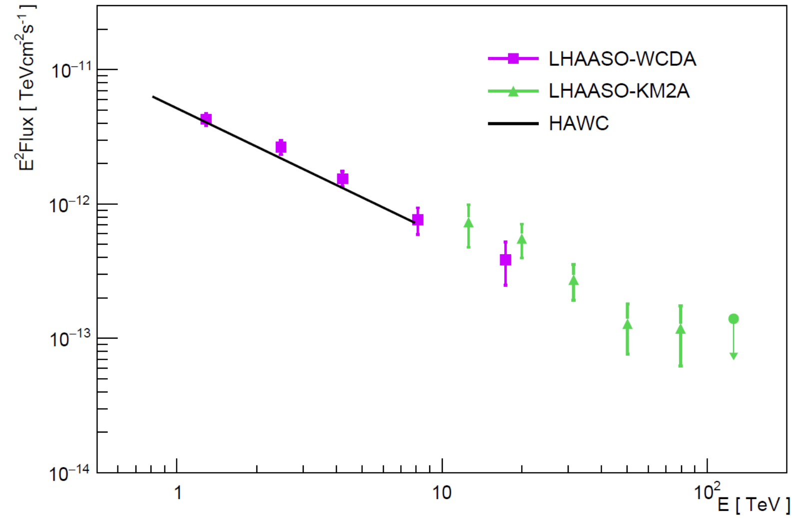

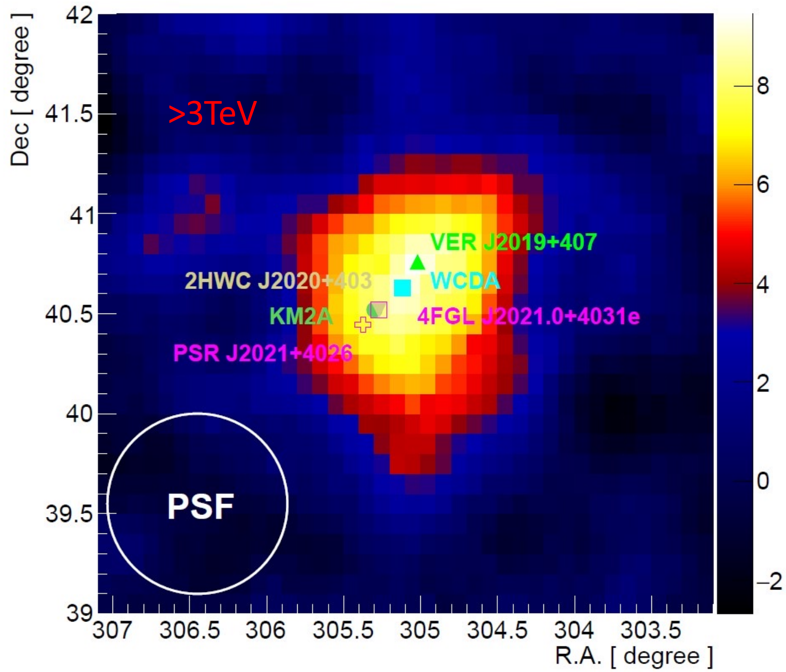

- gaussian： sigma = 0.374 +/- 0.040
- disk： radius = 0.592 +/- 0.056

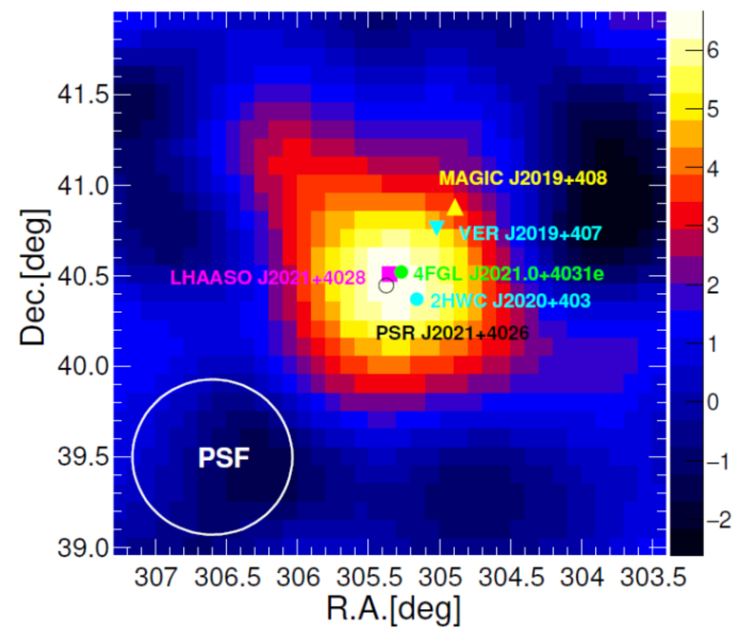

2: Hadronic vs Leptonic Models

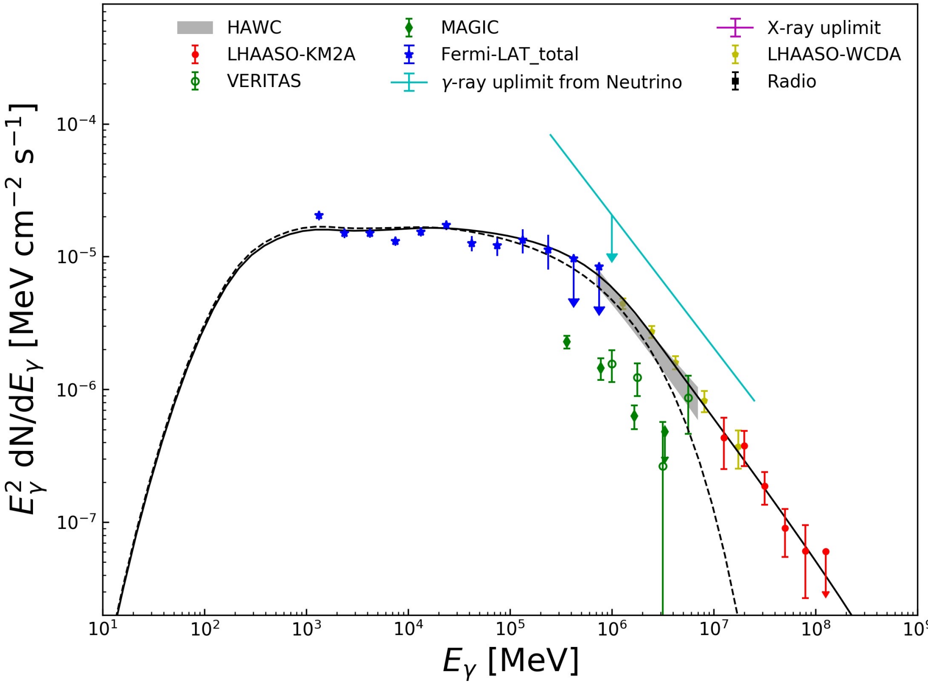

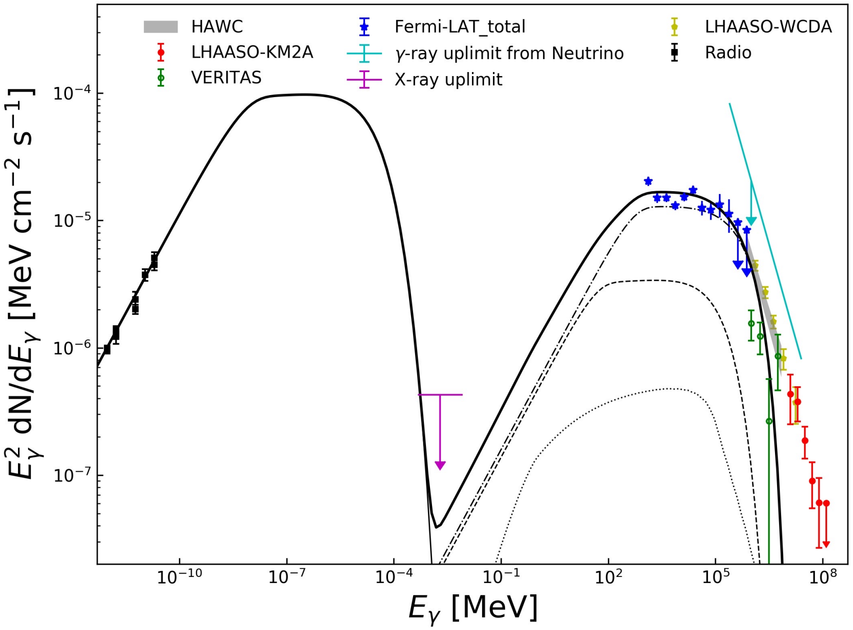

Hadronic with
an exponential cutoff of 10TeV (dotted)
a break at 4TeV (solid)
Index 2.1->3.1

Zeng et al. ApJ, 910, 78, (2021)

Leptonic with a ~17 μG B

Liu et al. RMPP, 6, 19, (2022)

Star Clusters

based on talk of

Ruizhi Yang

YMSC IN OUR GALAXY

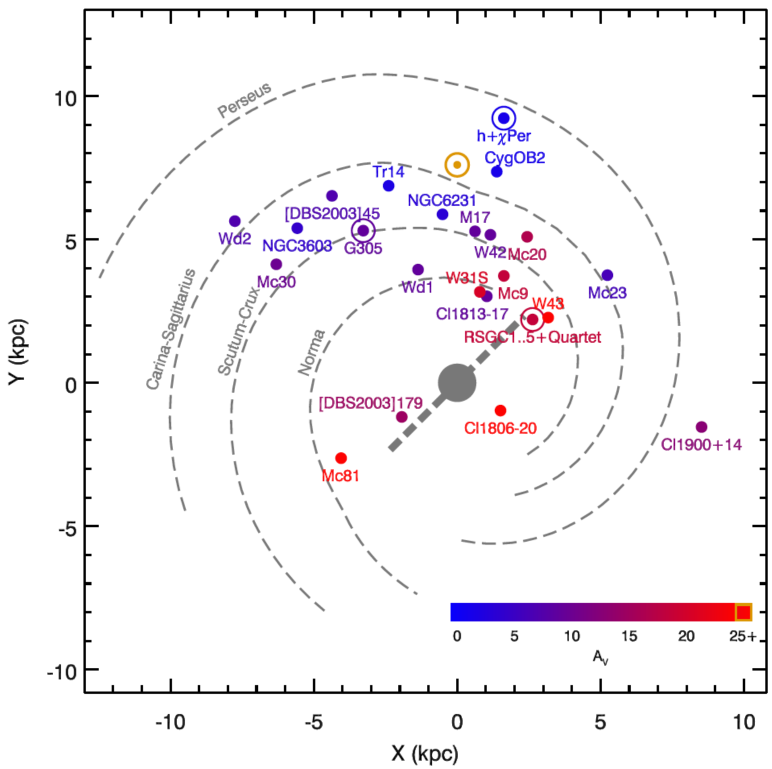

Davies et.al 2011

- ~20 in our Galaxy
- More to be discovered (high extinction in Galactic plane)

Stellar type	log[$\dot{M}$] $M_\odot$ yr^{-1}	V_∞ [km s^{-1}]
WNL	-4.2	1650
WNE	-4.5	1900
WC6-9	-4.4	1800
WC4-5	-4.7	2800
WO	-5.0	3500
O3	-5.2	3190
O4	-5.4	2950
O4.5	-5.5	2900
O5	-5.6	2875

- The wind power of a single young star can be as high as 1e37 erg/s

Gamma-ray emitting YMSC

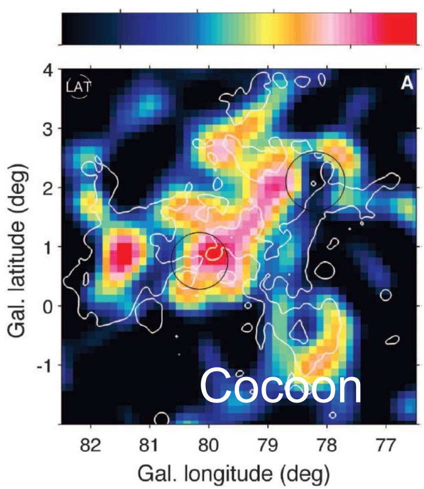

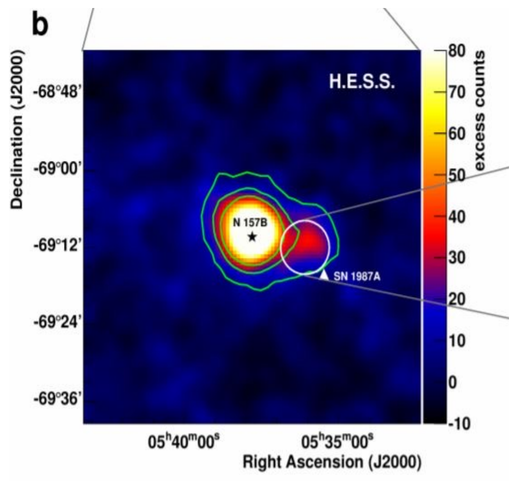

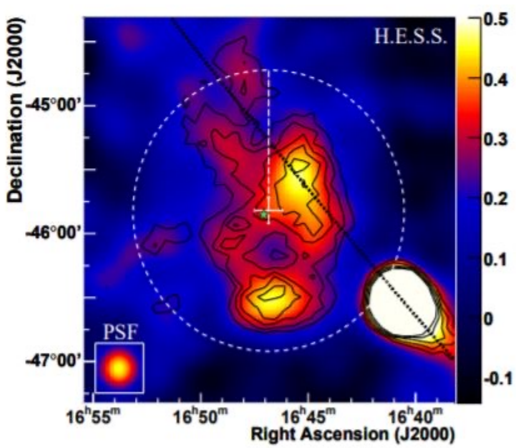

New GAMMA-RAY Source population:

Cygnus Cocoon(GeV-TeV)[Fermi 2012, HAWC2022]
Westerlund 1 (TeV) [HESS collaboration 2012]
Westerlund 2 (GeV, TeV？)[Yang et.al 2018]
NGC 3603 (GeV, TeV)[Yang et.al 2017]
W43 (GeV, TeV?) [Yang et.al 2020]
W40 (GeV) [Sun et.al 2019]
G25/RSGC 1[Sun et.al 2020]
Carina nebular [Ge et.al 2022]
M17 [Liu et.al 2022]

LHAASO VIEW ON CYGNUS

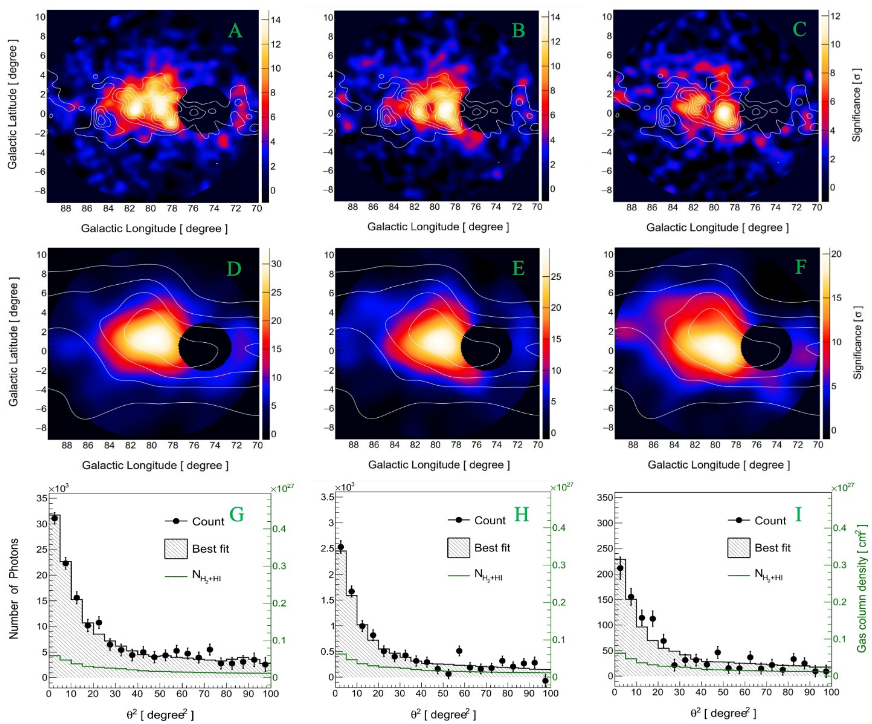

Huge bubble beyond ~10 degrees (200 pc)

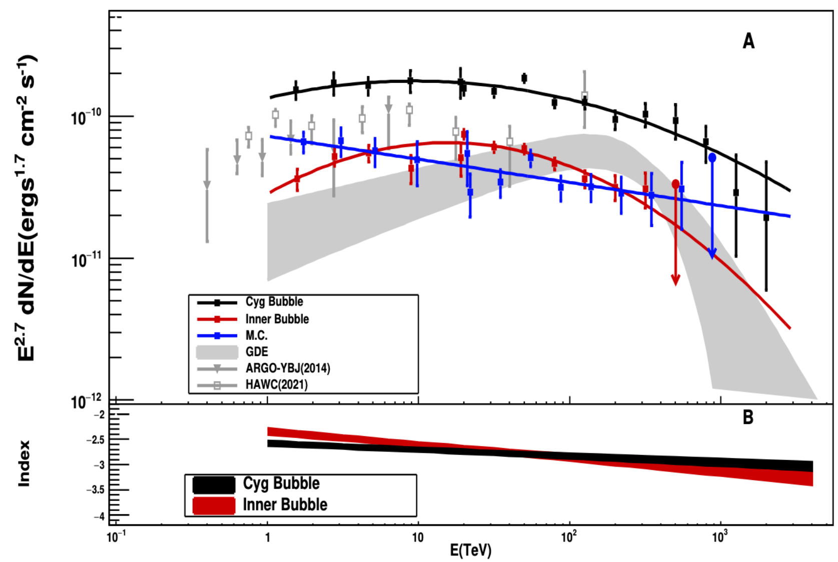

Curved and uniform spectral shape

inner bubble: r~3 degrees, similar to “cocoon”

cygnus bubble: r~10 degrees

LHAASO view on w43

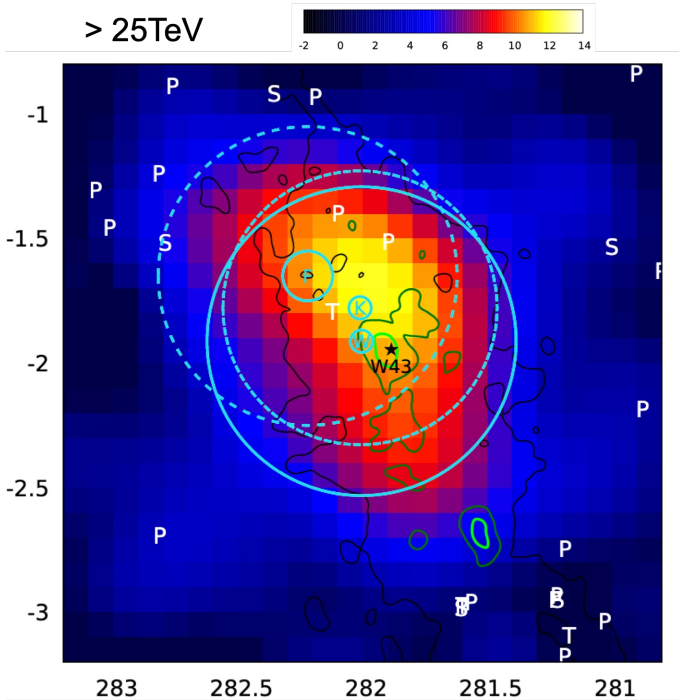

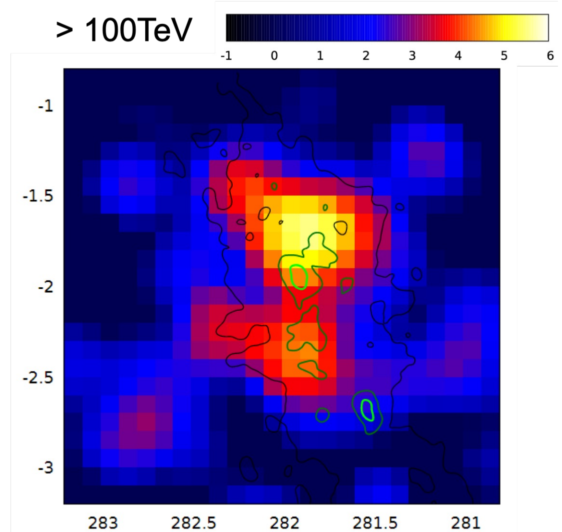

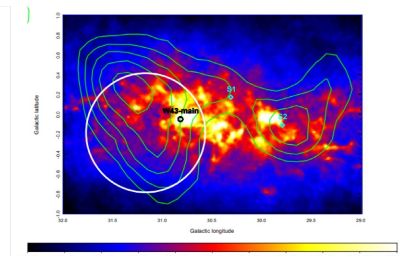

- •UHE gamma-ray emission reveal good correlation with dense gas
- •Spectrum up to PeV

Diffuse gamma-ray emission

based on talk of
Qiang Yuan

General picture of Galactic cosmic rays

© *I. V. Moskalenko*

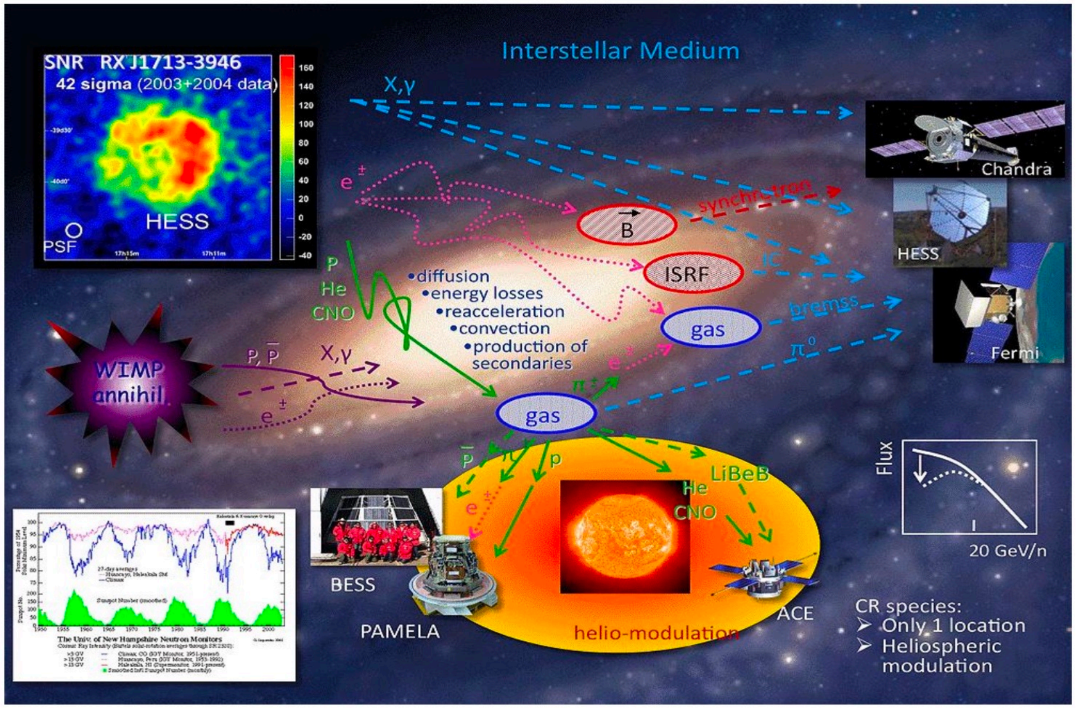

Acceleration at source

↓

Diffusion and Interaction

↓

Helio-sphere propagation

↓

Detection at the Earth

Diffuse γ rays are expected *a priori* to be produced by CR interactions during the propagation, and are thus powerful probe of CR propagation

Gamma/CR discrimination

$$R = \log\left(\frac{N_\mu + 0.0001}{N_e}\right)$$

$\log(E_{rec}/\mathrm{TeV})$	R for crab	R for diffuse
1.0 – 1.2	−5.11	−5.00
1.2 – 1.4	−5.24	−3.20
1.4 – 1.6	−5.95	−5.96
1.6 – 1.8	−6.08	−6.17
1.8 – 2.0	−2.34	−2.50
2.0 – 2.2	−2.35	−2.69
2.2 – 2.4	−2.36	−2.79
2.4 – 2.6	−2.36	−2.74
2.6 – 2.8	−2.36	−2.75
2.8 – 3.0	−2.36	−2.79

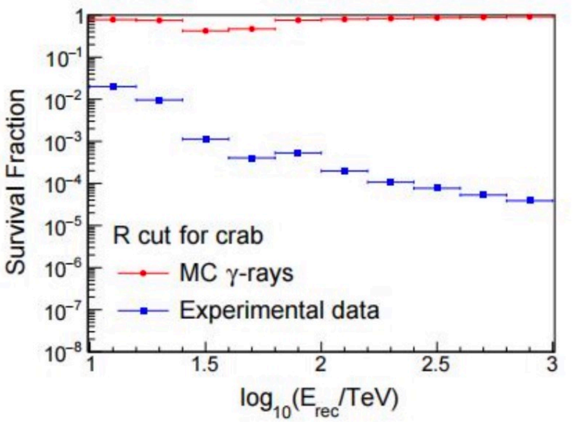

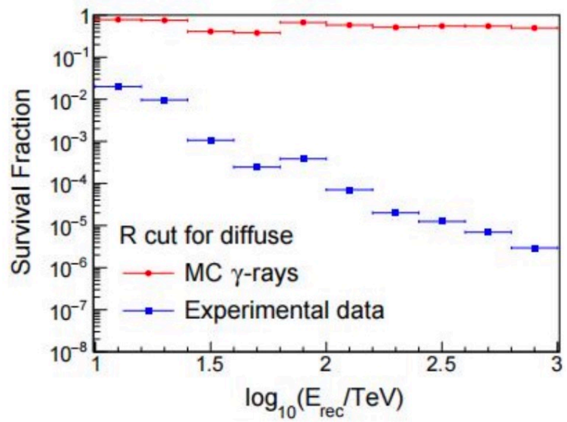

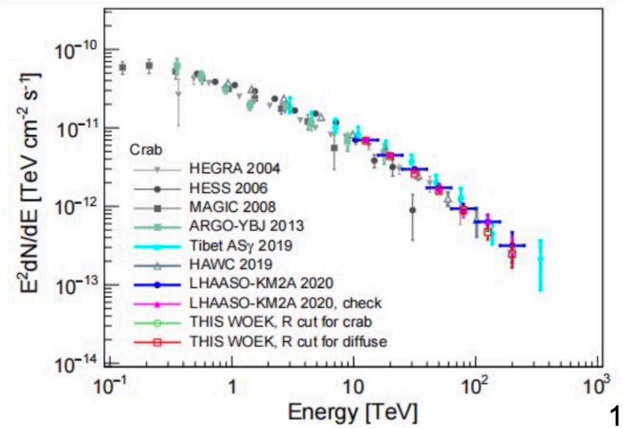

- R cuts adjusted from the Crab analysis to enable a higher $Q=S/B^{1/2}$ factor
- Efficiencies change from ~90% to ~60%

Mask LHAASO

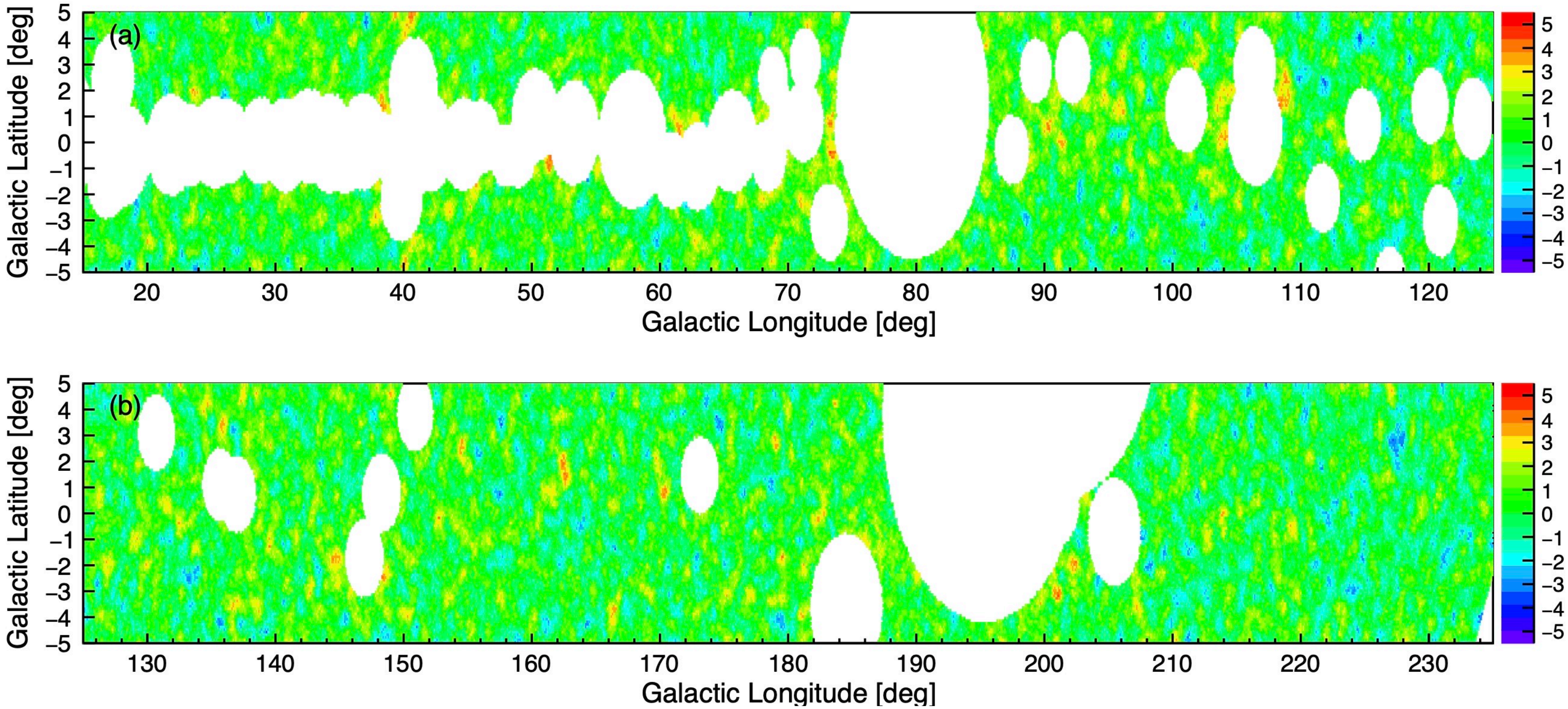

LHAASO collaboration arXiv: 2305.05372

Longitude and latitude profiles

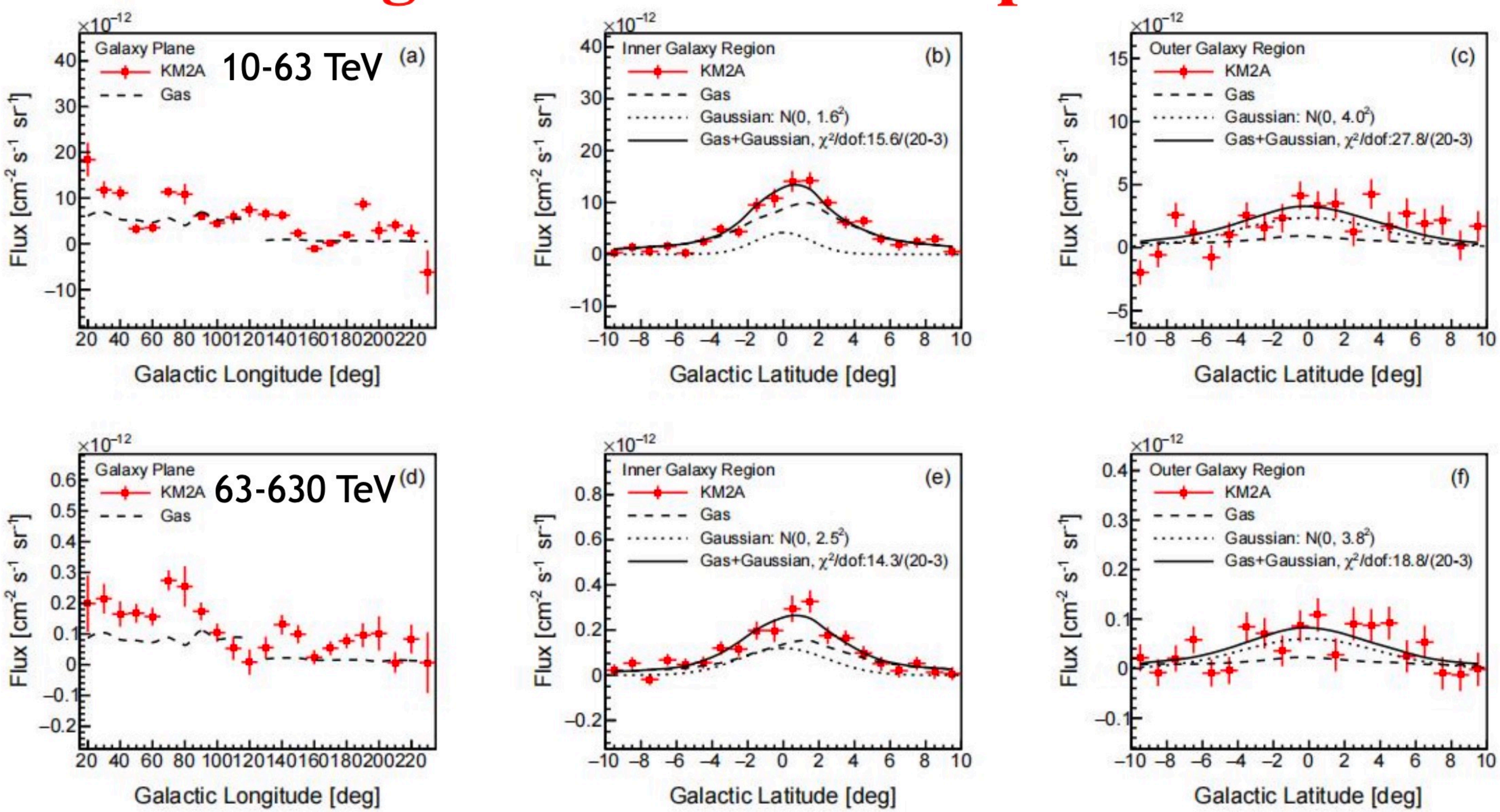

Adding a Gaussian latitude template does not improve the fittings significantly

LHAASO diffuse

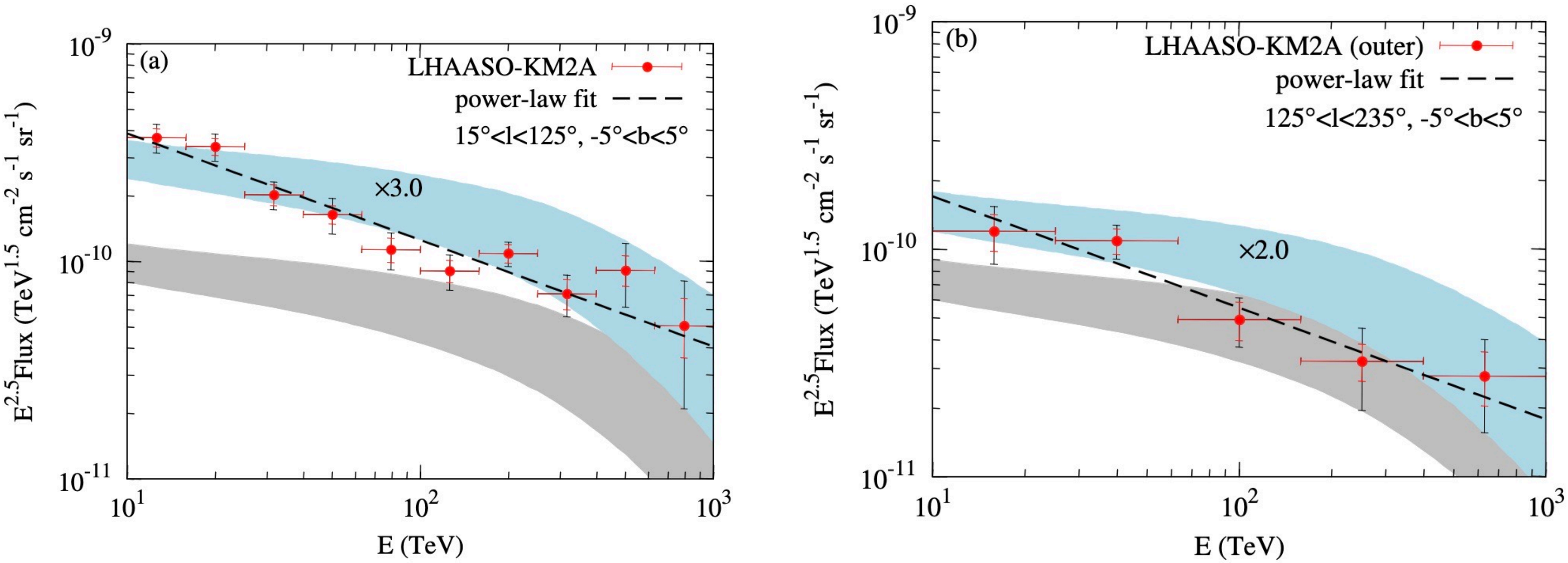

$$\Xi^{A,A'}(E,l,b) = \int_0^\infty \mathrm{d}s\, n_{\mathrm{gas}}^{A'}(\boldsymbol{x}) I_{\mathrm{CR}}^{A}(E,\boldsymbol{x})$$

$$I_\nu(E,l,b) = \sum_{A,A'} \int_E^\infty \mathrm{d}E'\, \Xi^{A,A'}(E',l,b) \frac{\mathrm{d}\sigma^{AA'\to\nu}(E',E)}{\mathrm{d}E}$$

arXiv: 2305.05372

Gamma-ray flux in inner and outer Galaxy

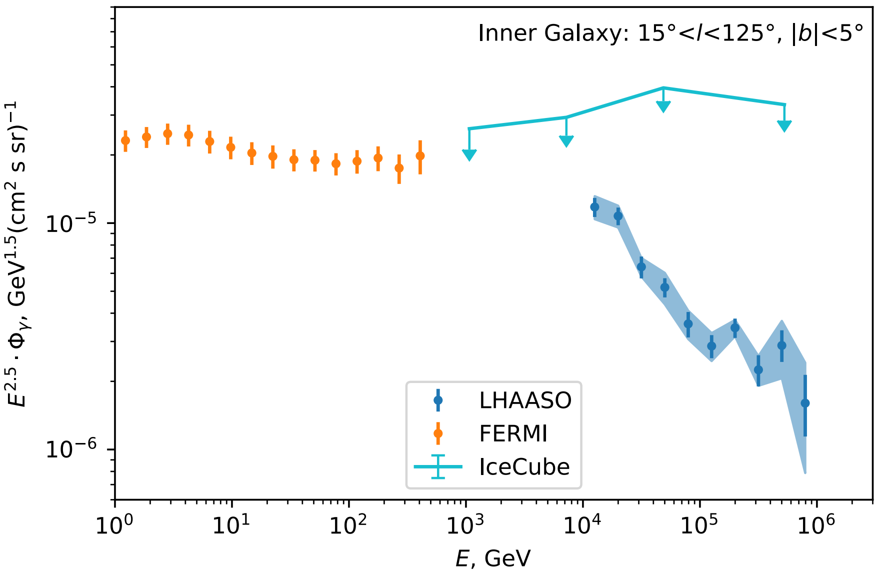

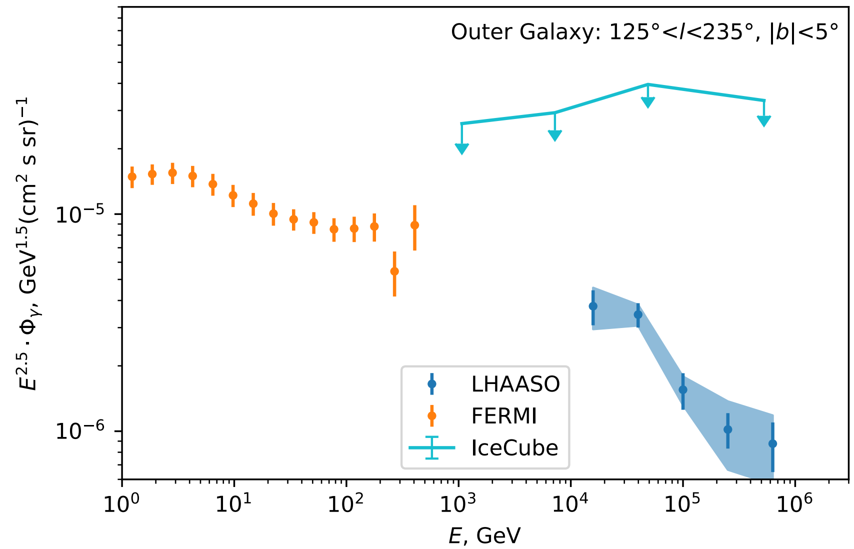

LHAASO data from LHAASO collaboration, 2305.05372

Fermi from R. Zhang et al, 2305.06948

IceCube data from IceCube 7 years limit on Kra-gamma model approximated to |b|<5

Gamma-ray flux in LHAASO is same 1/E^3,
but combination with Fermi looks different.

Energy coverage from sub-TeV to 10 TeV by WCDA

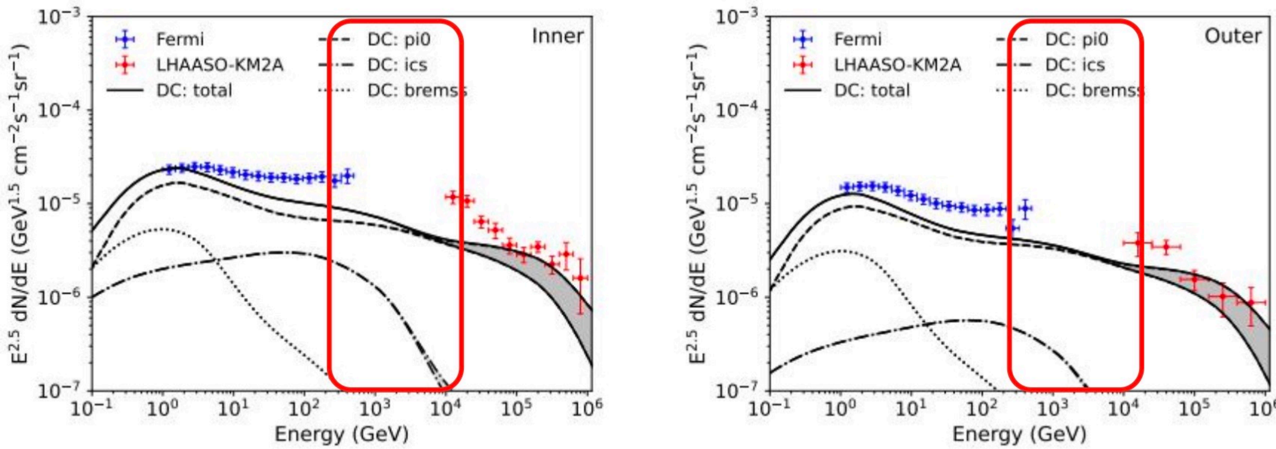

WCDA is expected to cover the energy range from sub-TeV to 10 TeV, and will perfectly bridge Fermi and KM2A.

1 PeV CR density in the Gal. plane

Lipari & Vernetto (2018)

G.Giacinti & D.S., 2305.10251

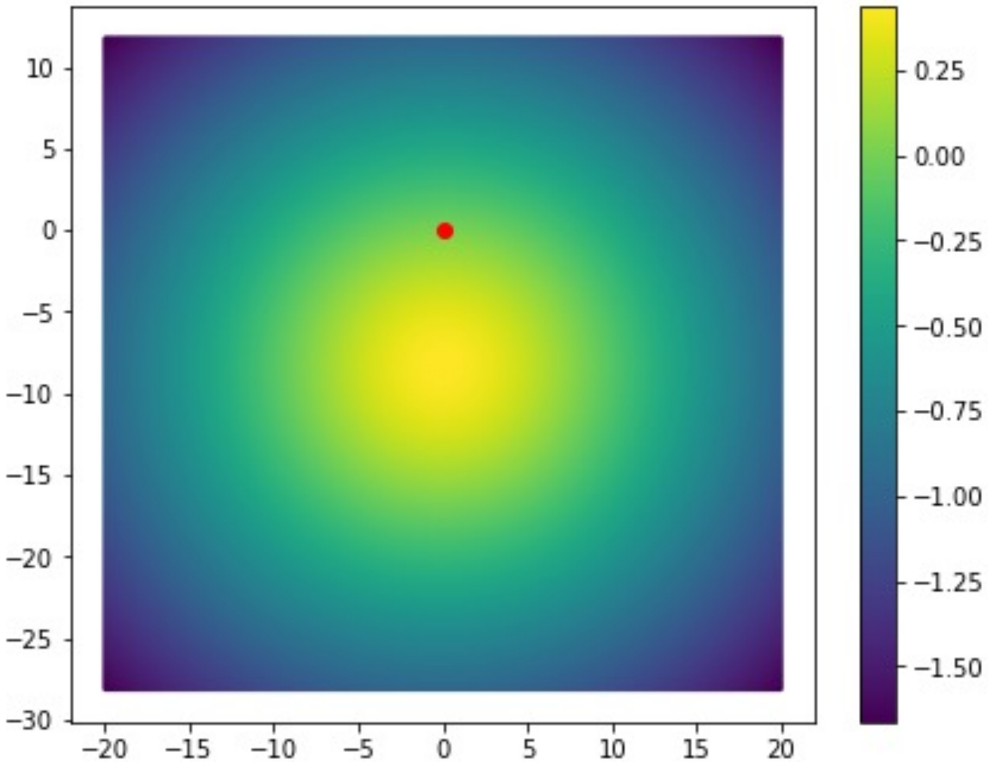

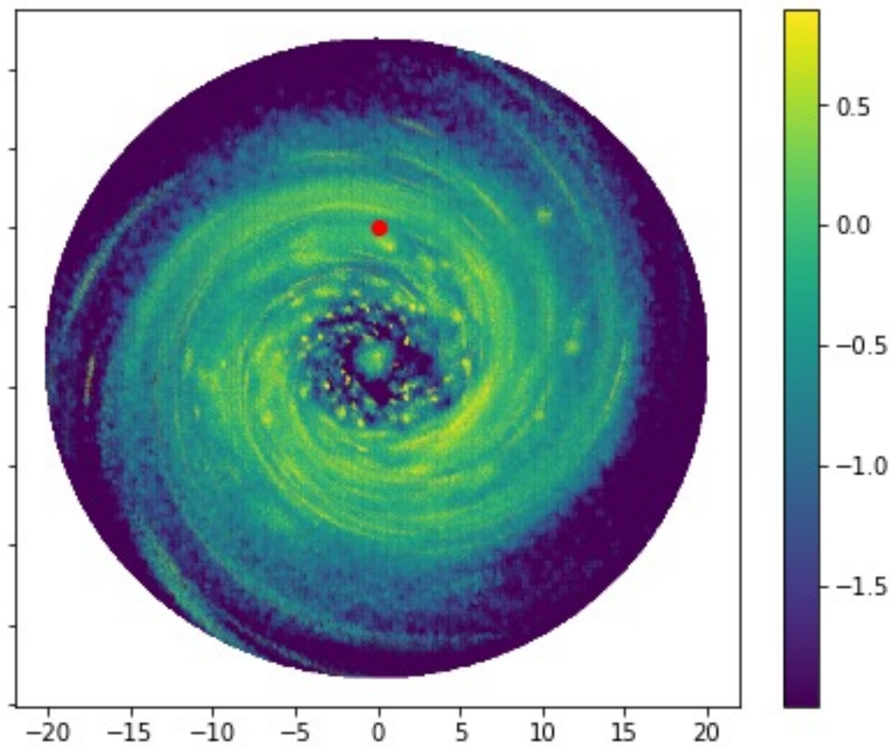

Talk by G.Giacinti

Gamma-ray and neutrino flux models from Galactic plane in inner and outer Galaxy

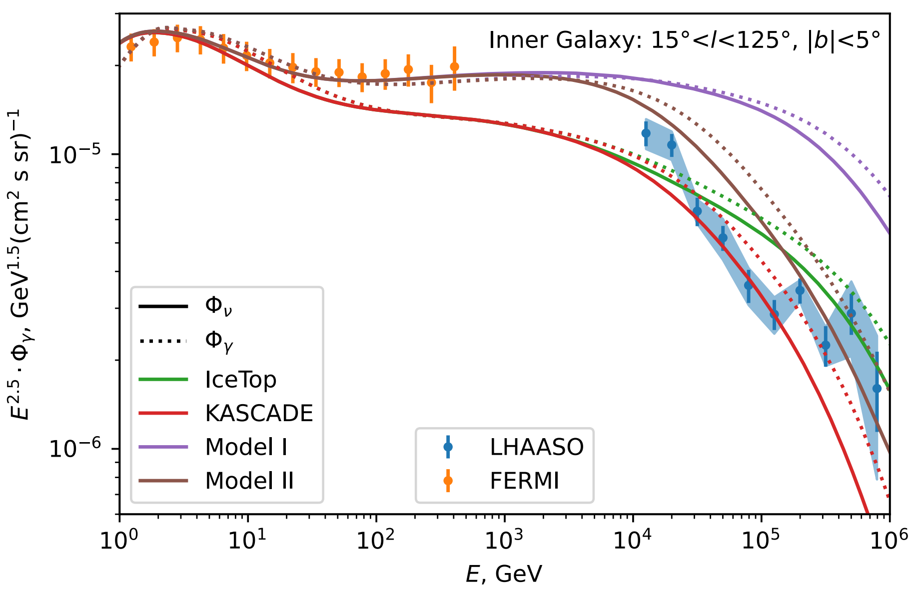

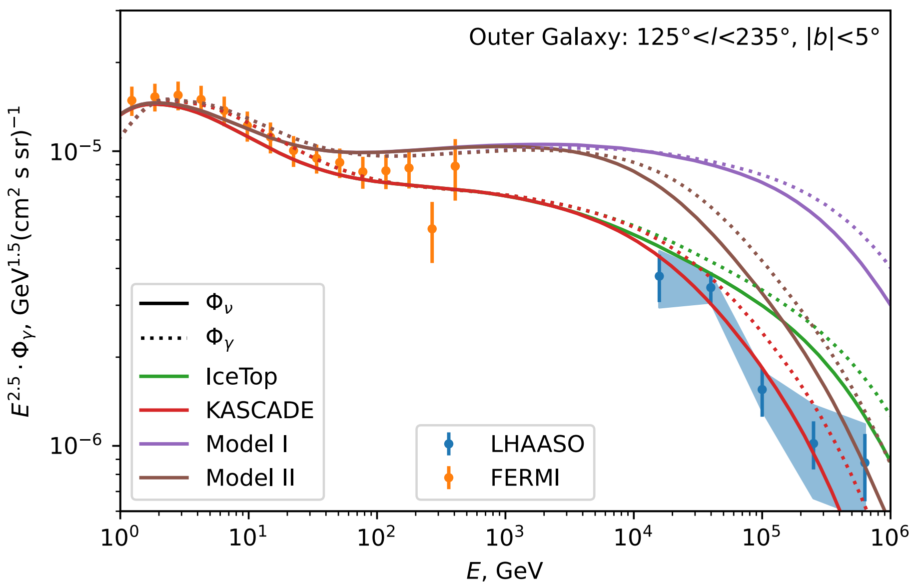

S.Koldobsky et al, ICRC 2023

Detection of GRB 221009A by LHAASO WCDA and km2a

based on talk of
Xiangyu Wang

GRB 221009A: brightest-of-all-time (BOAT) GRB

- Triggered on a weak precursor
- Fluence: >5e-2 erg/cm^2， low redshift (z=0.151)
- deriving an enormous energy $E_{\gamma,iso}$~$\mathbf{10^{55}}$ erg

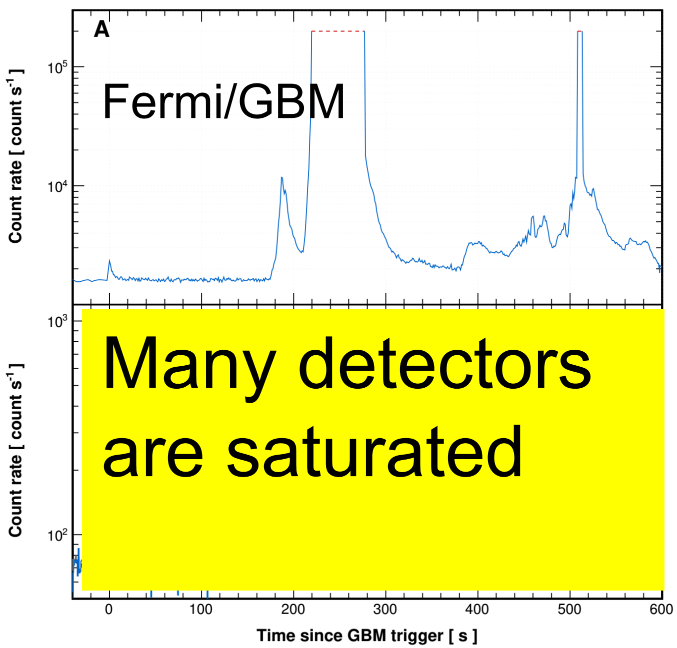

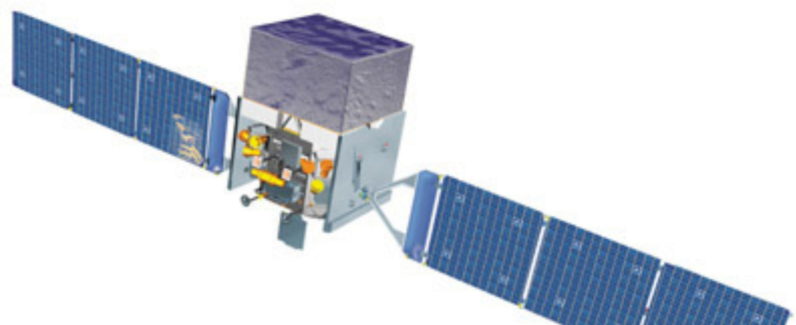

Fermi

GECAM/Konus-Wind Observations of GRB 221009A

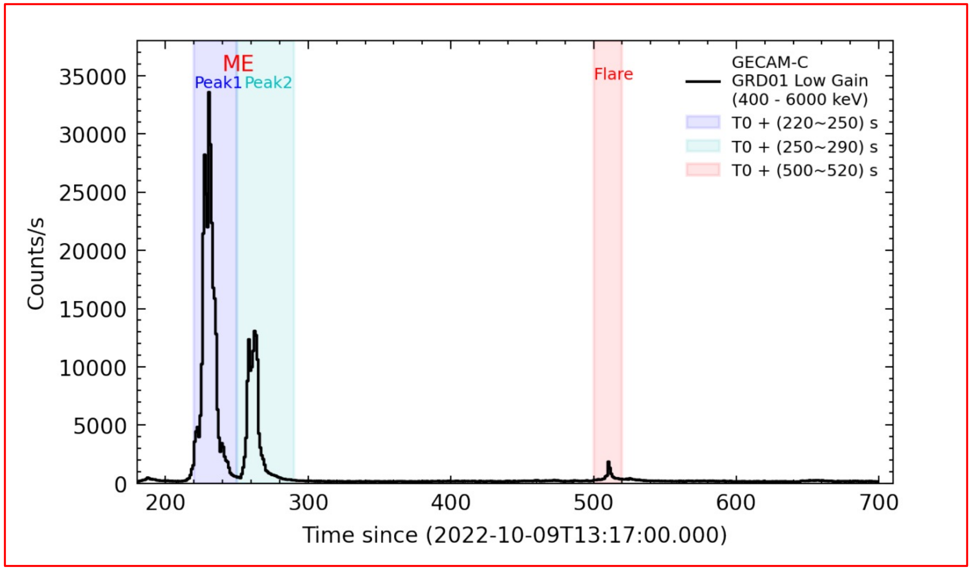

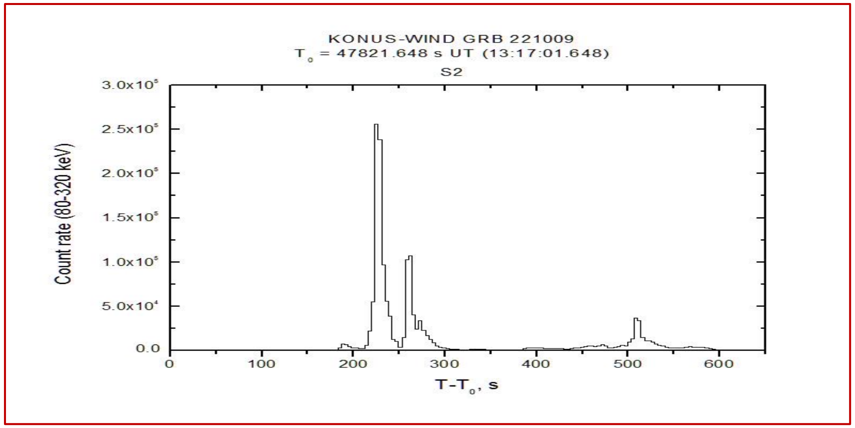

E_iso~ 1.5 × 10^55 erg

Mian peak 1 lasts ~10 s

GRB 221009A: A very rare event

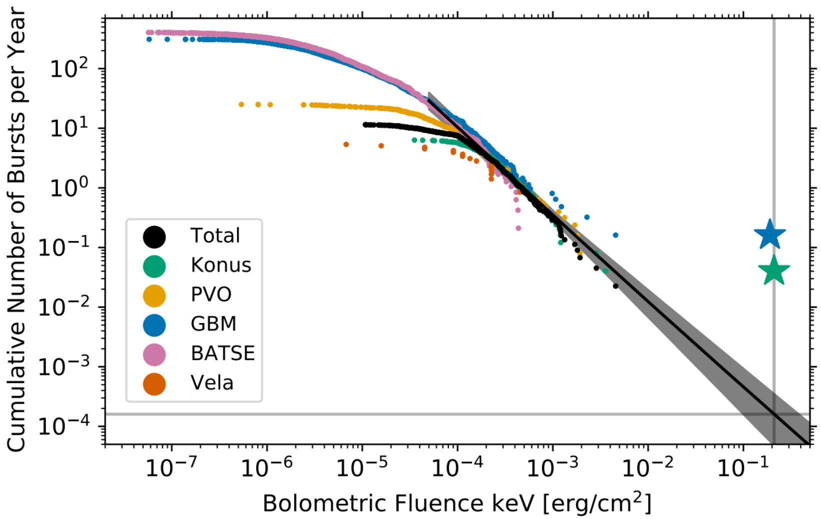

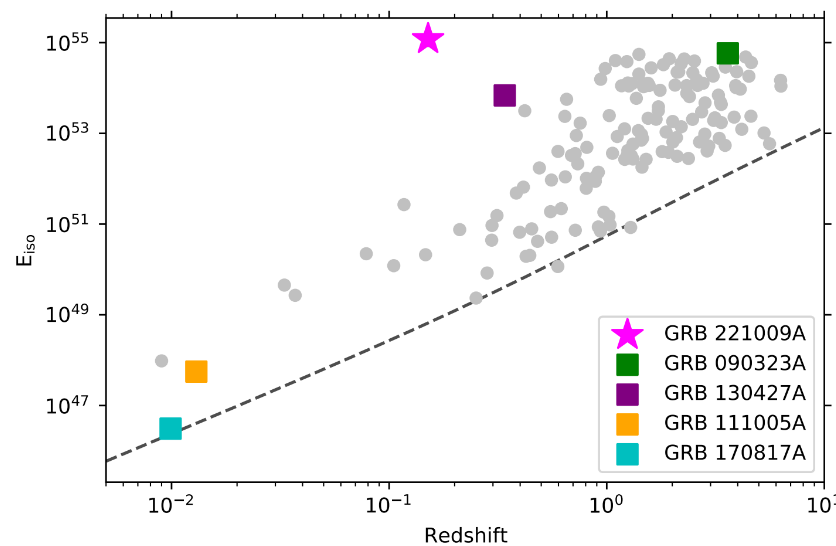

Fluence: >5 × 10 $^{-2}$ erg/cm^{2}

R_GRB≤ 6.1 × 10^{-4} Gpc^{-3} yr^{-1}

z=0.151 volume ~ 1 Gpc^3

R<10^-3 yr

Buns et al. 2023

LHAASO GRB221009A

- LHAASO detection of GRB 221009A: first GRB seen by a extensive air shower detector
- High statistics: >60,000 photons above 0.2TeV (LHAASO-WCDA)
- TeV count rate light curve: Smooth temporal profile – **external shock origin**

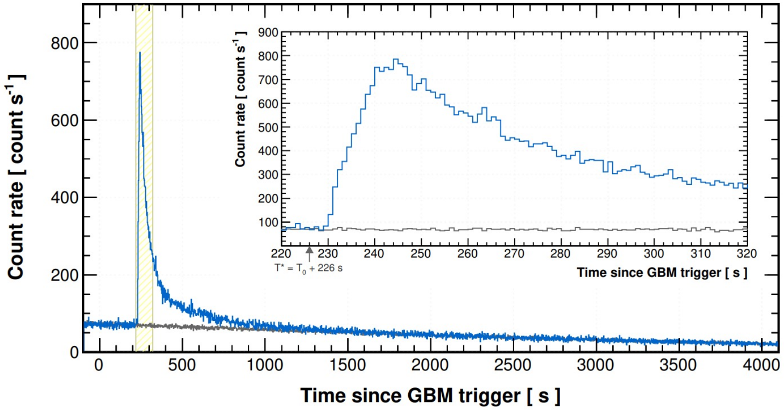

First time detection of the TeV afterglow onset !

MeV vs TeV light curves: external shock origin

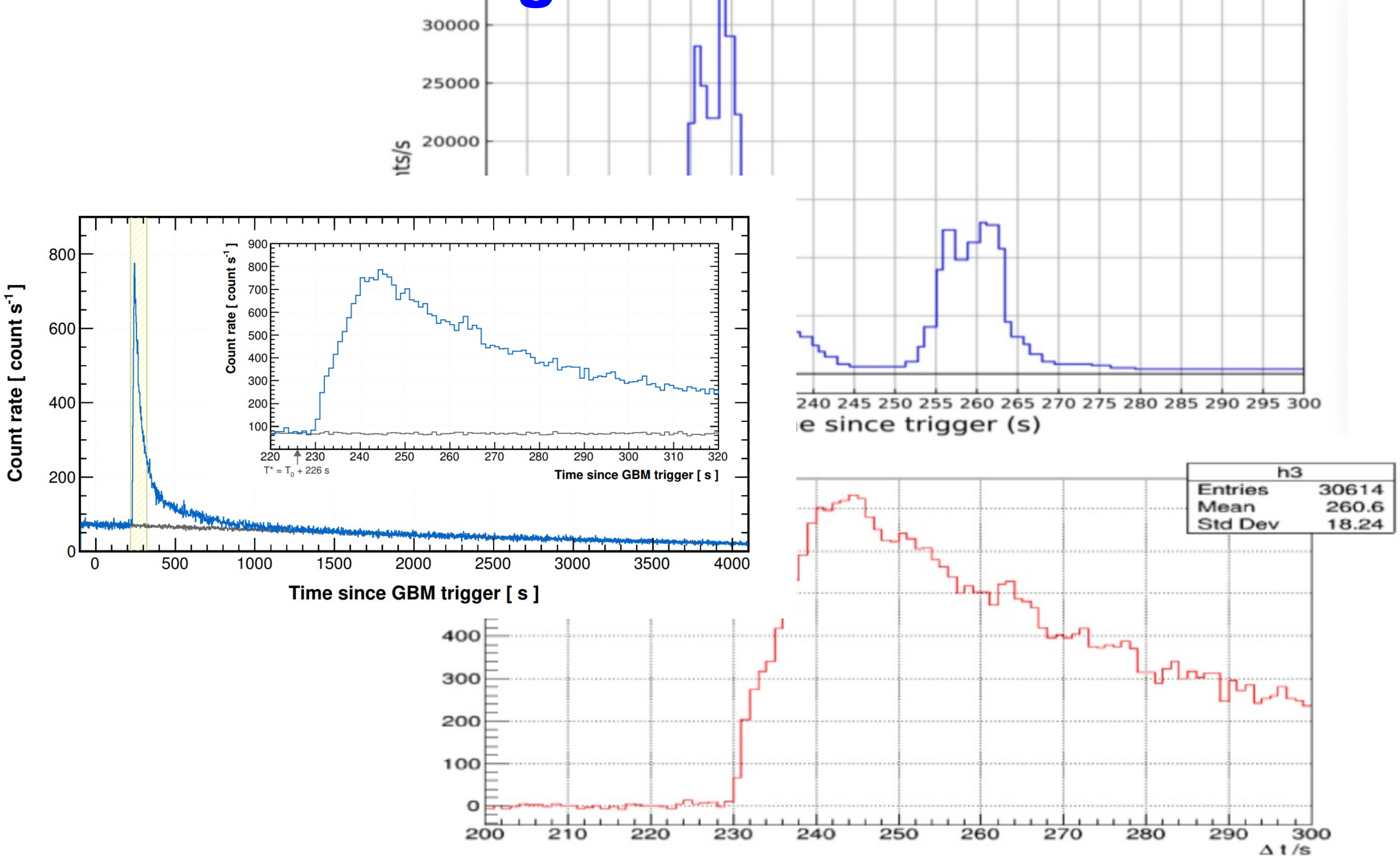

LHAASO, Science, June 8, 2023

SED measured by LHAASO-WCDA

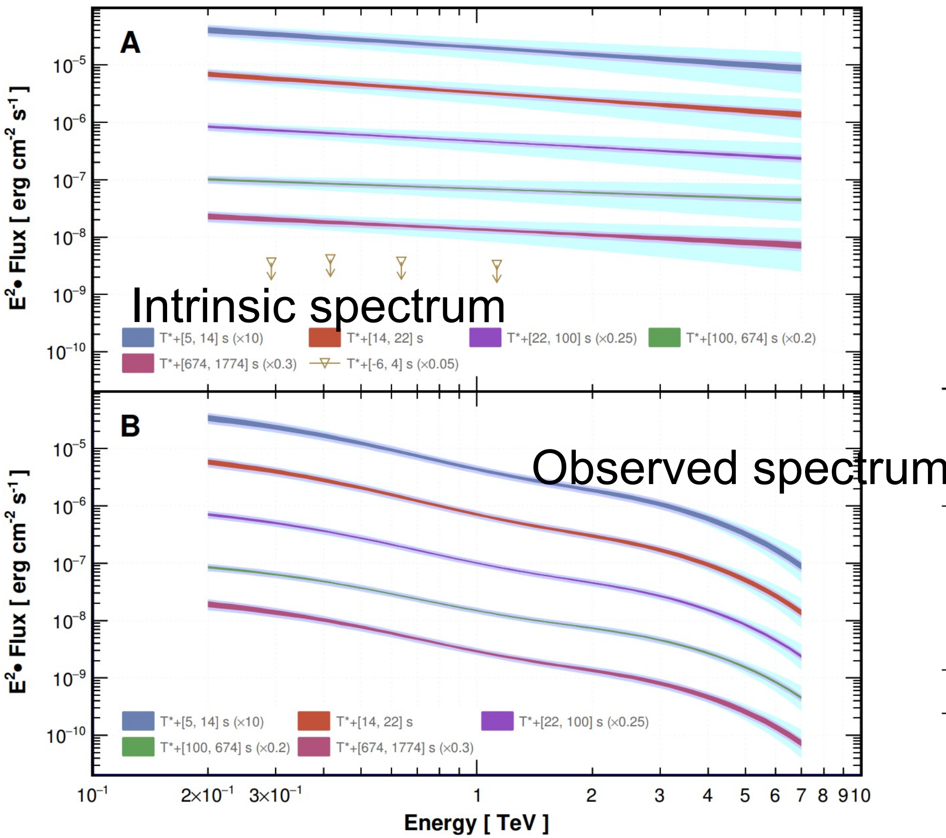

- .EBL model: A. Saldana-Lopez et al. (2021)

Time interval (seconds after T_0)	A (10^{-8} TeV^{-1} cm^{-2} s^{-1})	γ	$E_{\rm cut}$ TeV	χ^2/dof
Observed spectrum				
231–240	42.9 ± 2.7	2.983 ± 0.061	3.14 (fixed)	4.6/6
240–248	70.1 ± 3.8	3.006 ± 0.052	3.14 (fixed)	8.0/6
248–326	39.9 ± 1.0	2.911 ± 0.028	3.14 (fixed)	14.8/6
326–900	7.35 ± 0.16	2.788 ± 0.026	3.14 (fixed)	8.9/6
900–2000	0.959 ± 0.043	2.880 ± 0.067	3.14 (fixed)	2.9/5
Intrinsic spectrum, *standard* EBL				
231–240	127.3 ± 7.9	2.429 ± 0.062	\	3.1/6
240–248	208 ± 11	2.455 ± 0.054	\	6.5/6
248–326	117.8 ± 3.0	2.359 ± 0.028	\	8.7/6
326–900	21.77 ± 0.47	2.231 ± 0.026	\	3.4/6
900–2000	2.84 ± 0.13	2.324 ± 0.065	\	2.2/5

LHAASO, Science, June 8, 2023

1.Rising phase

- The rising phase: free expansion
- Fast rise: $\alpha_0 = 14.9^{+5.7}_{-4.0}$
- slow rise: $\alpha_1 = 1.82^{+0.21}_{-0.18}$
- Interpretation:

-TeV emission: assuming synchrotron Self-Compton emission

- Expected light curve: agrees with t $n \propto R^{-k}$

$$F_\nu = \begin{cases} F_m^{\rm IC}\left(\frac{\nu}{\nu_m^{\rm IC}}\right)^{-\frac{p-1}{2}} \propto t^{\frac{16-(9+p)k}{4}}\nu^{-\frac{p-1}{2}}, & \nu_m^{\rm IC} < \nu < \nu_c^{\rm IC} \\ F_m^{\rm IC}\left(\frac{\nu}{\nu_c^{\rm IC}}\right)^{-\frac{1}{2}} \propto t^{\frac{8-3k}{4}}\nu^{-1/2}, & \nu_c^{\rm IC} < \nu < \nu_m^{\rm IC} \\ F_m^{\rm IC}(\nu_m^{\rm IC})^{\frac{p-1}{2}}(\nu_c^{\rm IC})^{\frac{1}{2}}\nu^{-\frac{p}{2}} \propto t^{\frac{8-(2+p)k}{4}}\nu^{-\frac{p}{2}}. & \nu > \max(\nu_m^{\rm IC}, \nu_c^{\rm IC}) \end{cases} \quad (12)$$

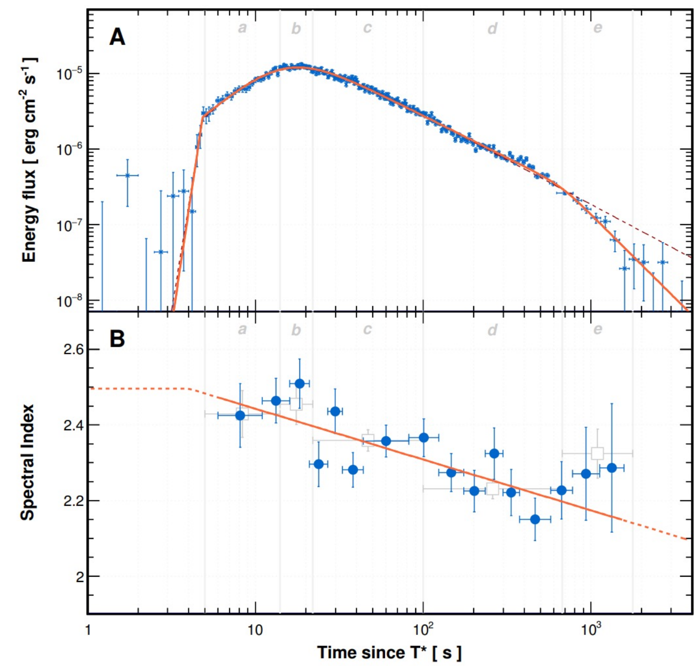

Fast rise phase is unusual: energy injectio

LHAASO, Science, June 8, 2023

What we've learnt from the GRB 221009A

Initial Lorentz Factor Γ_0

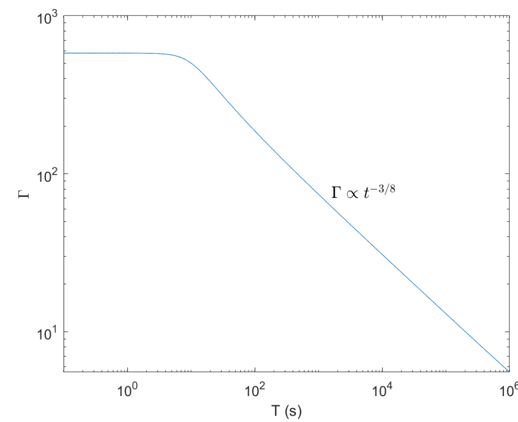

- From T* to the peak (energy-independent peak time), it takes

  ~18 s

- The bulk Lorentz factor is estimated as

$$\Gamma_0 = \left(\frac{3E_k}{32\pi n m_p c^5 t_{\rm peak}^3}\right)^{1/8} = 440 E_{k,55}^{1/8} n_0^{-1/8} \left(\frac{t_{\rm peak}}{18\,{\rm s}}\right)^{-3/8}$$

it is among the highest values for all GRBs

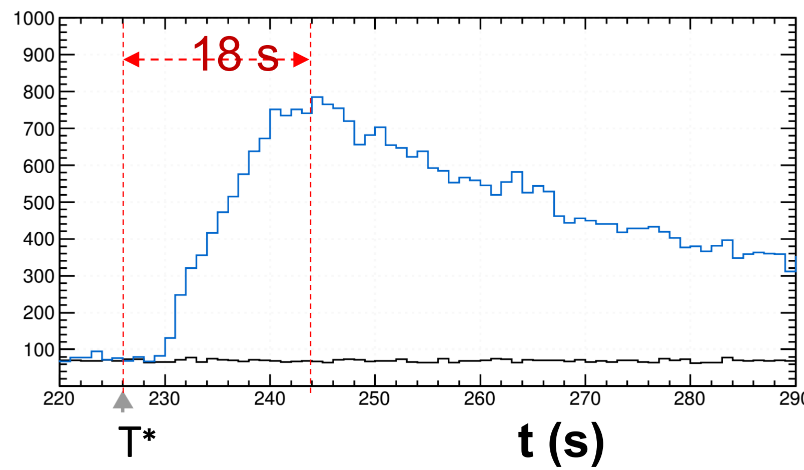

LHAASO, Science, June 8, 2023

A narrow GRB jet

- Jet breaks have been seen in optical/X-ray bands
- First time seeing a jet break at TeV band
- Helps to understand the total energy of the GRB

$$\theta_0 \; 0.6^\circ E_{k,55}^{-1/8} n_0^{1/8} \left(\frac{t_{\mathrm{b},2}}{670\,\mathrm{s}}\right)^{/8}$$

➢ assuming jet angles derived from the break time of the optical afterglow light curve, the collimation-corrected radiated energy is clustered around ~10^{51} erg.

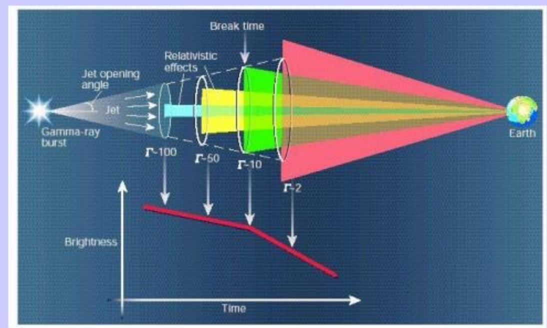

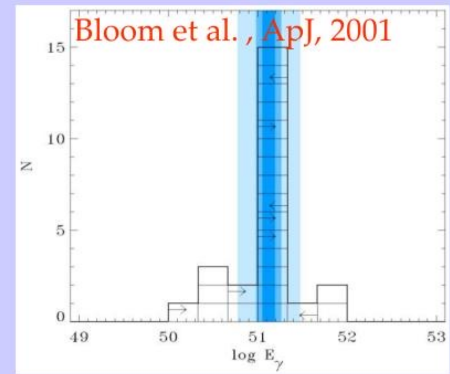

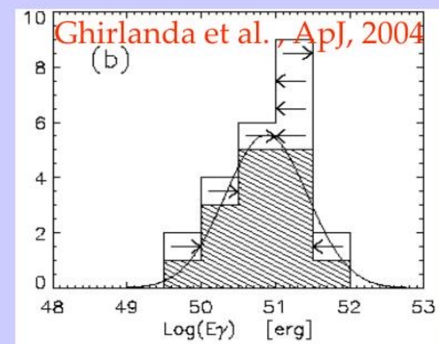

$$E_{\gamma,j} = E_{\gamma,\mathrm{iso}}\theta_0^2/2 \sim 7.5 \times 10^{50}\ \mathrm{erg}\, E_{\gamma,\mathrm{iso},55}(\theta_0/0.7^\circ)^2$$

What we've learnt from GRB 221009A

Upper limit in prompt phase

- The most strict limit on the prompt TeV emission

$R = F_{TeV}/F_{MeV} < 2 \times 10^{-5}$

1. A large $\gamma\gamma$ absorption optical depth ?
2. Or a magnetized jet?

$$R_{\rm in} \sim 2\Gamma_0^2 c t_v = 10^{15}\,{\rm cm}\,(\Gamma_0/440)^2\,(t_v/0.082\,{\rm s})$$

$$\tau_{\gamma\gamma} \sim \sigma_{\gamma\gamma} n_t' \frac{R_{\rm in}}{\Gamma_0} \sim 190 \left(\frac{R_{\rm in}}{10^{15}\,{\rm cm}}\right)^{-1} \left(\frac{\Gamma_0}{440}\right)^{-2} \left(\frac{\varepsilon_t}{h\nu_m}\right)^{\beta_1+1}$$

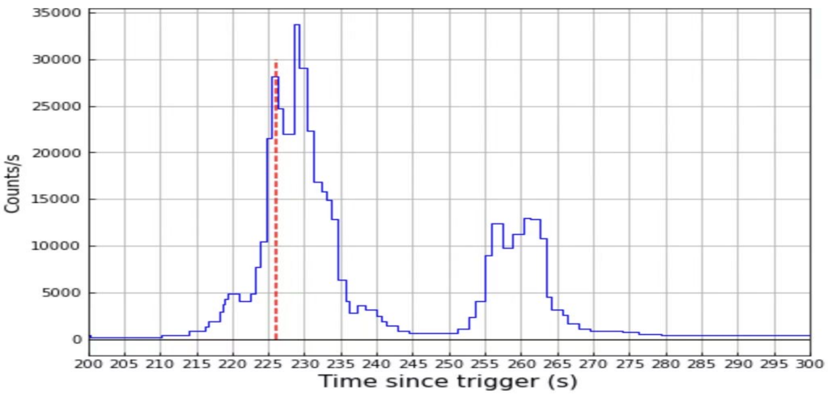

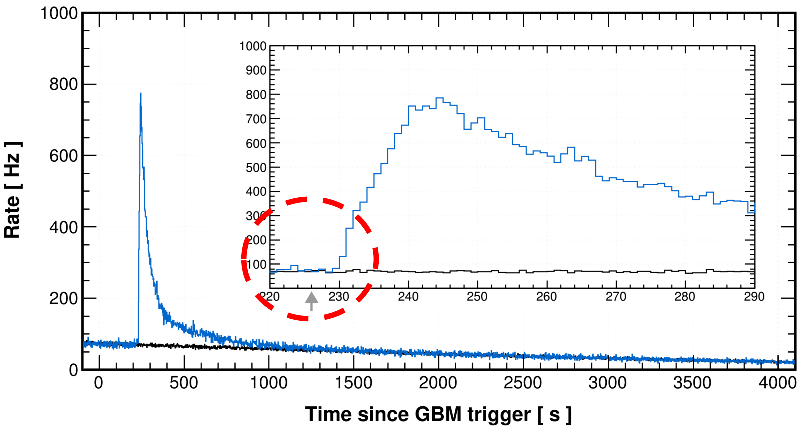

GRB 221009A KM2A

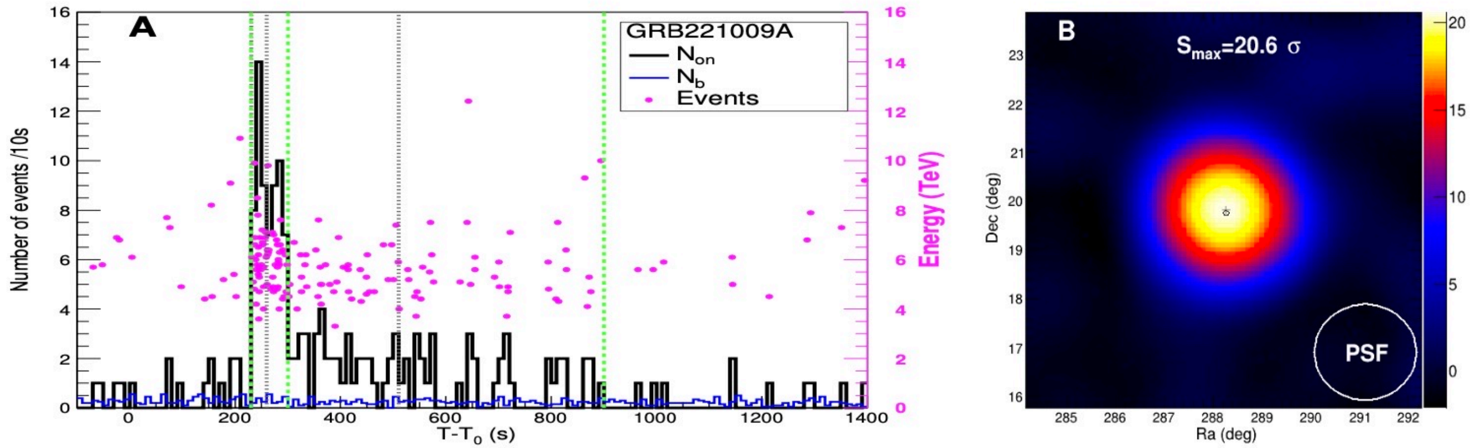

Figure 1: **The light curve and significance map of GRB 221009A obtained by KM2A.** (A) The gamma-ray-count light curve obtained by KM2A with each time-bin of 10s. The black curve indicates the events from the angular cone centered on the GRB, and the blue curve indicates the number of events due to cosmic ray background estimated from 20 similar angular cones at off-source directions with the same zenith angle. The gray dashed lines indicate the peak times of the multi-pulsed emission observed by GECAM-C (*10*) in the MeV band. The green dashed lines indicate the times of T_0+230s, T_0+300s, and T_0+900s. The pink points indicate the energy marked by the right label and the arrival time of each event. The energies of each event were reconstructed assuming the spectra shown in panel B of Figure 2. (B) The significance map around GRB 221009A as observed by KM2A. The plus sign and corresponding length denote the position and error determined by KM2A. The black circle denotes the position of the GRB reported by Fermi-LAT. The white circle shows the size of the PSF that contains 68% of the events.

LHAASO collab., Sci.Adv. 9 (2023) 46, adj2778 e-Print: 2310.08845

GRB 221009A км2а

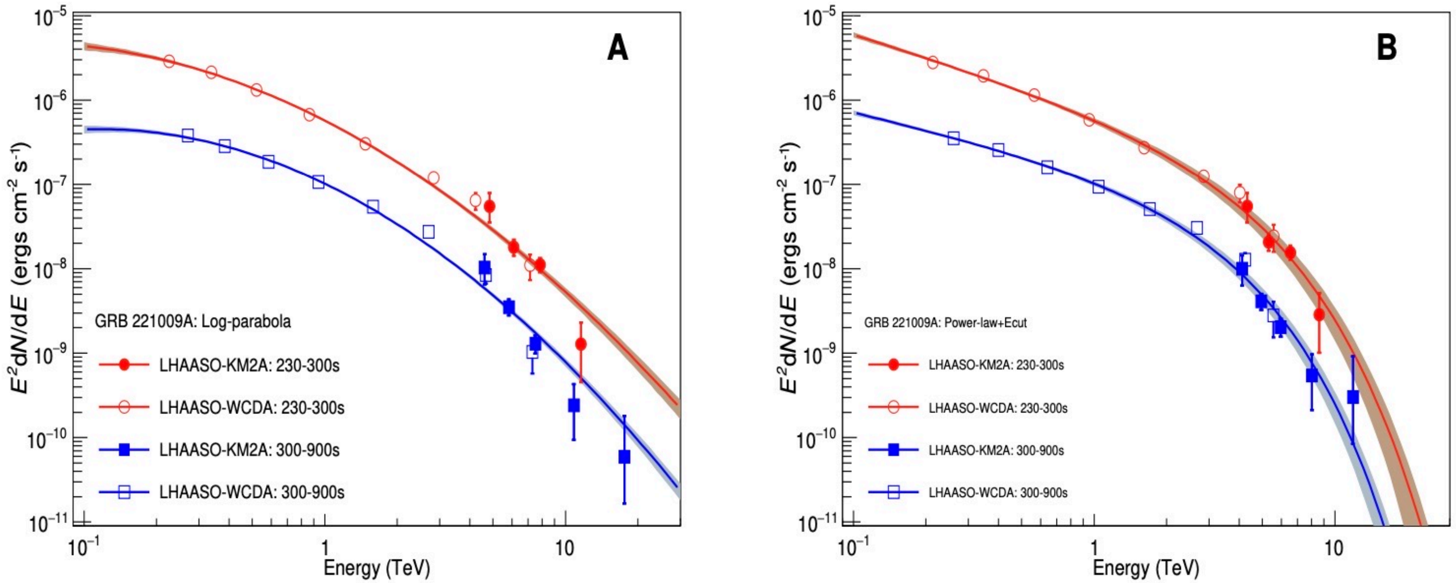

Figure 2: **Observed VHE spectra of GRB 221009A by LHAASO for the two intervals.** Interval 1 is from T_0+230s to T_0+300s (red points) and interval 2 is from T_0+300s to T_0+900s (blue points). The solid lines indicate the best-fitting results, and the shaded regions indicate the 1-sigma error region. (A) The log-parabola function is used to fit the observational data. (B) The power-law with exponential cutoff function is adopted to fit the observational data.

LHAASO collab., Sci.Adv. 9 (2023) 46, adj2778 e-Print: 2310.08845

GRB 221009A км2а

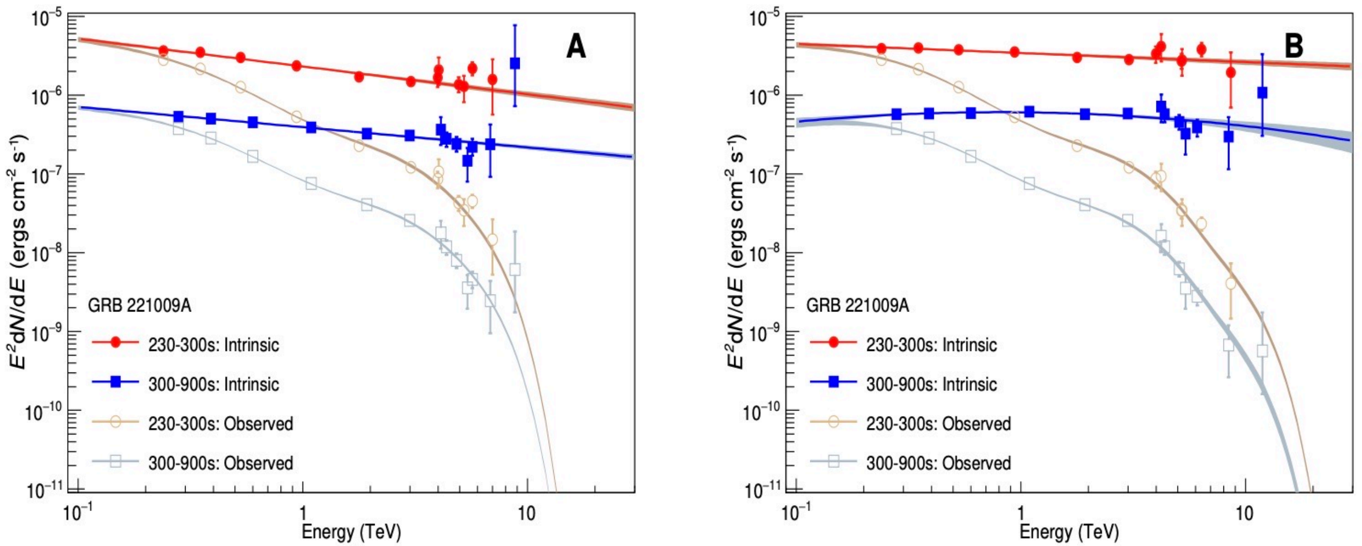

Figure 3: **Intrinsic VHE spectra of GRB 221009A corrected for EBL absorption.** (A) Filled points show the intrinsic spectrum of GRB 221009A corrected for EBL absorption using the model of Saldana-Lopez et al. 2021 (*17*). The red points are for interval 1 from T_0+230s to T_0+300s, and the blue points are for interval 2 from T_0+300s to T_0+900s. The solid lines indicate the best-fitting results using the power-law function, and the shaded regions indicate the 1-sigma error region. The unfilled points and shaded regions are corresponding observed spectra. (B) Filled points show the intrinsic spectrum of GRB 221009A corrected for EBL absorption using the LHAASO-constrained EBL model. The red solid line indicates the best-fitting result for interval 1, which is a power-law function, and the blue solid line indicates the best-fitting result for interval 2, which is a log-parabolic function. The points and shaded regions are similar to those in panel A.

LHAASO collab., Sci.Adv. 9 (2023) 46, adj2778 e-Print: 2310.08845

GRB 221009A KM2A

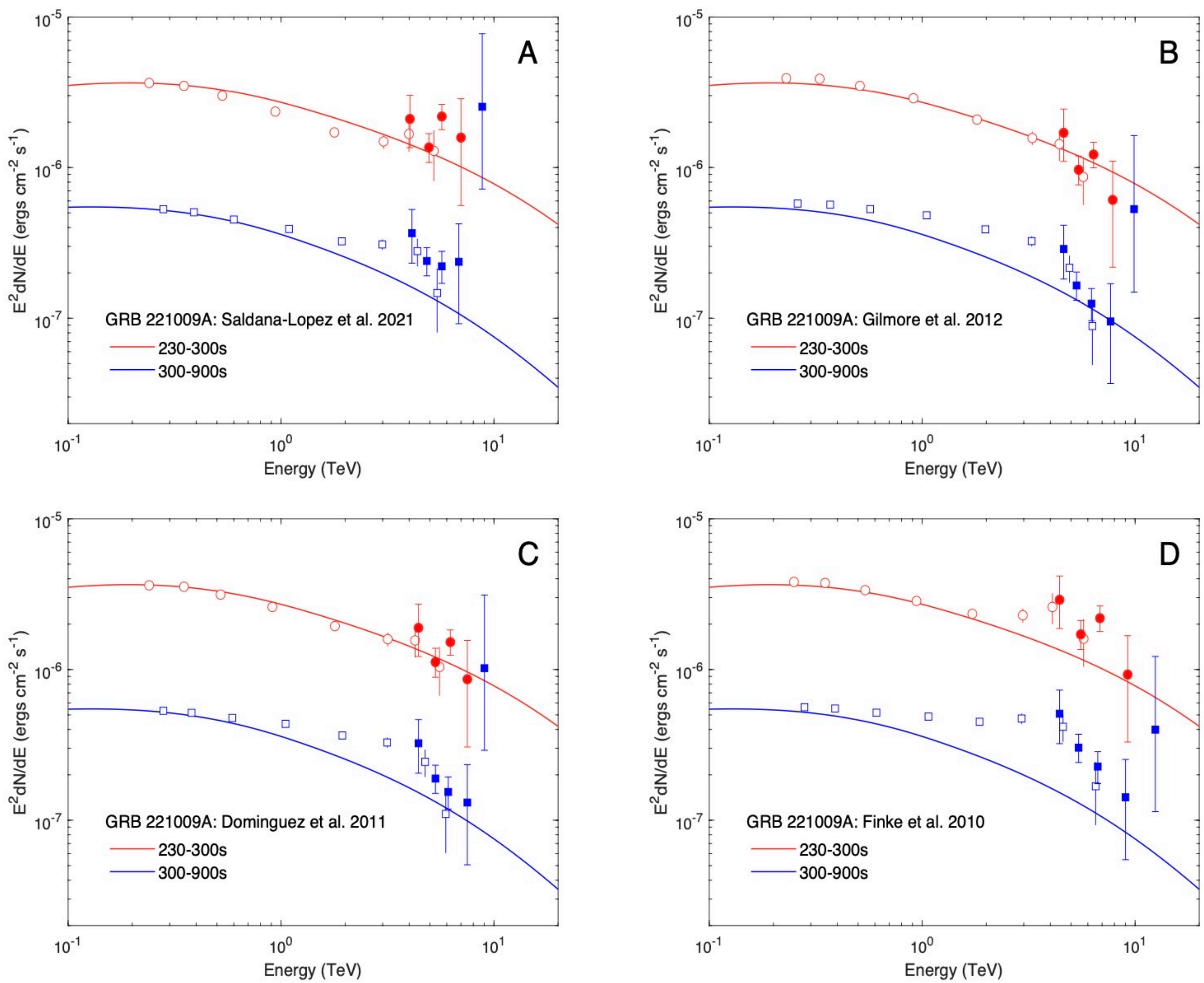

LHAASO collab., Sci.Adv. 9 (2023) 46, adj2778 e-Print: [2310.08845]

GRB 221009A summary

1. First time observing the onset of an TeV afterglow
2. This enables
   1. Setting the most strict limit on the prompt emission in the TeV band
   2. Finding an unusually fast rise phase
   3. Estimating the initial bulk Lorentz factor Γ_0 of the jet
3. Finding a jet break in the TeV light curve in its decay phase
   1. The narrowest jet of 0.8° (the earliest jet break), revealing the “core” of a structured jet
   2. A reasonable $E_{\gamma,jet} \sim 10^{51}$ erg with the beam correction
   3. **The unprecedently large fluence may be due to seeing the brightest core of a nearby GRB jet**
4. Signal at E>10 TeV is consistent with Standard Model. Constraints on intrinsic spectrum and on EBL models

Cygnus region with LHAASO

Cygnus region

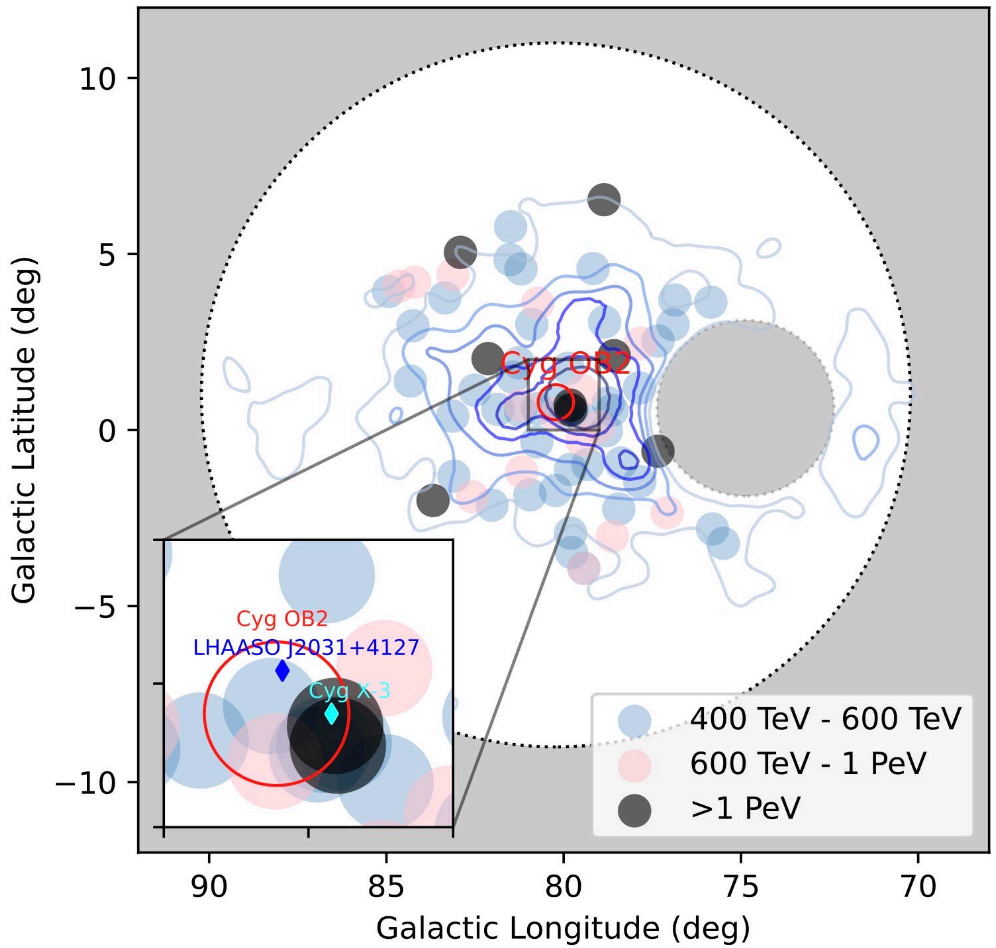

• *LHAASO collab.*, Zh.Cao et al, 2310.10100

Cygnus region

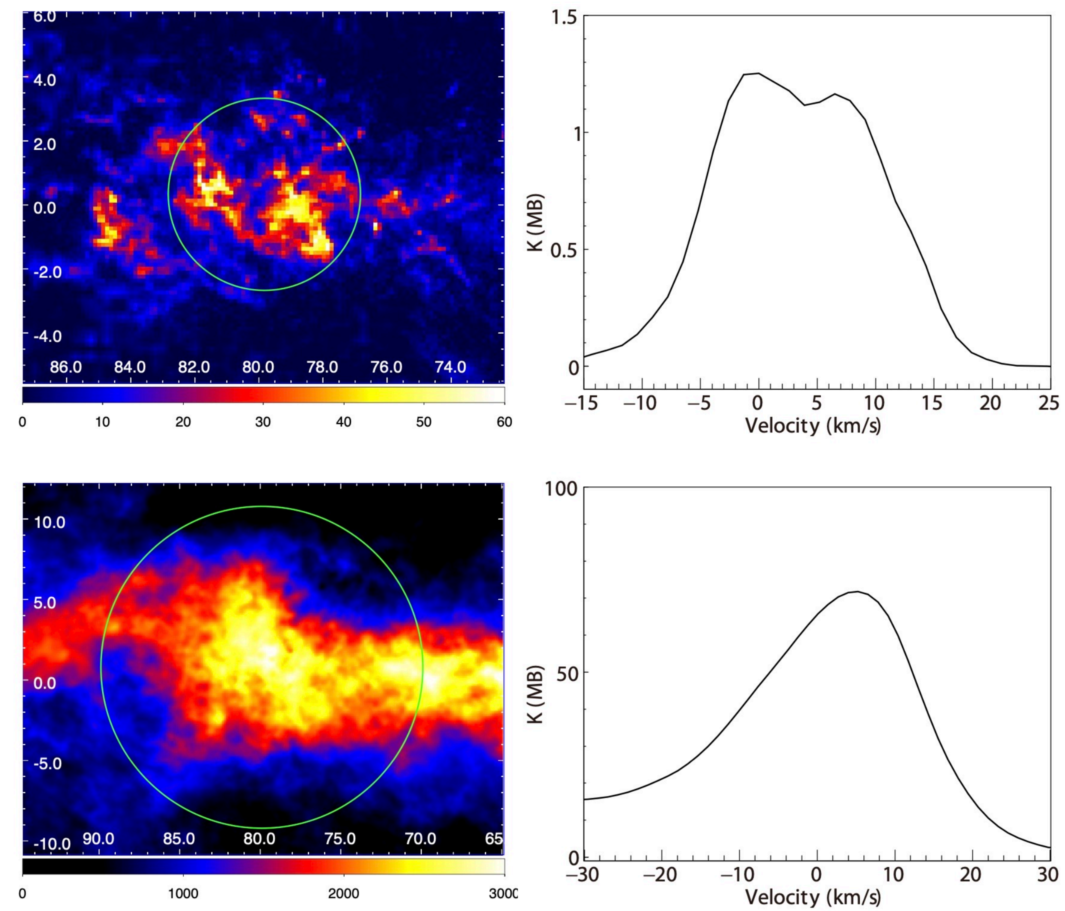

Figure 7: Left panels: ^{12}CO(top) and H I (bottom) intensity maps in Galactic coordinates (l,b) in degrees integrated over the velocity ranges -10 to 20 km s^{-1} and -20 to 30 km s^{-1}, respectively. The color denotes the intensity in unit of K km s^{-1} The regions delineated in green are used to estimate the astrophysical parameters for the molecular gas and atomic gas. Right panels: ^{12}CO and H I spectra of the regions indicated in left panels.

•*LHAASO collab.,* Zh.Cao et al, 2310.10100

Cygnus region

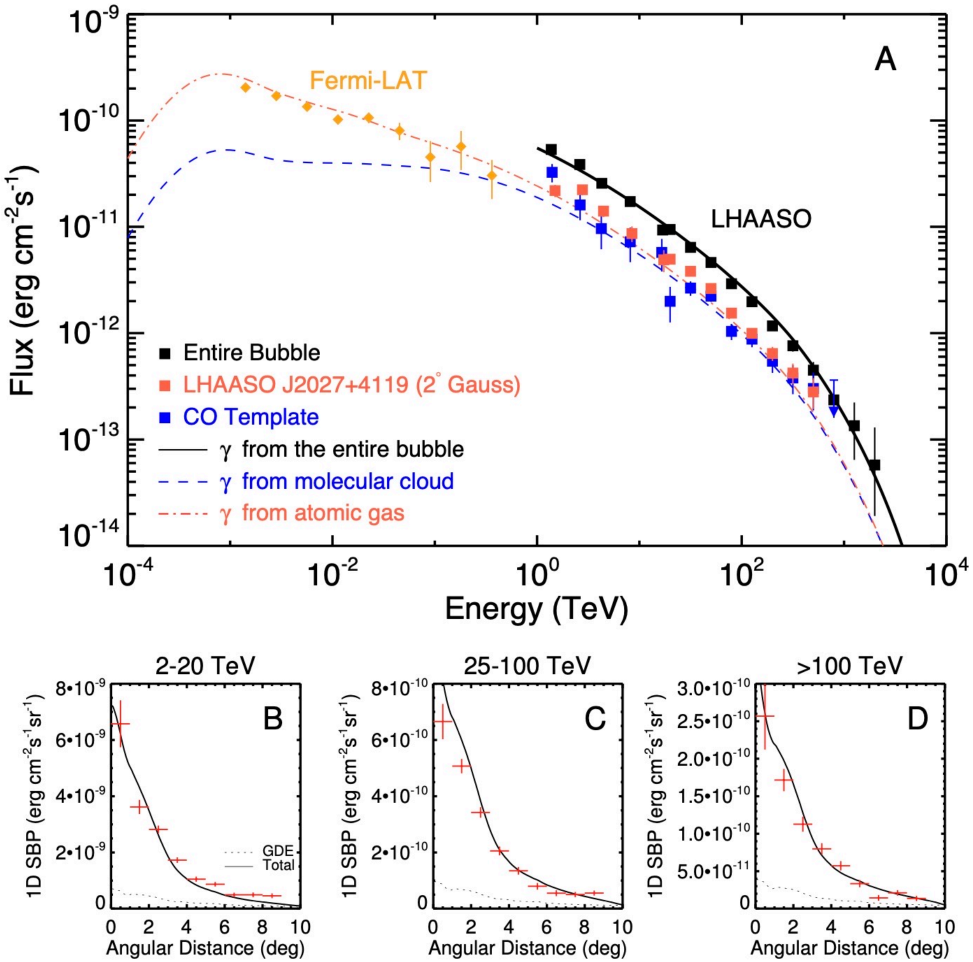

•*LHAASO collab.*, Zh.Cao et al, 2310.10100

Neutrinos from Cygnus region

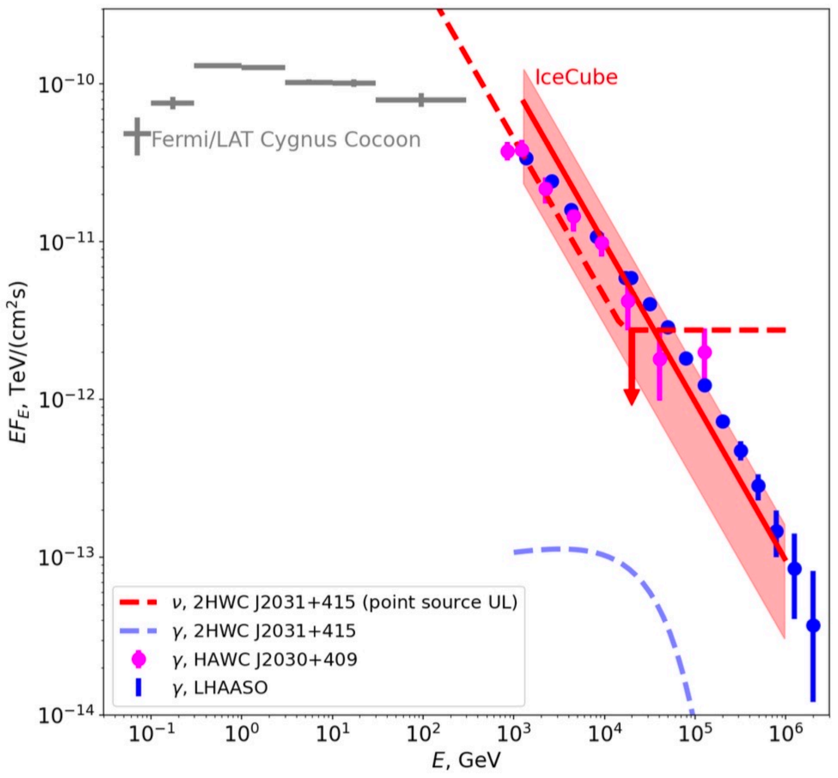

A.Neronov, D.S. and D.Savchenko, arXiv:2311.13711

Summary

- Construction of LHAASO finished in July 2021. LHAASO operates with almost 100% duty cicle. It's one year sensitivity is better compared to 50 hours for present Cherenkov telescopes above few TeV. Above 20 TeV it is better as compared to future CTA.
- LHAASO presented first catalog of 90 sources from about 2 first years of observation. 32 are new sources. Number of UHE gamma-ray sources above 100 TeV increased from 4 to 43 by LHAASO observations
  - 35 sources are PWN. Crab, Geminga, milisecond pulsar
  - 7 SNR, gamma-Cygni can not be explained by leptons
  - Star clusters Cygnus, w43
- Diffuse emission from Galaxy: new models requered
- GRB 221009A: detailed properties of GRB afterglow from 60000 photons in LHAASO WCDA and no new physics in KM2a, but constraints on EBL models/intrinsic spectrum
- Cygnus region: hadronic Pevatron source in central part.